

# SOUTHWEST RESEARCH INSTITUTE®

## Internal Research and Development 2016

---

The SwRI IR&D Program exists to broaden the Institute's technology base and to encourage staff professional growth. Internal funding of research enables the Institute to advance knowledge, increase its technical capabilities, and expand its reputation as a leader in science and technology. The program also allows Institute engineers and scientists to continually grow in their technical fields by providing freedom to explore innovative and unproven concepts without contractual restrictions and expectations.



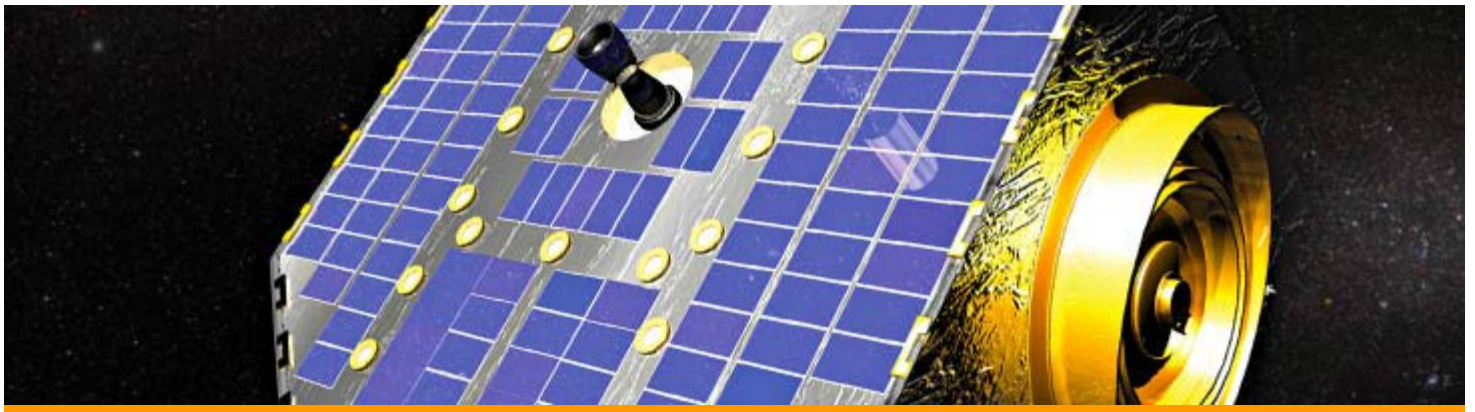
- [Space Science](#)
- [Materials Research & Structural Mechanics](#)
- [Intelligent Systems, Advanced Computer & Electronic Technology, & Automation](#)
- [Engines, Fuels, Lubricants, & Vehicle Systems](#)
- [Geology & Nuclear Waste Management](#)
- [Fluid & Machinery Dynamics](#)
- [Electronic Systems & Instrumentation](#)
- [Chemistry & Chemical Engineering](#)

Copyright© 2017 by Southwest Research Institute. All rights reserved under U.S. Copyright Law and International Conventions. No part of this publication may be reproduced in any form or by any means, electronic or mechanical, including photocopying, without permission in writing from the publisher. All inquiries should be addressed to Communications Department, Southwest Research Institute, P.O. Drawer 28510, San Antonio, Texas 78228-0510, [action67@swri.org](mailto:action67@swri.org), fax (210) 522-3547.

# SOUTHWEST RESEARCH INSTITUTE®

SwRI IR&D 2016 – Space Science

---



- Capability Development and Demonstration for Next-Generation Suborbital Research, 15-R8115
- Scaling Kinetic Inductance Detectors, 15-R8311
- Capability Development of Supernova Models, 15-R8498
- Fast Acquisition Multi-band High Resolution Spectrometer Development, 15-R8526
- Symplectic N-body Algorithms with Close Approaches (SyMBA), 15-R8539
- Radiation Hard ASICs for Space Imaging, 15-R8566
- Developing SwRI Capabilities for Detection of Isotopes of Lead, 15-R8570
- Stratospheric Compressor for Lighter-than-Air Vehicles, 15-R8575
- Investigation and Measurement of Balloon Dynamics at the Apex and Base of a Scientific Balloon, 15-R8577
- Feasibility Study and Definition of Requirements for a Satellite Ground Station, 15-R8578
- MASPEX Generation 2, 15-R8582
- The Development of an Enhanced Maximum Power Point Tracking (MPPT) Simulation Environment, 15-R8623
- Planet CARMA: Development of Venus Atmosphere Edition, 15-R8627
- Capability Development for Modeling Planetary Formation, 15-R8631
- Science Traceability Development and Engineering Trades in Preparation for a NASA Earth Ventures Instrument Proposal, 15-R8643

- Capability Development for Astrobiological Research, 15-R8646
- Understanding the Fluid Behavior of Planetary Regolith Materials, 15-R8651
- Evaluating Performance Limitations of Novel Processing Techniques for Next-Generation Space Sensors, 15-R8653
- Capability Demonstration of Pluto Photochemical Modeling for NASA Planetary Data Archiving, Restoration, and Tools Proposal, 15-R8658
- Radiation Testing of a Commercial RF Agile Transceiver for Spacecraft Applications, 15-R8661
- Constant Pressure Stratospheric Balloon (CPSB), 15-R8663
- Extension of SwRI's High Resolution Visible-Band Spectrometer into the Shortwave Infrared, 15-R8666
- Integrating SwRI Mass Memory Technology into a Focal Plane Array System, 15-R8669
- Testing Graphene Foils in a Space Plasma Instrument, 15-R8674
- Technology Development for Next-Generation Neutron Detector for Space Exploration, 15-R8675

# SOUTHWEST RESEARCH INSTITUTE®

SwRI IR&D 2016 – Materials Research & Structural Mechanics

---



- Assessment of Thermal Fatigue in Light Water Reactor Feedwater Systems by Fluid-Structure Interaction Analyses, 20-R8434
- Evaluate Atmospheric Microbiologically Influenced Corrosion Effects for Extended Storage of Spent Nuclear Fuel, 20-R8660
- Development of Computational Fluid Dynamics Framework for Characterization of High Energy Arcing Faults (HEAF) in Nuclear Power Plants, 20-R8680

# SOUTHWEST RESEARCH INSTITUTE®

SwRI IR&D 2016 – Intelligent Systems, Advanced Computer & Electronic Technology, & Automation

---



- [Detecting Distracted Drivers Using Vehicle Data, 10-R8496](#)
- [LTE System Security Research, 10-R8505](#)
- [Platform-Independent Evolutionary-Agile Optimization, 10-R8536](#)
- [Computational Performance Enhancements via Parallel Execution of Competing Implementations, 10-R8537](#)
- [Code Generation and Planning Engine for Self-Tuning Runtime Optimization, Project 10-R8538](#)
- [Automated Detection of Small Hazardous Liquid Pipeline Leaks, 10-R8552](#)
- [Select Superoptimization of Finite Element Analysis Tools, 10-R8563](#)
- [Subtle Anomaly Detection in the Global Dynamics of Connected Vehicle Systems, 10-R8571](#)
- [Construction Equipment Operator Training Simulators Technology Update, 10-R8572](#)
- [Assessing the Feasibility of Ranger in Kit Form, 10-R8590](#)
- [Deep Learning System for Robotic Pick Selection, 10-R8600](#)
- [Focused Automated Discovery of Telemetry Device Constraints, Project 10-R8626](#)
- [Optimization of Advanced Lattice-Boltzmann Models, Project 10-R8629](#)
- [Advanced Traffic Management Mapping Technologies: Linear Referencing, Vector Representation, and Multiple Raster Layers, 10-R8634](#)

- Large-Scale Robotic Aircraft Painting Technology Research and Development, 10-R8640
- Automated Engine Hot-spot Detection at Standoff Distance, 10-R8644
- High Performance Streaming Data Processing, 10-R8677
- Using SequenceL Parallel Programming Language to Improve Performance of Complex Simulations, 16-R8540
- Investigation of Computational Methods for Modeling Bird Strike Impacts on Aircraft Structures, 18-R8477
- Algorithms to Improve the Speed of the Numerical Model Based on the Lattice-Boltzmann Method, 18-R8541
- Improving the Efficiency of Computations Involving the Ballistic Impact of Full-Scale Structures of Composite Materials, 18-R8564
- Development of a New Numerical Model to Simulate Chemotaxis-driven Bacterial Transport for Treatment of Tumor Cells and Mitigation of Bacterially-mediated Pipeline Corrosion Problems, 18-R8602
- Computational Model Development and Validation for Additive Manufacturing Simulation, 18-R8650
- Dynamic Response of Steel-Plate and Concrete Composite Small Modular Reactor Structures Under Explosive and Seismic Loads, 20-R8433

# SOUTHWEST RESEARCH INSTITUTE®

SwRI IR&D 2016 – Engines, Fuels, Lubricants, & Vehicle Systems

---



- Investigation into Engine Wear Map Development with Radioactive Tracer Testing, 03-R8479
- Lubricant Impact on Fuel Economy — Correlation between Measured Engine Component Friction and Vehicle Fuel Economy, 03-R8502
- Experimental Investigation of Co-direct Injection of Natural Gas and Diesel in a Heavy-duty Engine, 03-R8522
- Combustion Chamber Design Optimization for Advanced Spark-Ignition Engines, 03-R8551
- Transient Durability Analysis of Aluminum Cylinder Heads, 03-R8611
- Low Cost, High Brake Mean Effective Pressure, High Power Density Diesel Engine, 03-R8617
- Fast Catalyst Light-Off on a Heavy-Duty Natural Gas Engine, 03-R8620
- Dilute Combustion Assessment in Large Bore, Low Speed Engines, 03-R8633
- Fuel Economy Effect of Advanced Vehicle Hardware, 03-R8649
- Validating Using Laser Scan Micrometry to Measure Surface Changes on Non-Concave Surfaces, 08-R8562
- Development of a New PAH Method for Process Oils, 08-R8625

# SOUTHWEST RESEARCH INSTITUTE®

SwRI IR&D 2016 – Geology & Nuclear Waste Management

---



- Investigation of Drought Intensity and Periodicity in South Texas Using Chemical Records in Bat Guano Cores, 20-R8519
- Distinguished Lecture Series and Invited Review Paper, 20-R8588
- Mechanical Stratigraphy and Natural Deformation in the Austin Chalk, 20-R8637
- Developing an Integrated Methodology to Estimate Geologic Stress States, 20-R8654
- Integrated Use of Structural Geologic Framework and Unstructured Numerical Models of Groundwater Flow, 20-R8659
- Mission Data Selection and Digital Terrain Modeling for Assessing Seasonal Flows on Mars, 20-R8662

# SOUTHWEST RESEARCH INSTITUTE®

SwRI IR&D 2016 – Fluid & Machinery Dynamics

---



- Proof-of-Concept Development of a Traversing Hot-wire Anemometer for Natural Gas Applications, 18-R8593
- Field Testing of Rotating Equipment Vibration Modes Using Operational Modal Analysis, 18-R8608
- Hydrogen and Methane Gas-Phase Detonations, 18-R8614
- A Fundamental Assessment of KISSC and JR Tearing Resistance Curves in Sour Brine Environment, 18-R8618
- Development and Validation of Liquid-Liquid Separation Modeling Techniques, 18-R8622

# SOUTHWEST RESEARCH INSTITUTE®

SwRI IR&D 2016 – Electronic Systems & Instrumentation

---



- Improved Spatial Resolution for an Earth-Observing Infrared Spectrometer, 10-R8621
- Compound-Eye Based Ultra-Thin Cameras, 14-R8545
- Multivariate Statistical Process Control for Cooling Towers, 14-R8656

# SOUTHWEST RESEARCH INSTITUTE®

SwRI IR&D 2016 – Chemistry & Chemical Engineering

---



- [Exploration of Encapsulation Methods of Subunit Vaccines, 01-R8576](#)
- [Enhancing the Efficacy of a Chlamydia Subunit Vaccine through Encapsulation, 01-R8584](#)
- [Development of a Low-Cost Robust Circulating Fluidized Technology for the Sustainable Production of Biofuels and Biobased Products, 01-R8585](#)

## 2016 IR&D Annual Report

---

### Capability Development and Demonstration for Next-Generation Suborbital Research, 15-R8115

#### Principal Investigator

S. Alan Stern

Inclusive Dates: 01/01/10 – Current

**Background** — Research applications for new-generation suborbital vehicles include, but are not limited to, microgravity sciences, space life sciences, Earth and space sciences, land use, education and public outreach (EPO), technology development and demonstration/space systems development and demonstrations (including TRL raising). The primary research advantages of these vehicles include more frequent access to the space environment, lower launch cost compared to conventional sounding rockets, capability for human operator presence, better experiment affordability, gentler ascent and entry compared to sounding rockets, extended periods of turbulence-free microgravity, and increased time in the 250,000 to 400,000 ft (80 to 120 km) region of the atmosphere (the "Ignorosphere").

**Approach** — Our long-term business interests in these vehicles are:

- To exploit them for planetary, astronomical, microgravity, aeronautical, and auroral research.
- To provide research-related common systems (flight computers, data recording racks, etc.) and payload integration services to NASA and/or vehicle providers.
- And to provide instrumentation, payload specialists, and flight project expertise to research groups, both domestic and overseas, working in this area.

Therefore, the overarching objective for this project is to put SwRI in the lead of the burgeoning suborbital research field using next-generation, manned vehicles by becoming one of the first, and quite possibly the first, organization to fly payloads with research payload specialists on these vehicles. This will open up to SwRI a series of new business opportunities including funded research and hardware development projects, ground and flight system task-order contracts associated with next-generation suborbital work, and providing payload specialists for next-generation suborbital work.

**Accomplishments** — Flight experiments were selected (SWUIS-A for remote sensing; JSC



*Figure 1: PI Stern and Co-I Durda completed pressure suit testing and centrifuge evaluation in November 2011.*

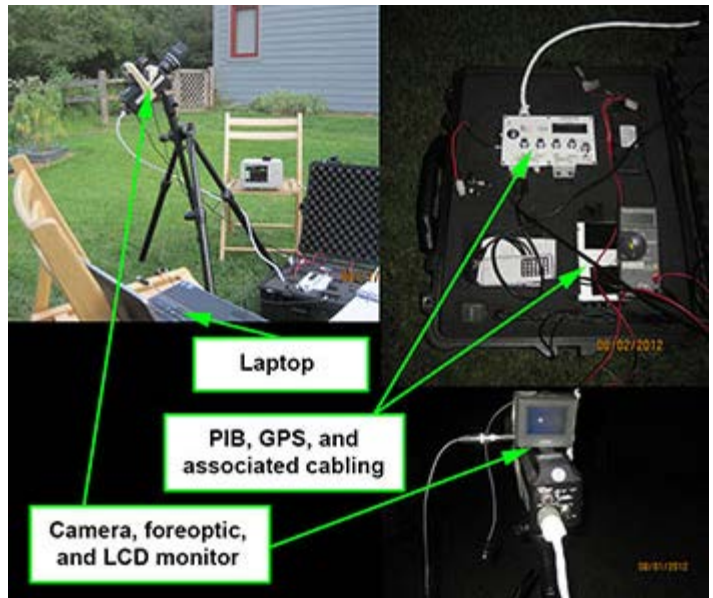


*Figure 2: The SWUIS experiment was upgraded and re-calibrated during laboratory and field ops in August/September 2012.*

biomed harnesses for life science work; BORE [Box of Rocks Experiment] for microgravity research). We secured personnel for SWUIS-A refurbishment, checkout, and calibration, and began refurbishment of the instrument. We completed the design and initiated construction of the BORE microgravity experiment. We received and test-fitted a JSC biomed harness that forms the basis of one of our three suborbital flight investigations. We initiated discussions with XCOR, Virgin Galactic, and Space Adventures regarding flight assignments, terms, and conditions on their suborbital vehicles. We constructed a flight requirements matrix to determine which flight providers are suitable for which of our experiments.

We completed a second set of F-104 training flights, with focused, in-flight investigations to (1) evaluate the wearability and function of the AccuTracker II biomedical harness with standard crew flight suits and life support equipment during typical g-loads, and (2) test the design concept for our BORE microgravity experiment during zero-g parabolas. We completed a zero-g training flight that included initial zero-g training and team exercises to refamiliarize/practice personal mobility and experiment handling operations in zero-g conditions.

We completed construction of the BORE microgravity experiment. The Blue Origin configuration of the BORE microgravity experiment successfully passed vibration testing. FAA Class II and Class I medicals for each SwRI payload specialist were completed in order to maintain expected suborbital flight medical qualification standards.

We designed the SwRI Payload Specialist Team mission patch, and initiated discussions with two companies on a collaborative effort to test/evaluate a pressure suit under launch g-loads. We completed pressure suit familiarization training and undertook centrifuge training to test/evaluate the pressure suit under launch g-loads.

We completed an upgrade and re-calibration of the SWUIS experiment for flight, and initiated planning for high altitude (75,000 ft) flight training in F-104 and F-18 aircraft. Additionally, we negotiated early flight test phase spaceflights with XCOR, and continued aerobic jet aircraft training. We completed flight data requirements and collection plans for each suborbital experiment.

We requested and received flight integration requirements documents and initiated work to



*Figure 3: Closeout photo of the BORE payload, delivered to Blue Origin's west Texas launch site in preparation for its April 2, 2016, suborbital spaceflight.*

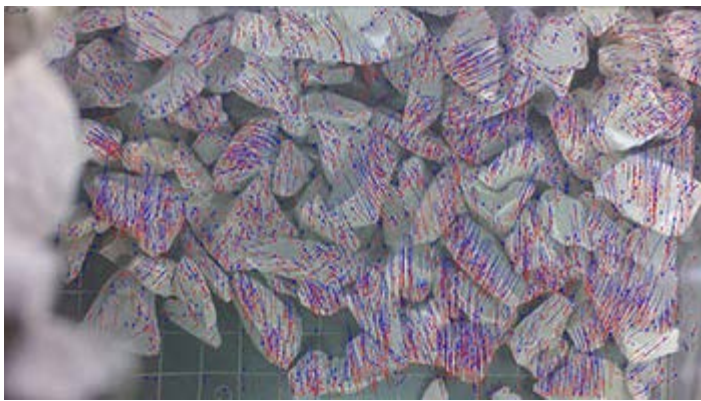


*Figure 4: Frame grab from video data from the Box-of-Rocks Experiment (BORE) flown on Blue Origin's April 2, 2016, suborbital spaceflight, showing the use of software for simultaneously tracking multiple features on many floating particles (i.e., the tracking "blips" – red and blue tracks – superimposed on the video frame).*

Blue Origin of a new Benchtop Payload Controller, etc.).

BORE successfully flew its first suborbital spaceflight aboard Blue Origin's New Shepard rocket on April 2, 2016. The payload performed flawlessly and recorded high-quality video data of the settling behavior of two different asteroid regolith simulants in microgravity. This was the first flight of science payloads on New Shepard, and Blue Origin marked the event by broadcasting pre-recorded video "tours" of the experiments; SwRI's contribution is archived online at <https://www.youtube.com/watch?v=dugpPEp2y78>.

The project is presently in a dormant state to conserve funds while waiting for the Virgin Galactic and XCOR vehicles to enter operational service in 2017/2018, at which time payload integration will commence and flight training will be completed.

complete these documents, and clarified crew training requirements with both XCOR and VG.

We checked out all three of our flight experiments after over a year in storage. We built BORE and SWUIS experiment flight boxes and developed flight checklists, conducted a successful test of both experiments, and validated checklists in zero-gravity parabolic aircraft flights.

A two-year, no-cost extension was approved for this project in December 2016, extending the project to 1 January 2019. We conducted annual battery change for the biomonitor flight experiment (required annual maintenance to prevent loss of programmed settings).

We prepared the BORE payload for flight aboard the Blue Origin suborbital vehicle in early spring 2016 (including cleaning and reconfiguring internal parts after the November 2013 zero-g test flight, reconfiguring for new data cameras provided by Blue Origin, reprogramming and testing the new flight software after delivery from

## 2016 IR&D Annual Report

---

### Scaling Kinetic Inductance Detectors, 15-R8311

#### Principal Investigators

[Peter W. A. Roming](#)

Michael E. Epperly

Omar D. Granados

B. David Moore

Michael D. Lillywhite

Gregory S. Winters

Inclusive Dates: 05/07/12 – 10/06/15

**Background** — Charged coupled devices (CCDs) and hybrid complementary metal-oxide-semiconductor (CMOS) detectors have dominated the field of optical and IR imaging. Despite their dominance, they lack simultaneous timing and spectral information, and only have good quantum efficiencies over a narrow wavelength range. Superconducting tunnel junctions (STJs) and transition edge sensors (TESs) have alleviated these shortcomings, but suffer from the major challenge of constructing large format arrays required for most imaging applications. Kinetic inductance detectors (KIDs) are a relatively new superconducting technology that have many of the desirable characteristics of STJs and TESs, but have great promise for creating large-scale formats like current CCDs and CMOS detectors for precision scientific, military, and medical imaging.

Current approaches for multiplexing KID arrays rely on detecting resonance changes by injecting a source signal with multiple frequency components. Source signal frequencies are designed to match each sensor element's unique resonant frequency. The array output is then a signal with multiple frequency components. The array's spectral response is measured with no photons present. When photons are absorbed by an element, its resonant frequency changes indicating the detection of a photon.

While this method has been proven to enable photon detection, it has two key drawbacks. The first is in device characterization. Each element is designed with a different resonant frequency, but due to manufacturing tolerances and variation due to temperature, the exact frequency is unknown. Each array element requires individual characterization to identify its resonant frequency under precisely controlled conditions. A second, even greater challenge is that the resonant frequency of each element changes with micro-Kelvin changes in temperature. This necessitates in-system re-calibration of the resonant frequencies. Source signal and processing electronics then need to be modified with the new set of frequencies. Large numbers of array elements exacerbate the problem.

**Approach** — The multi-frequency source signal is replaced with a wideband signal source. The wideband source enables every element in the array to resonate, producing a notch in the frequency spectrum, as long as its resonant frequency is within the band of interest. The wideband source causes each sensor element to resonate, and the array's spectral response will contain a notch at each sensor element's resonant frequency. Instead of needing to calibrate each element to determine its resonant frequency, a measurement of the response is taken during dark conditions, and only changes in resonances need to be detected for photon detection. We use three different wideband sources and compare their performance: white noise, wideband pulse, and maximal-length sequence (MLS).

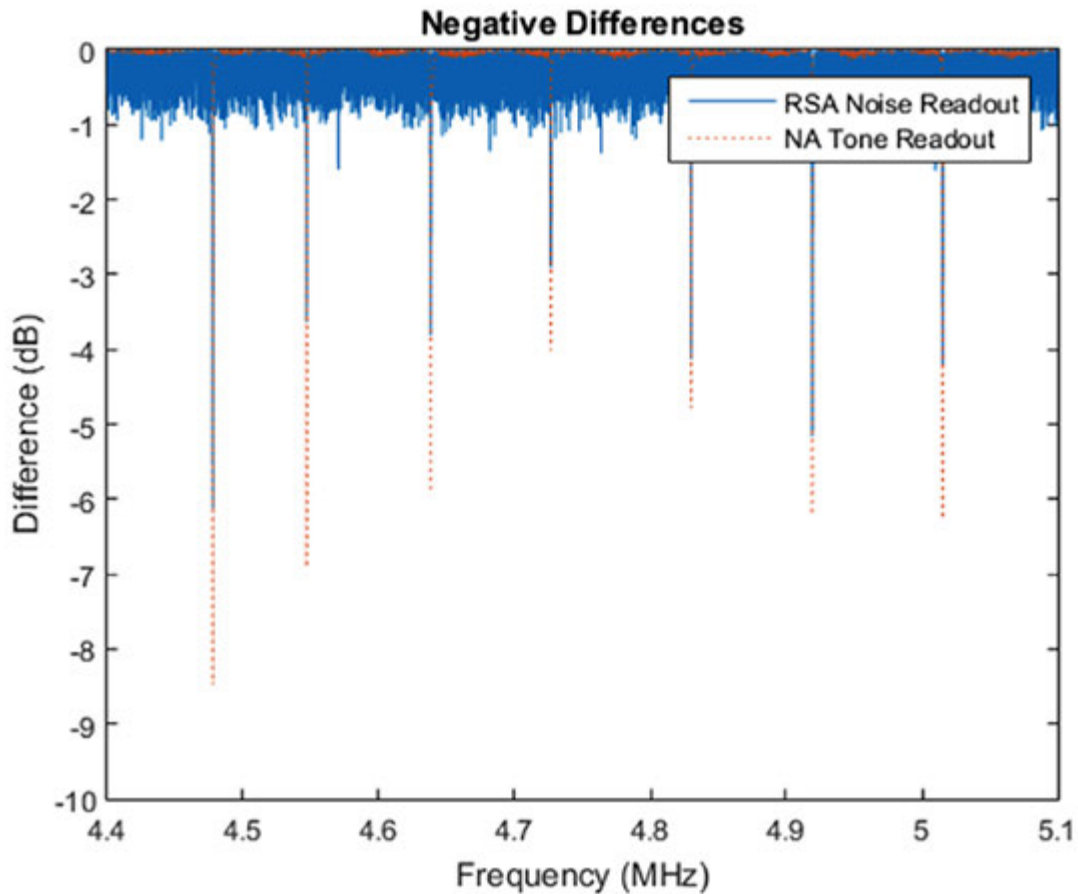


Figure 1: Difference plot between the MLS versus the network analyzer methods.

**Accomplishments** — Our "high"-temperature KID was packaged, placed in our cryocooler, and tested with a network analyzer to determine the location of the resonant frequencies for each pixel. A noise source generator and channelizer output electronics were built for measuring the noise-induced resonant frequencies. We tested the three different wideband sources and found that the white noise source is insufficient for consistent readout, wideband pulse requires higher analog-to-digital converter (ADC) dynamic range than available for accurate readout, and MLS provided the most promising results (Figure 1). We also tested the notch strength for our high-temperature KID as a function of temperature and found that above ~2.4K the notch strength is significantly weakened.

## 2016 IR&D Annual Report

---

### Capability Development of Supernova Models, 15-R8498

#### Principal Investigators

[Amanda Bayless](#)

Peter Roming

Rob Thorpe

Inclusive Dates: 10/01/14 – 04/01/16

**Background** — One of the crucial processes for shaping the composition of the universe is the death of massive stars ( $>8 M_{\text{Sun}}$ ) manifested as supernovae (SNe). Understanding this process is important as it has a significant impact on our understanding of cosmology, chemical enrichment, galaxy evolution, star formation rate, stellar evolution, compact object remnants, circumstellar medium, and dust formation. The purpose of this project is to develop a new analysis tool, the SuperNovae Analysis aPplication (SNAP), which will allow us to explore the physics of these stellar explosions.

**Approach** — SNAP consists of an observational database containing archived data from past SNe events, a model database with models that span a range in parameter space, and correlation software that compares the observations and the models. This is an improvement over current methods of data analysis as individual SNe are modeled one at a time using various codes that make assumptions regarding the underlying physics. By comparing sets of models with several observations, we are starting to understand which assumptions are valid, what the span of parameters space is, and how models can be improved. SNAP benefits observers as now new SN can be compared with existing models in real time. We currently discover approximately one SN daily. With the new surveys going on-line (e.g. LSST in 2018), we will find approximately 100,000 annually. SNAP allows an assessment on which SNe should have follow-up observations.

**Accomplishments** — The SNAP database is available at [snapdb.space.swri.edu](http://snapdb.space.swri.edu) and the descriptive public page is at [snap.space.swri.edu](http://snap.space.swri.edu). Figure 1 shows the basic database structure. The initial comparison software is complete and a paper has been submitted to AAS Journals. Further developments include adding more models and observations and adding features to the correlations software. This continuation of work is funded by a three-year grant from NASA. Initial results describing the database were presented in a poster at the annual meeting of the American Astronomical Society (AAS). Current results were presented at the 2017 AAS meeting as an oral presentation and poster.

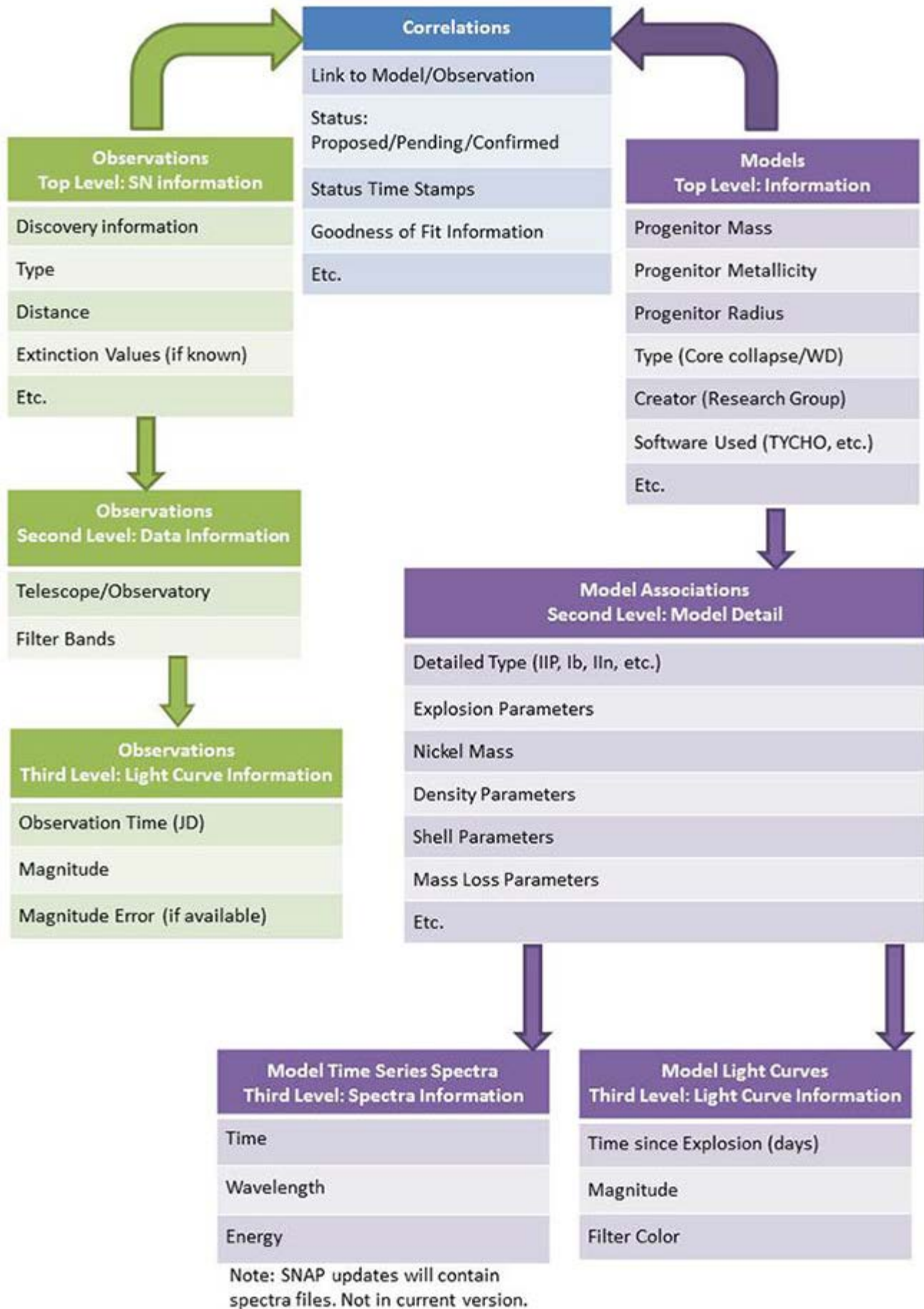


Figure 1: The flow chart for the database structure outlining the three databases in SNAP: Observations, Models,

*and Correlations.*

---

**2016 IR&D | IR&D Home**

## 2016 IR&D Annual Report

---

### **Fast Acquisition Multi-band High Resolution Spectrometer Development, 15-R8526**

#### **Principal Investigators**

[Michael W. Davis](#)

Thomas K. Greathouse

Kathleen E. Mandt

Peter W.A. Roming

Gregory S. Winters

Inclusive Dates: 01/01/15 – 04/04/16

**Background** — SwRI has a nearly 20-year history of designing, integrating, testing, and launching ultraviolet spectrographs. However, small, low-resource, capable near-IR spectrographs are needed to address NASA's Earth Science goals. This project developed the design of such a small, low-resource near-IR spectrograph and built a laboratory prototype.

**Approach** — The goal of this project was to design and demonstrate a prototype compact multiband spectrograph with optical performance competitive to existing larger instruments. The time and budget limitations of the project necessitated a design that could be tested with visible light, yet was still viable in the infrared. The end product would be a laboratory spectrograph rated at Technical Readiness Level 3, high enough for consideration for further development funding by NASA.

**Accomplishments** — A compact multiband near-IR spectrograph was designed using all-reflective optics. This spectrograph formed the basis for the CHIME instrument to be proposed to NASA in a future Earth Ventures Instrument proposal. A simplified variant of this design was built and tested in an SwRI optics and detector laboratory. The tests used a visible HeNe laser for simplicity and cost reduction, but the results can be scaled to the near-IR wavelengths of interest to NASA Earth Ventures missions. The design proved to have a resolving power of 28,000 at 632 nm. The echelle grating design means that the resolving power will hold out to 1,600 nm. The testing raised the maturity of the design to Technical Readiness Level 4, more than high enough to propose for future NASA opportunities.

## 2016 IR&D Annual Report

---

### **Symplectic N-body Algorithms with Close Approaches (SyMBA), 15-R8539**

#### **Principal Investigators**

[Kevin J. Walsh](#)

Harold F. Levison

Glen Mabey

David K. Kaufman

Julien Salmon

Inclusive Dates: 03/10/15 – 12/04/15

**Background** — The objective of this project was to migrate our planetary accretion code, SyMBA, to use graphics processing units (GPUs). The gravitational N-body code SyMBA was developed at SwRI, and has led to numerous advances in planet formation studies. It is valuable to the planetary science community because of its unique capabilities – owing to its symplectic algorithm it can support the number of timesteps and close encounters necessary for billion-year integrations of planetary building blocks interacting, colliding, and growing. This code had previously been limited to run on single processors or across a small number of cores in parallel. However because of poor scaling, simulations can take months or even years. The primary problem is the close encounter algorithm that allows SyMBA to remain symplectic while handling close encounters between bodies, which relies on recursion and a complex interaction tracking algorithm.

**Approach** — Originally designed to handle computation only for computer graphics, current GPUs enable highly pipelined general-purpose computing. We set an objective of porting the entire code to run on GPUs, as we expected this would lead to the best code performance. The two major problems that needed to be solved were the recursive function call for timestep halving and the encounter list sorting and manipulation for parallel GPU calculations. We produced three new versions of the code, splitting computation between CPU and GPU two different ways, and also one version entirely running on the GPU using Portland Group compilers and their OpenACC code and compilation products running on NVIDIA hardware.

**Accomplishments** — We attained a relative speedup of approximately 15 in some regions of parameter space, particularly those that maximized the pure N-body aspect of the code and the split effort between CPU and GPU. This advancement will allow us to do more realistic simulations and attack a new class of problems.

## 2016 IR&D Annual Report

---

### Radiation Hard ASICs for Space Imaging, 15-R8566

#### Principal Investigators

[Peter W. A. Roming](#)

Michael E. Epperly

Michael A. Koets

Inclusive Dates: 07/01/15 – Current

**Background** — Cross-delay line (XDL) micro-channel plates (MCPs) have been the detector of choice for ultraviolet (UV) imaging and spectroscopic applications over the last decade. Notwithstanding their predominance in the field, these sensors lack the combination of high positional resolution, large number of pixels, capability to observe bright sources, low operational voltages, small volume, and low power encoding electronics. Recent advances in the next-generation UV detectors — cross-strip (XS) MCPs — have addressed many of these issues. Despite this significant progress, low-power encoding electronics are still lacking. An additional need is to be able to track sources with the detector itself, rather than an extremely stable platform, to reduce production and operational costs.

**Approach** — We have developed a combined hardware-software (HSW) concept that incorporates sensor electronics, event detection, centroid processing, alignment, and image compression to deliver a compact low power encoding electronic system that also functions as a star tracker. We will develop and validate this new HSW capability for handling data supplied by these state-of-the-art XS MCPs via two key tasks. First, we will design new interface electronics for these sensors and implement them in a compact, power-efficient ASIC. Second, we will create the image processing algorithms required for generating the data products from the sensor electronics and investigate implementation options for the algorithms that are appropriate for use on small spacecraft.

**Accomplishments** — A new interface electronics design is completed in preparation for an integrated circuit fabrication. We also completed correlation-based alignment and localization algorithms, and coding and testing of sparsification and anti-coincidence logic for ASIC.

## 2016 IR&D Annual Report

---

### Developing SwRI Capabilities for Detection of Isotopes of Lead, 15-R8570

#### Principal Investigators

Tom Whitaker

F. Scott Anderson

Inclusive Dates: 07/01/15 – 06/30/16

**Background** — The purpose of this project was to extend SwRI's Laser-Ablation Resonance Ionization Mass Spectrometry (LARIMS) technique for radiometric dating to the Pb-Pb method. Radiometric dating is the principal method used by geologists to determine the age of rocks and other objects. We have previously successfully developed LARIMS to rapidly determine the age of a sample comparing isotopes of Rb and Sr with essentially no sample preparation. This is accomplished by selectively ionizing Sr using lasers whose wavelengths are tuned to electronic resonances in Sr. The process is then repeated 2 to 3 microseconds later for Rb, separating the ion formation for the two elements in time. The isotopes are then analyzed in a time-of-flight mass spectrometer (TOF-MS). This project extended our dating capability to Pb-Pb dating, which is based on the fact that  $^{206}\text{Pb}$  and  $^{207}\text{Pb}$  are stable end products, respectively, of  $^{238}\text{U}$  and  $^{235}\text{U}$  decay. The advantage of the Pb-Pb system for LARIMS is that only a single element must be analyzed, simplifying the instrumentation and avoiding inter-element fractionation effects.

**Approach** — Laser wavelengths were generated for the three-step resonance ionization scheme shown in Fig. 1. Samples were introduced into a multi-bounce TOF-MS, and a small spot was ablated with a frequency-quintupled Nd:YAG laser (213 nm). Ions formed in the ablation process were prevented from entering the mass spectrometer using pulsed electric fields. The neutral Pb atoms were ionized with high specificity by the wavelengths shown in Figure 1. These laser-induced ions were accelerated into the the TOF-MS for isotope analysis. The samples could be repositioned so that hundreds of different spots could be analyzed and the resulting isotope signals plotted to form an isochron. Figure 2 shows the selectivity of the resonance ionization process for analysis of Pb in Standard Reference Material (SRM)-610 containing 426 ppm Pb with an intentionally introduced isobaric contaminant ( $\text{HfO}_2$ ). The red line shows the signal (offset by 1 mV) when one of the resonance lasers is turned off. None of the  $\text{HfO}_2$  contaminant is visible.

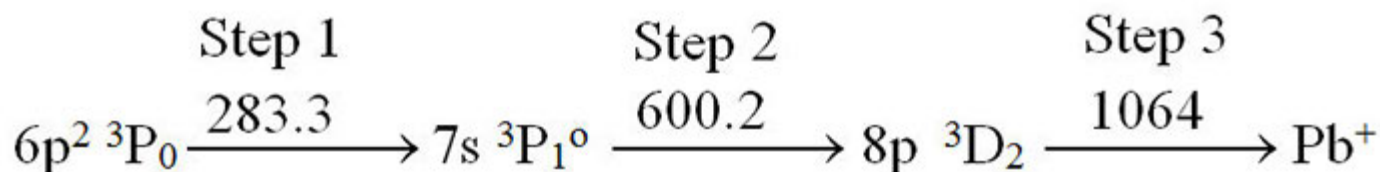


Figure 1: States and wavelengths (nm) required for resonance ionization of Pb atoms.

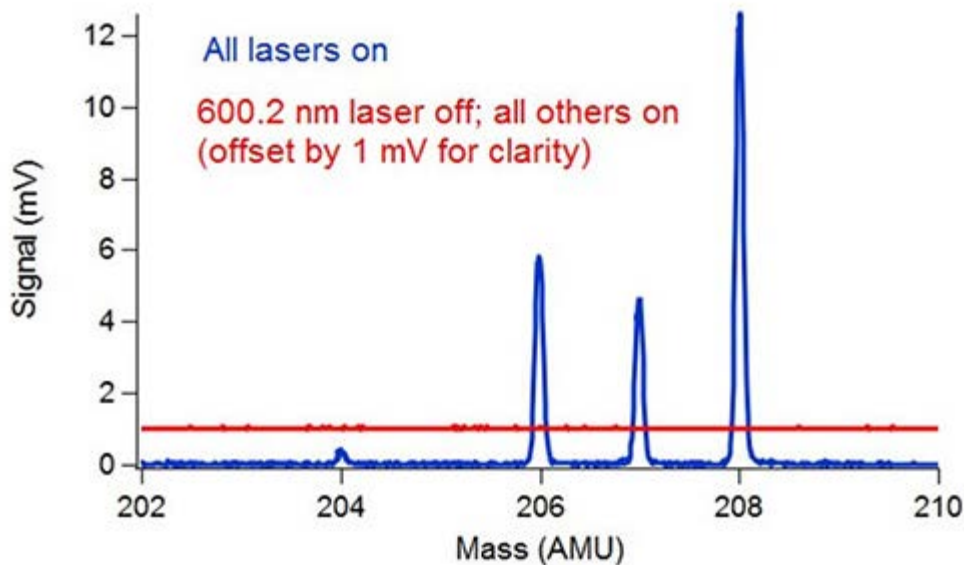


Figure 2: LARIMS spectrum of SRM-610 containing isobaric contaminant.

**Accomplishments** — Dates were obtained for a Kuehl Lake Zircon (measured age  $1070 \pm 50$  Ma; actual 1.067 Ma), and the La Paz Icefield lunar meteorite (LAP)-02205 (measured age  $3170 \pm 50$  Ma; actual 2990 Ma). The LAP-02205 sample had significant modern Pb contamination. This gave two distinct sets of points on two different slopes. We were able to separate these two sources of Pb, and the agreement within 200 Ma of the accepted value shows that the technique is useful even when other sources of Pb are present at high concentrations. We also generated an isochron, shown in Figure 3, for the Miller Range (MIL)-05035 lunar meteorite. Even though this sample contains only 0.405 ppm total Pb, we were able to obtain an age of  $3880 \pm 80$  Ma, in good agreement with the literature value of between 3800 and 3900 Ma.

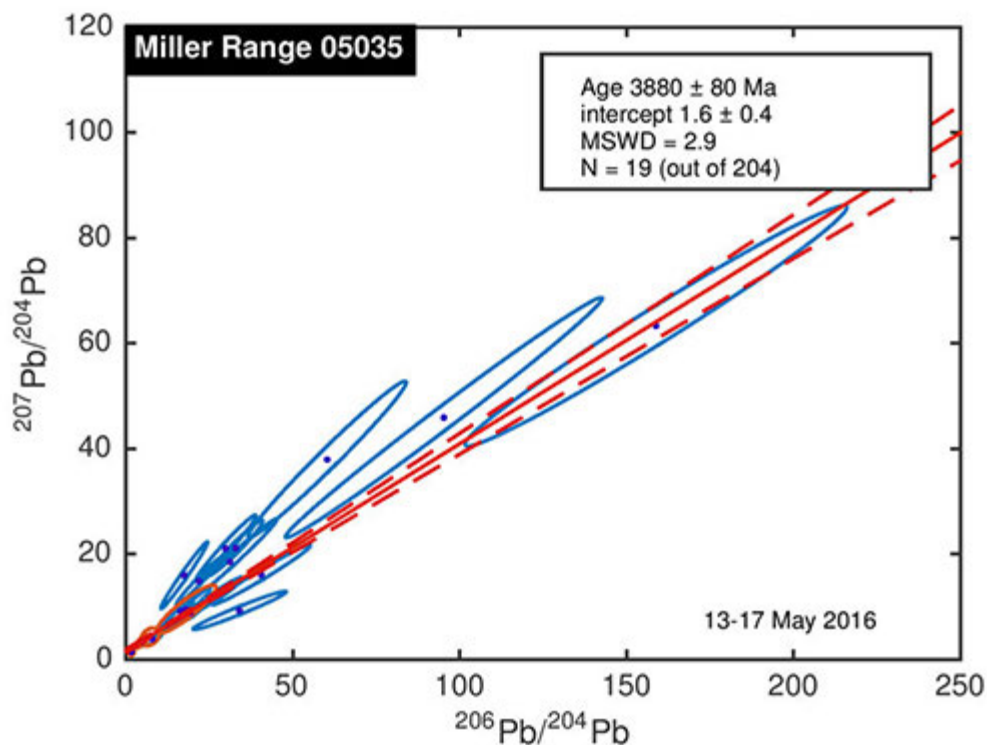


Figure 3: LARIMS isochron for MIL-05035. Because of the low concentration of Pb in this sample, only 19 points out of 204 that we analyzed had adequate signal to noise to be used in the isochron.



## 2016 IR&D Annual Report

---

### Stratospheric Compressor for Lighter-than-Air Vehicles, 15-R8575

#### Principal Investigators

[James Noll](#)

Grant Musgrove

Inclusive Dates: 07/13/15 – 02/18/16

**Background** — A vehicle with trajectory control and persistent operation capabilities up to 120,000 feet altitude does not currently exist and is a game-changing technology sought for military and scientific applications. Lighter-than-Air (LTA) vehicles are uniquely suited to long-endurance operation at these altitudes. The extremely low air density and steady winds at these altitudes makes long duration guidance and control of LTA vehicles impractical using traditional means of thrust. Low power directional control of the LTA vehicle can be achieved by driving the vehicle to different altitudes and exploiting wind differences in different strata. Technology that enables efficient movement of air into and out of an LTA vehicle's ballonet allows repeatable altitude changes for long-duration flights, thus allowing flight path control of the system over long distances.

**Approach** — The objective of this research was to determine and characterize the best method to add air mass to an LTA vehicle for altitude and trajectory control applications in the stratosphere. A matrix of performance parameters for compressors that facilitate altitude control of LTA vehicles was generated. Preliminary design concepts for the compressor aerodynamic flow path were developed using a one-dimensional analysis. The results of this preliminary design were used to formulate initial requirements and size the supporting systems for the stratospheric compressor. A review of the overall system feasibility concluded that further study was warranted in a second phase of study.

In Phase II, a three-dimensional simulation of the aerodynamic flow path was performed using computational fluid dynamics (CFD) software. The performance capabilities were updated and the derived requirements for the supporting systems were updated. Thermal performance in the radiation dominated environment of near space operation was analyzed. In addition, a preliminary design for test equipment and procedures to assess compressor performance characteristics will be generated.

**Accomplishments** — In Phase I of this project, preliminary compressor designs for buoyancy control at high altitudes were created. Feasibility of the designs was assessed based on mass and power of compressor systems. Findings in Phase I indicate there are viable compressor designs for achieving trajectory control of LTA platform suited for small commercial and military payloads intending to fly over specific targets, as well as large scientific payloads with capability to steer away from population centers. The Phase II study validated assumptions made in the initial aerodynamic modeling, investigated strategies for heat management, and developed test methodology for performance evaluation of stratospheric compressor systems.

## 2016 IR&D Annual Report

### Investigation and Measurement of Balloon Dynamics at the Apex and Base of a Scientific Balloon, 15-R8577

#### Principal Investigators

I. Steve Smith, Jr.

James Noll

Brock Martin

Ethan Chaffee

Inclusive Dates: 07/10/15 – Current

**Background** — The large balloon reflector (LBR) (Figure 1) is a 10-meter aperture (20m diameter), inflated, spherical THz antenna designed to fly on a large scientific balloon at 120,000 to 130,000 feet. The realization of a large, near-space, 10-meter class reflector for THz astronomy and microwave/millimeter-wave remote sensing and telecommunications has long been a goal of NASA and the DoD. The LBR is one of 12 concepts selected in 2013 out of ~550 submissions by the NASA Innovative Advanced Concept (NIAC) program to conduct a fast-paced design study. The LBR team consists of SwRI, University of Arizona (UA), Applied Physics Laboratory (APL), and Jet Propulsion Laboratory (JPL). The concept was originally conceived between UA and SwRI.

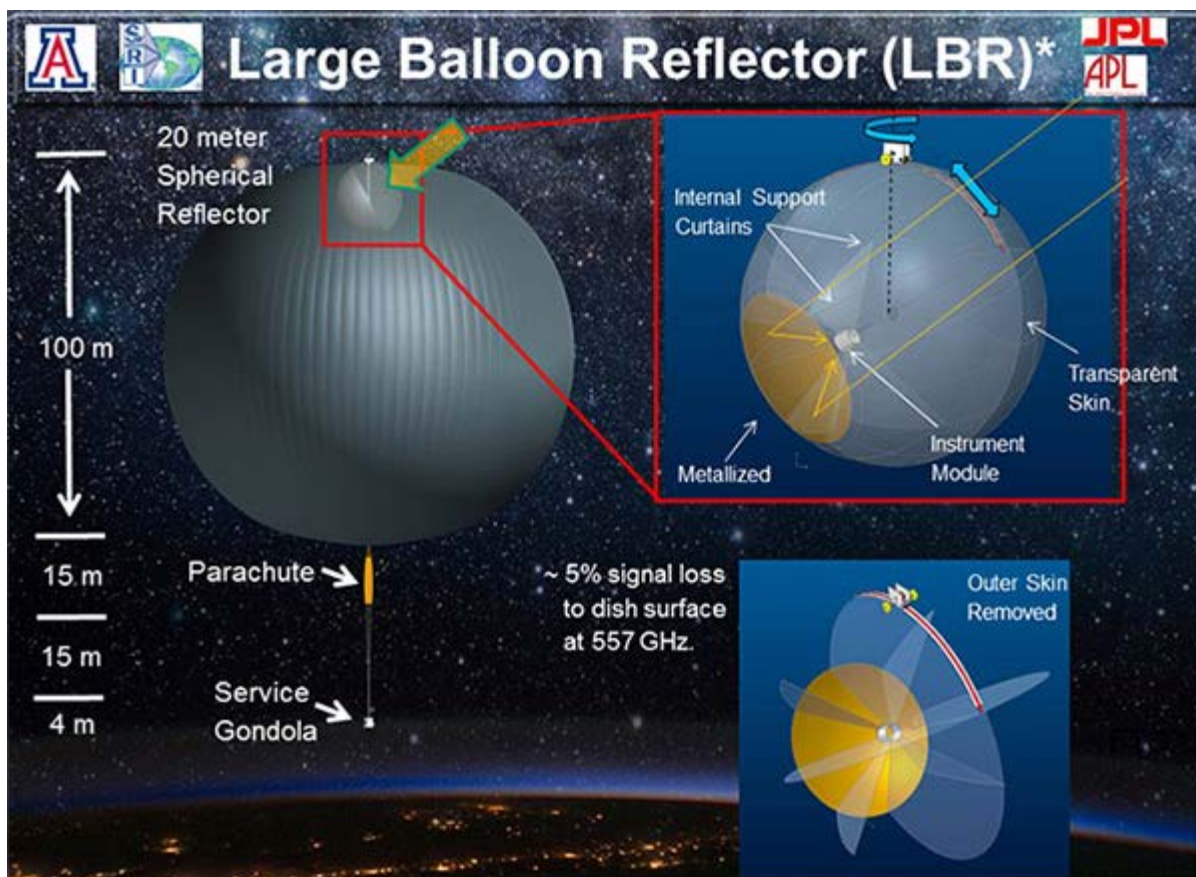


Figure 1: Large balloon reflector concept

LBR has won both Phase I and II funding under the NIAC program. During our Phase II mid-term review on April 27, 2015, the review panel wanted to see quantitative evidence that locating LBR within the carrier balloon instead of tethering it below the payload gondola provided a sufficient pointing stability advantage to warrant the additional operational complexity. Since there is little or no data for the balloon apex dynamics or simultaneous data between the apex and a suspended payload, additional data was needed. In late May, NASA's Science Mission Directorate authorized a free piggyback balloon test flight so we could obtain the required data. This was contingent on us getting flight instrument packages flight ready in time for the flight in late August; the next opportunity would not occur until a year later. They indicated that once we have this data in-hand, we would be in a strong position to propose and obtain funding to fly a LBR engineering model.

**Approach** — The objective of this project was to develop two flight packages to obtain simultaneous dynamics data from both the apex of a balloon and its suspended payload under the same flight conditions. This data would then be used to quantitatively answer the question of whether it was better to place the LBR at the balloon apex or from the payload. To accomplish this task, we needed to:

1. Construct small, efficient instrument packages using COTS hardware to be flown at the apex of a scientific carrier balloon and on the payload gondola suspended below it. The packages will leverage the experience and hardware gained in recent SwRI efforts and will contain accelerometers, inclinometers, temperature sensors, and cameras. The instrument packages will be used to measure the flight dynamics data (three-axis accelerations, rotations, magnitudes, rates, frequency, modes, etc.).
2. The measured dynamics data will be used to constrain and validate numerical models. We will perform a differential analysis of the relative merits of locating LBR in the top of the stratospheric balloon or tethered below the payload gondola. These results will be used to position us for the next phase of development and funding.

**Accomplishments** — We were able to successfully design, fabricate, test, and integrate two LBR sensor packages (LBRSP): an up-looking balloon apex and a down-looking gondola sensor. As part of the package, we were also able to integrate a UA star camera (Figure 2). Both packages, apex and gondola, were able to link and transmit data to each other via an onboard Wi-Fi for data redundancy in the event one was damaged or lost.

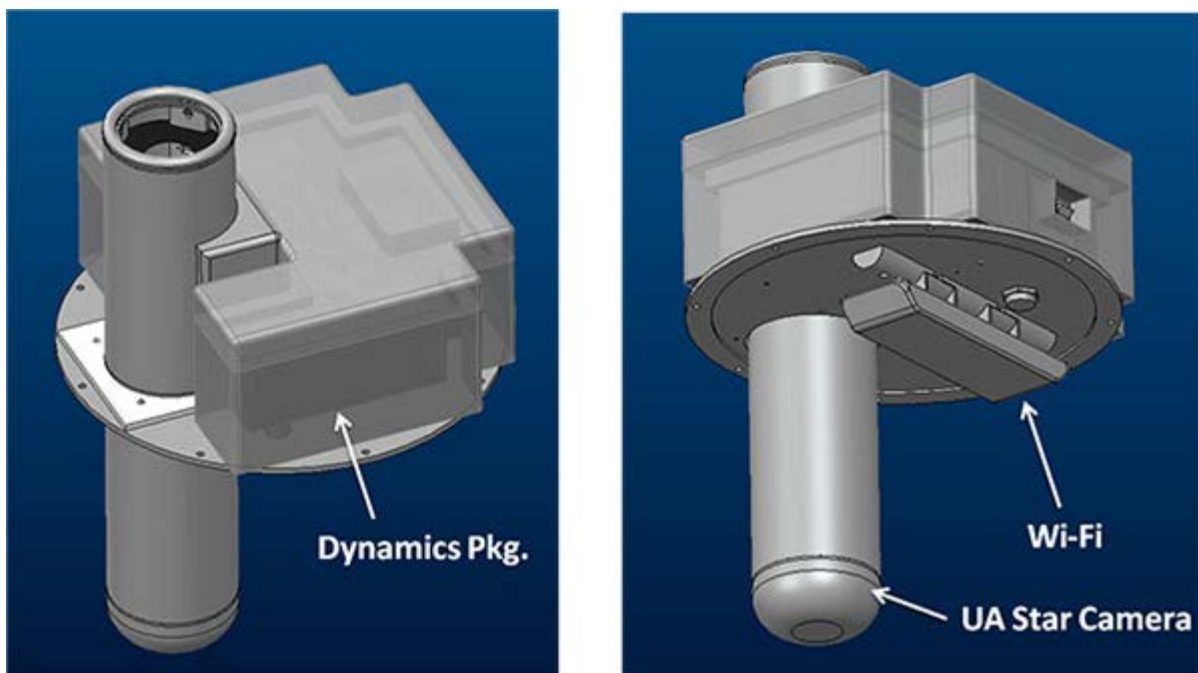


Figure 2: LBRSP mechanical layout

The NASA piggyback flight was conducted from Fort Sumner, N.M., on September 4, 2015. An image of the balloon and gondola can be seen in Figure 3. The LBRSPs were able to acquire, record, transmit, and receive data for the entire flight lasting a total of 7.5 hours, including the ascent, float, and descent. All instrumentation was successfully recovered.



*Figure 3: Balloon and gondola just before launch*

Initial data analysis has been completed adequately to successfully fulfill the objectives of this effort. The apex data shows that there are several oscillation modes at the apex of the balloon, but all of these modes have periods longer than 5 seconds. The strongest modes are at 8.2 sec., 22.5 sec., and ~300 sec. These are relatively low frequencies that are easier to compensate in a pointing system. The gondola jitter is much more pronounced than the apex. The gondola shows several short period oscillations between 2.0 and 0.8 seconds that are much more difficult to compensate with a pointing system. In summary, from a pointing control point of view, it is preferable to have the LBR at the balloon apex than suspended from the gondola.

## 2016 IR&D Annual Report

---

### Feasibility Study and Definition of Requirements for a Satellite Ground Station, 15-R8578

#### Principal Investigators

[Greg Fletcher](#)

Tom Jaeckle

Inclusive Dates: 07/20/15 – 05/20/16

**Background** — The goal of this project was to design a ground station for communication with Earth orbiting spacecraft that provides the most versatile set of capabilities available. SwRI has developed a robust NASA mission management capability, including roles as Principal Investigator, Project Manager, Mission Systems Engineering, Mission Operations, Spacecraft Bus provider, and instrument/payload provider. SwRI has developed numerous capabilities over time to support these efforts. The last significant capability to be developed is the ability to provide uplink and downlink of our own mission commanding and data. This capability signifies a level of institutional and programmatic maturity that provides a competitive advantage in the spaceflight industry, particularly for missions. Beyond our own missions, there is a market for providing uplink/downlink services to external customers. The research objective for this project was to develop the design, identify a location suited to a ground station, understand the market needs, and develop a business case that would not only pay for the cost and maintenance of a 13-meter ground station, but provide a long-term revenue stream.

**Approach** — A model of the operational scenarios was developed that incorporated data related to current capabilities and technologies, such as frequency band, antenna gain, geophysical locations of existing network assets relative to the selected site, and overpass predictions (both number and frequency of occurrence). Key parameters from the model results were fed into a set of financial models to ensure the business case was viable. Figure 1 shows a 13-meter ground station configured with similar capabilities to the proposed SwRI ground station. The image was provided by L-3 Datron, who will supply



Image courtesy of L-3 Datron

*Figure 1: The SwRI-proposed ground station will be similar to this configuration.*

much of the ground station hardware.

**Accomplishments** — The model results indicated that a ground station at the geophysical coordinates of SwRI, equipped with S, X and Ka-Band receivers with an S-band transmitter would fill gaps in current network capabilities for uplink/downlink of Earth orbiting spacecraft data and commanding. Partnerships with NASA's Near Earth Network (NEN) and commercial spaceflight assets were endorsed by NASA and network partners Universal Space Network (USN) and Kongsberg Satellite Services (KSAT). The SwRI ground station will support its own missions, and cooperate as part of a global communications network. Costs for constructing a 13-meter ground station were developed, and quotes received from suppliers. Business case models indicated that the revenue stream will pay for the initial cost, maintenance, and operation, while providing SwRI with a competitive edge for NASA mission development.

## 2016 IR&D Annual Report

### MASPEX Generation 2, 15-R8582

#### Principal Investigators

J. Hunter Waite

Greg Miller

Christopher Glein

Inclusive Dates: 08/06/15 – Current

**Background** — The purpose of this project is to integrate and test the latest generation of multi-bounce time-of-flight mass spectrometer at a system level with hardware developed at SwRI. This integration comprises the ground support equipment, software components, digital acquisition processor, ultra-stable high-voltage power supplies, ion extraction pulsers, timing, and acquisition with calibration techniques for mass assignment. These activities support upcoming proposals for demonstrating new research applications of MASPEX within NASA's New Frontiers program.

**Approach** — The proposed tasks are:

- Develop and integrate the MASPEX instrument control and data acquisition software.
- Develop the next-generation MASPEX detector system with modifications found during the current test and development phases of the Europa vacuum cover feed through to interface the detector to MBTOF 5 (developed under the ICEE program).
- Develop a MASPEX closed-ion source with modifications discovered in the final phase of testing, and integration with MBTOF 5.
- Develop the next generation of the high-stability, temperature-controlled laboratory power supplies (the FRIDGE) and integrate into the Europa prototype.
- Characterize the life characteristics of the MASPEX High Conductance Valve (developed under the Tech Dev program).
- In response to an unforeseen opportunity to propose for a New Frontiers "ocean

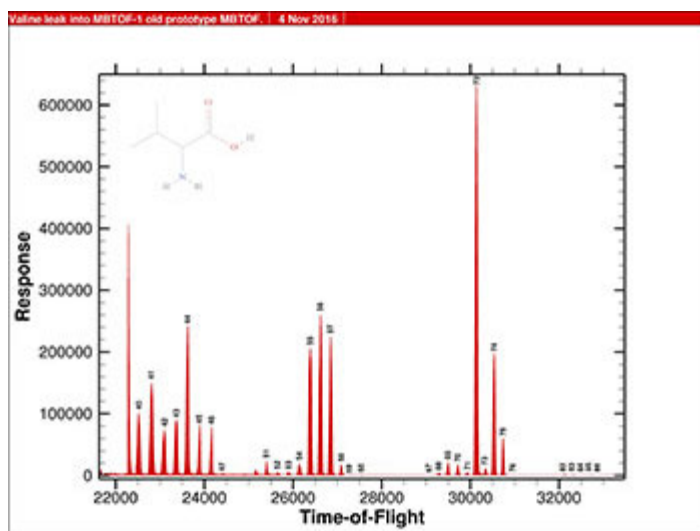


Figure 1: Amino acid solutions in the ion source.

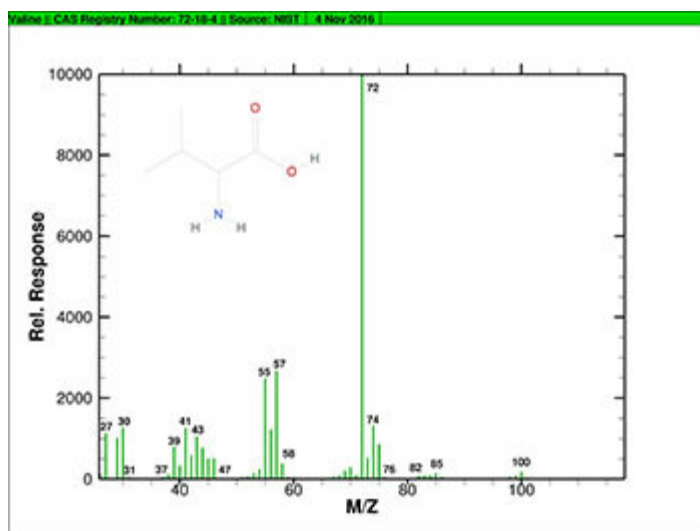


Figure 2: Data compared with a reference mass spectrum.

worlds" mission, laboratory work was initiated to support the science objectives and demonstrate the technical capabilities of MASPEX for the Enceladus Life Finder (ELF) mission.

**Accomplishments** — The goals of the first four tasks were successfully achieved. The completion of Tasks 2 and 3 was transferred to the MASPEX Europa contract. Task 5 was suspended as a result of changes in the valve design.

The first-generation multi-bounce mass spectrometer was refurbished under this project to make measurements of amino acids and hydrocarbon gases, in support of the ELF proposal. A graduate student was recruited and trained for this project. The instrument was configured to accept amino acid solutions into the ion source, and measurements were successfully made (Figure 1). The consistency of the data with a reference mass spectrum (Figure 2)

supports the argument that MASPEX can measure these building blocks of life in the Enceladus plume. Standardized hydrocarbon gases were purchased, and isotopologue measurements are now being completed to demonstrate the capabilities of MASPEX to accurately and precisely determine carbon and hydrogen isotopes in methane as a test for life on Enceladus (Figure 3).

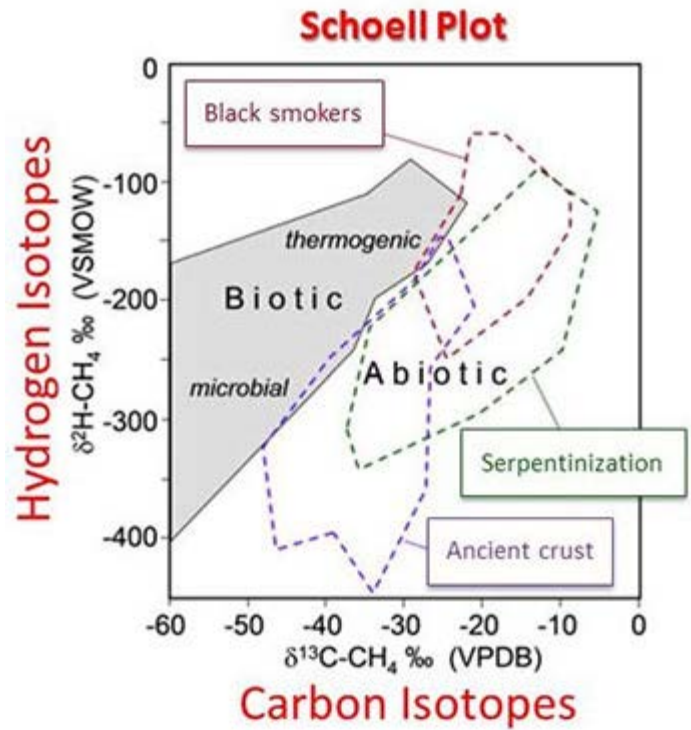


Figure 3: Isotopologue measurements demonstrated MASPEX.

## 2016 IR&D Annual Report

---

### The Development of an Enhanced Maximum Power Point Tracking (MPPT) Simulation Environment, 15-R8623

#### Principal Investigators

[John Stone](#)

Steven Torno

Carlos Nuñez

Gray Dennis

Robert Bolanos

Inclusive Dates: 01/18/16 – 05/18/16

**Background** — By far, the most common power source for spacecraft is the sun, converted into usable energy by an array of solar cells. For small satellites where efficiencies are vital, the best approach to efficient solar array power extraction is to use a maximum peak power tracker (MPPT). A MPPT configuration places a DC-DC buck converter between the solar panel and the spacecraft loads and battery, and the MPPT controller uses solar array telemetry to pull the appropriate amount of power for the system operating point. The drawback of MPPT techniques is the complexity of the circuitry and the associated power dissipation in the buck converter and Field Effect Transistor (FET) switching operation. Recent efforts at improving efficiency for an in-house MPPT pointed to a large mismatch between the modeled MPPT performance and the actual hardware, resulting in an inability to accurately predict the response of the physical circuit to proposed improvements. The purpose of this project was to improve and validate MPPT simulation models against actual hardware.

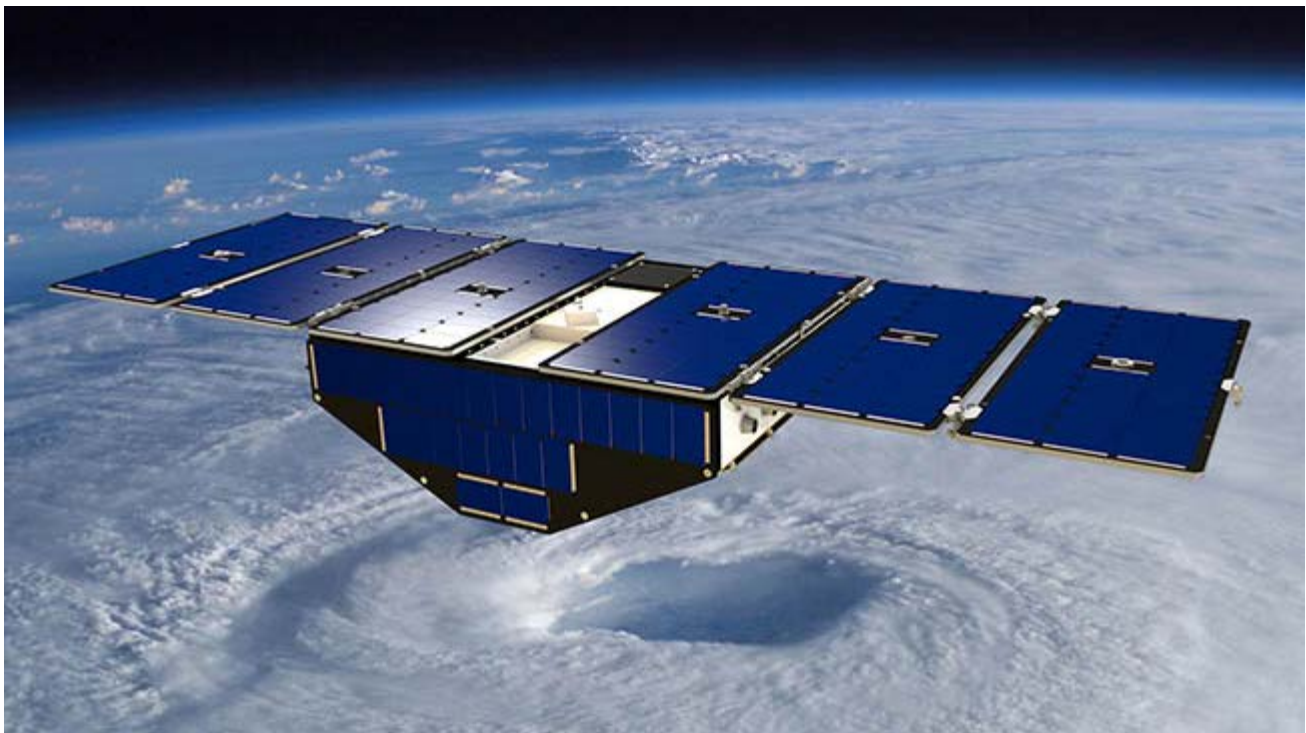


Figure 1: Typical SwRI-designed small satellite with deployed solar arrays.

**Approach** — Initially, a baseline simulation model of an existing SwRI-designed MPPT was established, and measurements of a test board compared to simulation results. An iterative model improvement process was then followed of adding/adjusting various circuit parasitic elements measured on the board, with special attention paid to the lead inductances of the FET and diodes as well as the capacitance of the PWB planes. Each simulation component addition/change was compared to the measured baseline, and the final model applied to various MPPT configurations to gauge accuracy.

**Accomplishments** — The simulation modeling of the initial MPPT was finalized and accurate to within 2.8 percent on efficiency, and the same knowledge and methods learned were applied to another project's MPPT design (with a different topology) resulting in a mismatch between the revised simulation and measured efficiency of less than 2 percent. Additionally, the topology of the original MPPT test board was modified and simulated, with the revised simulation model accurate to within 2.9 percent. This is significantly better than the initial simulation predictions of both MPPT converter efficiencies, and raises the confidence level in our simulation environment noticeably. The improved simulation environment will provide tangible benefits for several upcoming projects.

## 2016 IR&D Annual Report

### Planet CARMA: Development of Venus Atmosphere Edition, 15-R8627

#### Principal Investigators

Kandis Lea Jessup

Erika Barth

Inclusive Dates: 01/25/16 – 05/25/16

**Background** — The purpose of this project was to develop the Venus module of the SwRI-based Planet CARMA (Community Aerosol and Radiation Model for Atmospheres) solver, which allows accurate and efficient modeling of microphysical and radiative processes in any planetary atmosphere through modular inputs to a core (standardized) Radiative Transfer (RT) and microphysics code. Our motivation in developing this tool was that the long-term evolution of climate on Venus and other planets is dependent on the planetary albedo which is determined by both cloud particle properties, and the chemistry that maintains the supply and formation of the clouds.

**Approach** — CARMA solves the continuity equation for aerosol particles (vertical transport, coagulation, cloud formation, and growth) and calculates their radiative effects in a column of atmosphere. To construct our Venus CARMA we use a Venus temperature/pressure profile, molecular weight and viscosity from a CO<sub>2</sub> atmosphere, eddy diffusion based on a combination of models from the literature, and a fixed water vapor profile. The composition of the particles is defined by three groups:

- Meteoric Dust CN - 1.3 nm radius particles created through a Gaussian-shaped production equation, peaking at 83 km.
- Sulfur Aerosol CN - 10.4 nm radius particles created through a Gaussian production equation representing photochemical production, peaking at 61 km.
- H<sub>2</sub>SO<sub>4</sub>+H<sub>2</sub>O Cloud - Particles are represented for a range of sizes, 1.64 nm to 30 μm.

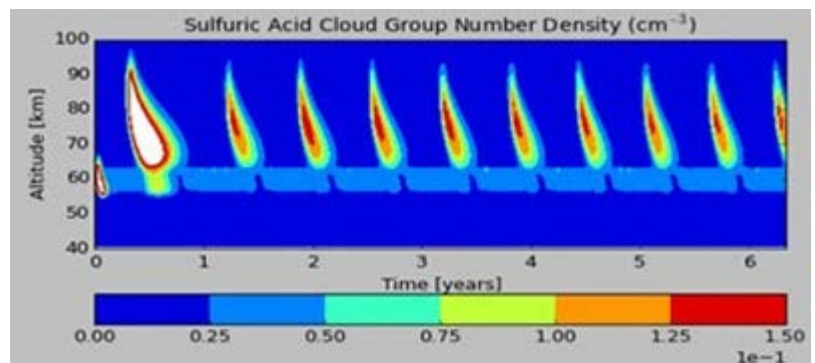


Figure 1: Model results showing H<sub>2</sub>SO<sub>4</sub> clouds produced by Venus CARMA. The periodicity is related to the time it takes to resupply H<sub>2</sub>SO<sub>4</sub> vapor after a nucleation event has occurred; time variation in the Venus clouds has been noted in the literature.

In our simulations the dust and sulfur particles serve as condensation nuclei (CN) for the H<sub>2</sub>SO<sub>4</sub> clouds. The effects of a solution of H<sub>2</sub>O and H<sub>2</sub>SO<sub>4</sub> are included in the equations for vapor pressure, liquid density, and surface tension. The nucleation process prescribes the initial formation of the cloud particles. Condensation growth and evaporation then control how the particles change in size in reaction to the humidity level of the environment, assuming a static water vapor profile.

**Accomplishments** — We have created a physically consistent microphysics model that operates with H<sub>2</sub>SO<sub>4</sub> and H<sub>2</sub>O mixtures at Venus temperatures and pressures. The model compares favorably with other work in the literature and includes additional capabilities.



## 2016 IR&D Annual Report

---

### Capability Development for Modeling Planetary Formation, 15-R8631

#### Principal Investigator

David Nesvorny

Inclusive Dates: 02/20/16 – 06/20/16

**Background** — The purpose of this project was to develop a software capability to model the formation and early dynamical evolution of planetary systems discovered by NASA's Kepler telescope, where two or more super-Earths and Neptune-size planets have close-in, tightly packed orbits. These properties motivate us to consider the formation and dynamics of planetary systems in the presence of a protoplanetary gas disk. The previous approaches to this problem can be divided into two categories. The first category is to use a hydrocode and model a small number of nearly fully formed planets in the presence of a gas disk. The focus of these studies is typically the physical structure of the disk itself, and the torques exerted by the disk on planets. This approach is incapable of addressing a more complex dynamical interaction of bodies emerging in the disk. The second category consists in using a more efficient N-body integrator, but ignore the gas disk hydrodynamics and instead mimic the disk torques directly in the N-body integrator by adding artificial force terms. This approach is capable of generating insights into complex orbital dynamics involving a large number of bodies, including their close approaches, collisions, and orbital reconfigurations. Their interaction with gas is only approximate, because the hydrodynamical aspect of the system is only crudely taken into account.

**Approach** — We developed a new code that is capable of following a large number of planetesimals, planets, and pebble-sized bodies that form and dynamically evolve in a protoplanetary gas disk. The code is the most universal tool available in the planetary science community to study the early evolution of planetary systems. The scalability of the code was tested on NASA's Pleiades computer. Using a large number of CPUs it is now possible to follow the dynamical evolution of Earth-mass or more massive planets over a significant fraction of the gas disk lifetime.

**Accomplishments** — Figure 1 shows a preliminary test of the code, where 16 Earth-mass planets were seeded in the inner part of a protoplanetary disk. The gas disk was assumed to have an inner cavity near 0.15 AU. The system was integrated for 100,000 years with the new code. Early dynamical instabilities reduced the system to three planets with masses 4, 5 and 7 Earth masses, which remained stable for the rest of the simulation. The final orbital period ratios were 1.78 and 1.50, indicating a compact configuration that is reminiscent of the properties of the Kepler systems.

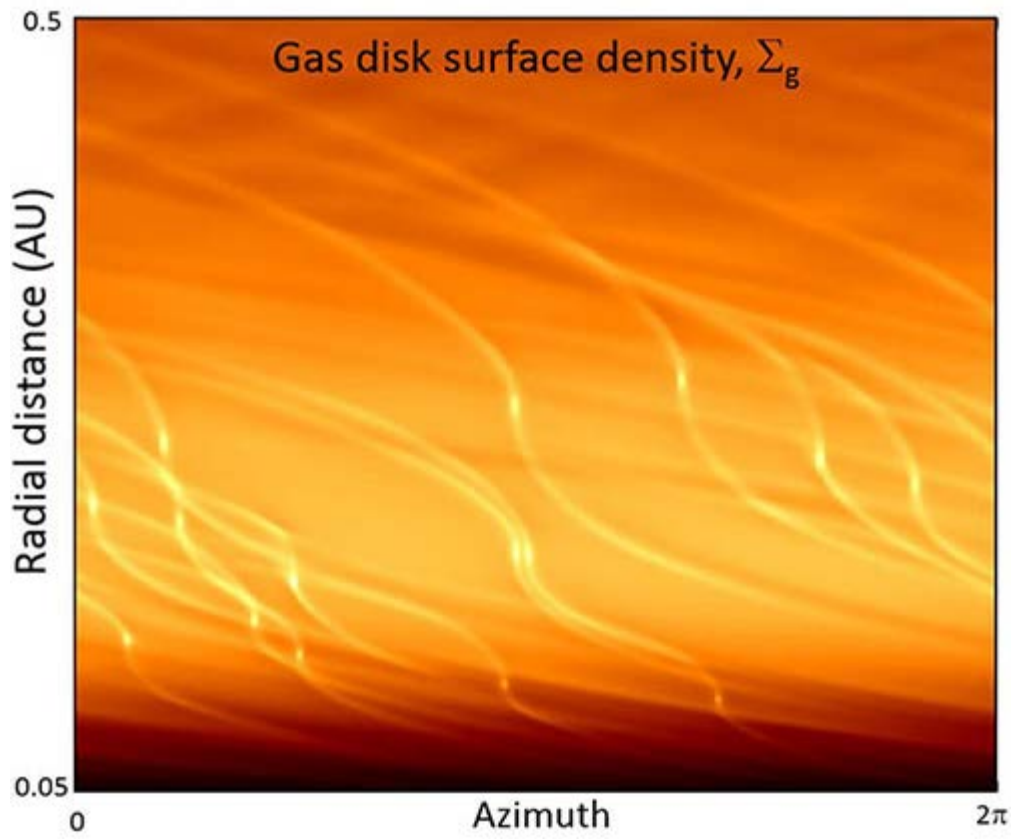


Figure 1: Inner part of a protostellar disk with embedded Earth-mass protoplanets.

## 2016 IR&D Annual Report

---

### Science Traceability Development and Engineering Trades in Preparation for a NASA Earth Ventures Instrument Proposal, 15-R8643

#### Principal Investigators

[Kathleen Mandt](#)

Alejandro Soto

Michael Davis

Mark Tapley

Adrienn Luspay-Kuti

Scot Rafkin

Inclusive Dates: 04/01/16 – 08/01/16

**Background** — SwRI is internationally recognized as a leader in instrument development for Earth and planetary missions. A prime example of this strong leadership is the ultraviolet spectrometer (UVS) program, which has four instruments currently in flight and two selected for flight on future missions. The reputation, experience, and technological capabilities developed under the UVS program place SwRI in a strong position to grow a parallel program of IR spectrometers that has a major science goal of meeting critical needs in Earth atmospheric science. The purpose of this project was to lay the foundation for a competitive NASA Earth Venture Instrument (EVI) proposal. The most critical element of a competitive instrument proposal is the science traceability matrix (STM). For NASA instrument proposals, the STM visualizes the flow of the proposed project from science goals and objectives to measurements that would be made to achieve the objectives. An effective STM clearly demonstrates that the instrument proposed for the project will meet the goals outlined in the proposal and provide scientific closure. The STM also drives the engineering requirements, and an early completion of the STM maximizes the time available to identify and then close technical trades with a robust and low risk implementation plan.

**Approach** — We divided the proposed work into seven tasks that describe a logical progression of activities necessary to achieve the goal and to produce the STM deliverables:

- Task 1 – Determine the highest value science that might be targeted by our instrument.
- Task 2 – Generate focused science goals that address the science identified in Task 1.
- Task 3 – Determine measurement requirements needed to address the science goals.
- Task 4 – Determine through iterative trade studies whether the instrument as currently designed or with reasonable modification can meet the measurement requirements, including adequate margin.
- Task 5 – Determine the operational requirements needed to achieve the science goals.
- Task 6 – Repeat Task 2–5 if necessary.
- Task 7 – Determine Command and Data Handling (C&DH) requirements.

**Accomplishments** — Under this project, we successfully developed a preliminary STM for the EVI proposal and an additional STM for another instrument development program announced by NASA after funding was approved for this project, the Instrument Incubator Program (IIP).

## 2016 IR&D Annual Report

---

### Capability Development for Astrobiological Research, 15-R8646

#### Principal Investigators

[Kathleen Mandt](#)

Walter Huebner

Amanda Bayless

Adrienn Luspay-Kuti

Joey Mukherjee

Edward Patrick

Inclusive Dates: 04/01/16 – Current

**Background** — Life precursors in the form of complex organic molecules have been discovered in molecular clouds around nearby young stars, inside meteorites, and in cosmic dust arriving at Earth from asteroids, meteoroids, and comets. Considerable international efforts in astrobiology are currently underway: (1) observationally with telescopic spectroscopy in various wavelength regions, (2) instrumentally with space missions to planets, comets, and asteroids, (3) laboratory simulations and experiments, and (4) theoretical model calculations using experimental and theoretical chemical reaction rate coefficients and other data. The objective of this project is to contribute to the fourth category of research by adapting and expanding an established complex model of the chemistry that takes place in the comae of comets to model chemistry in the solar nebula. The long-term goal is to determine how these complex organic molecules formed in the same conditions under which asteroids, meteoroids, and comets formed.

**Approach** — We have identified four technical objectives that will help us meet this goal and have divided the work into six tasks that target each of these objectives:

- **Objective 1:** Update the databases used by the model to include the necessary elements and molecules to simulate the production of complex organic molecules
- **Objective 2:** Update the existing model's computer program to handle the new species as well as the physical processes
- **Objective 3:** Update the model's computer program to simulate physical processes relevant to the production of complex organic molecules
- **Objective 4:** Validate the model by comparison with similar simulations

**Accomplishments** — During the first half of this project we worked simultaneously on Objectives 1-3 and made significant progress on each. We have begun to update the cross section database, PhIDRates, and the reaction rate database. We completed the process of including 18 chemical elements in the chemistry equation writer program and the coupled differential equation solver program and are currently testing the code to make sure it operates properly. We have begun research on the inclusion of gas-grain reactions in the model. Finally, we have determined the appropriate input parameters for model simulations and have prepared a series of points that are being used for testing the model. As this is an ongoing project, more work will be conducted over the next several months.

## 2016 IR&D Annual Report

---

### Understanding the Fluid Behavior of Planetary Regolith Materials, 15-R8651

#### Principal Investigators

[Danielle Y. Wyrick](#)

Hakan Başağaoğlu

Justin Blount

Alan P. Morris

Inclusive Dates: 04/01/16 – 04/01/17

**Background** — Common to all solid planetary bodies is surface regolith, unconsolidated material typically comprised of dust and broken rock fragments. On Earth, the regolith contains high amounts of organic material and biological weathering, and is subjected to effective aeolian and fluvial processes that serve to round individual grains and sort sediments by size. Less well understood is the behavior of regolith materials on airless bodies, where minimal erosional processes keep individual grains at a high degree of non-sphericity. Gully formations and fluvial-like features on the small asteroids Vesta and Helene have been attributed to several hypotheses, but none has explored the role of grain size and shape distribution on the dynamic and static behavior of the regolith on airless planetary bodies. Understanding the effects of grain shape and size has significance beyond geology, including targeted drug delivery. Recent advances at SwRI in multi-phase Lattice-Boltzmann numerical modeling, including simulating non-Newtonian fluids, suggests that 2D simulations of densely packed multiple angular-shaped particles is not only feasible, but may have wide ranging modeling applications in both geological and biomedical fields.

**Approach** — The objectives of this project are twofold: to understand how grain size and shape affect material properties such as cohesion, friction angle, and porosity, as well as dynamic behavior such as angle of repose; and to improve existing SwRI modeling capabilities of complex geologic and biologic problems by including arbitrary shape particles and Bingham fluid-flow behavior. Existing models have already been translated to allow for computational optimization of the code, including increasing the number of modeled particles, size, shape, and fluid type. Current upgrades to the Lattice-Boltzmann modeling approach, including non-Newtonian viscosities such as dilatant, pseudoplastic, and viscoelastic fluid flows, will be augmented with Bingham fluid capabilities, allowing for modeling of a wide range of conditions, from creeping (low Reynolds numbers) to moderately turbulent flow regimes.

**Accomplishments** — The project is currently in progress, with early experimental and modeling tasks completed. If successful, this new modeling approach would not only help resolve outstanding questions regarding the fundamental behavior of regolith materials on airless bodies, but more importantly, the increased modeling capabilities will allow for immediate applications toward the space science and biomedical fields.

## 2016 IR&D Annual Report

---

### Evaluating Performance Limitations of Novel Processing Techniques for Next-Generation Space Sensors, 15-R8653

#### Principal Investigators

[Miles Darnell](#)

Mike Koets

Jennifer Alvarez

Inclusive Dates: 04/01/16 – 04/01/17

**Background** — Within the past few years, SwRI has successfully entered new markets in applications involving high data rate (giga bits per second (Gbps)) signal processing and data management. New market opportunities center on the demand for sophisticated, high-performance signal processing systems for small spacecraft. The levels of complexity and performance required by these new applications significantly exceeds SwRI's current heritage with space-based signal processing systems. Emergence of new commercial space-qualified components has changed both the scope of what is practical for these applications and the approaches best suited to the implementation of these systems.

**Approach** — The investigation is exploring the use of modern, high-speed digital-to-analog and analog-to-digital converters and the latest space-hardened field programmable gate arrays (FPGA). These components are essential to many of the target applications. Recently developed converters provide extremely high sample rates (measured in billions of samples per second). Interfacing to these new converters presents fundamental new challenges both in the analog electronics associated with the converters and in the management of digital data streams. The feasibility of a novel FPGA-based interface architecture to support the high throughput of these converters is being modeled and analyzed. Assuming positive results, the architecture will be realized as new prototype hardware that will serve as a true measurement of performance and a proving ground for tailored high-speed processing algorithms.

**Accomplishments** — The novel architecture has passed through the modeling and analysis phase. Limitations of the architecture have been characterized. These limitations only narrow the range of applications for the novel architecture and in general prove the feasibility of the architecture. Analysis shows that meeting a throughput of 38.4 Gbps is feasible. Prototype hardware is being designed prior to fabrication. Presently the printed circuit board design is being modeled and simulated in detail for both signal and power integrity design correctness.

## 2016 IR&D Annual Report

### Capability Demonstration of Pluto Photochemical Modeling for NASA Planetary Data Archiving, Restoration, and Tools Proposal, 15-R8658

#### Principal Investigators

[Adrienn Luspay-Kuti](#)

Kathleen Mandt

Kandis-Lea Jessup

Vincent Hue

Inclusive Dates: 04/22/16 – 08/22/16

**Background** — The purpose of this project was to develop a photochemical model for Pluto's atmosphere to set the foundation of a critical part of a proposal submitted to NASA's Planetary Data Archiving, Restoration, and Tools (PDART) program. The recent flyby of the New Horizons spacecraft provided the first close-up view of Pluto's atmosphere, with critical details about its composition. New Horizons confirmed that Pluto's atmospheric composition (primarily nitrogen and methane) and chemistry is strikingly similar to that of Saturn's largest moon, Titan. Both atmospheres exhibit complex chemistry initiated by solar ultraviolet light, ultimately leading to the production of complex molecules and organic haze. Photochemical modeling is a powerful tool to better understand the physical and chemical processes at work in planetary atmospheres. In this project, we applied our team's extensive experience with Titan photochemical modeling to develop a state-of-the-art Pluto photochemical model based on the most recent New Horizons measurements.

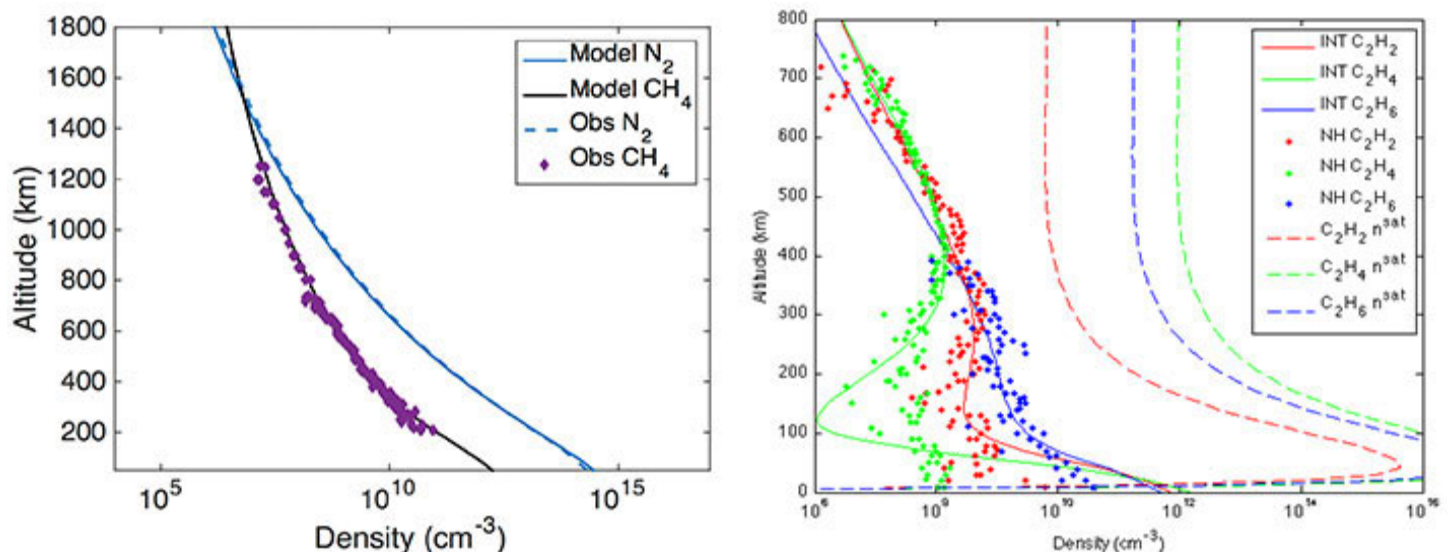


Figure 1: Comparison of Pluto model results to observations of the major (left) and minor hydrocarbon (right) species.

**Approach** — We adapted our existing and well-established in-house Titan photochemical model to Pluto's atmospheric conditions. We updated four key components of the model: the thermal profile based on the most recent New Horizons flyby measurements; photon absorption by updating the temperature-dependent high-resolution photoabsorption cross sections, chemistry by the incorporation of carbon monoxide, and the eddy diffusion profile. We then tested and validated our updated Pluto atmospheric

model until reasonable agreement with the New Horizons observations was achieved (Figure 1). Our results indicated that condensation and sticking to aerosols play an important role in Pluto's atmosphere, and the lower altitudes of the atmosphere cannot be appropriately represented with photochemistry alone. Thus, we incorporated condensation and aerosol sticking into the model.

**Accomplishments** — We successfully created a working, full-chemistry model of Pluto's atmosphere. Description of the Pluto model with preliminary results was included in a NASA PDART proposal, which was greatly strengthened by the efforts of this project. Through this project, we established credibility in modeling the atmosphere of Pluto, expanded our existing planetary atmospheric modeling program, and increased funding opportunity for upcoming NASA proposals.

## 2016 IR&D Annual Report

---

### Radiation Testing of a Commercial RF Agile Transceiver for Spacecraft Applications, 15-R8661

#### Principal Investigators

[Roberto Monreal](#)

Jim Hollen

Jennifer Alvarez

Inclusive Dates: 05/23/16 – 09/23/16

**Background** — Cost has become a key constraint in the space industry, pushing the market for small- and low-cost spacecraft and payloads. SwRI has developed radio hardware for specialized terrestrial applications using the latest advances in cellphone technology. Such radios are cross cutting into space-based applications. In particular, a radio frequency (RF) integrated circuit (IC), the Analog Devices AD9361, enables radios with very small size, low power, and high performance at a low cost. The radio subsystem satisfies key characteristics for low cost spacecraft radio frequency payloads, but the performance of the AD9361 in a radiation environment was unknown. While it is not necessarily suitable for every class of space mission, the performance, features, and cost of the AD9361 make it ideal for certain types of technology demonstration missions. The purpose of this project was to test the AD9361 under radiation conditions and assess the results against candidate mission scenarios.

**Approach** — The technical approach focused on conducting single event effects (SEE) radiation testing on several AD9361-equipped test boards. The test campaign was streamlined to focus on testing with heavy ions at Texas A&M University's Cyclotron Test Facility. This testing allowed characterization of the transmitter, receiver, and input power in response to increasing heavy ion linear energy transfer (LET) levels. The testing characterized the susceptibility to single event latch-up (SEL) plus "soft" failures in which the failure was able to be cleared by a device reconfiguration or re-initialization.

**Accomplishments** — The results are promising for the classes of mission that are being targeted for application of the AD9361. Of utmost importance is that the device did not experience SEL events up to an LET of 52 (MeV/cm<sup>2</sup>-mg). Additionally, the AD9361 was shown to be infrequently susceptible to SEE manifestations that do not damage the device and can be overcome by resetting or re-initializing the device, or rewriting the configuration to the device. Calculations using orbit and radiation prediction tools show that this would happen at a rate of approximately one or two failures per 10 years for candidate orbits. An operationally acceptable mitigation for targeted missions would be to reset or reprogram the AD9361 every few weeks.

## 2016 IR&D Annual Report

---

### Constant Pressure Stratospheric Balloon (CPSB), 15-R8663

#### Principal Investigators

[William D. Perry](#)

Ethan Chaffee

Inclusive Dates: 05/23/16 – Current

**Background** — Stratospheric balloons are used for a wide range of science, military, and commercial applications. In many of these applications, flight durations of days or weeks are needed. These balloons provide a platform to support instruments, surveillance, and communication systems above most of the Earth's atmosphere, providing clear view of the sky and a wide view of the Earth. Constellations of balloons can provide communications and internet service to large areas of the world that presently do not have the needed telecommunications infrastructure.

This project investigates a concept for a novel new constant pressure stratospheric balloon system. Presently, there are two basic types of stratospheric balloons, zero pressure and super pressure. Zero-pressure balloons are cost effective and reliable, but the flight duration is limited. Super-pressure balloons provide long-duration flight, but are much less reliable and must be fabricated from expensive, very high strength material.

The CPSB (constant pressure stratospheric balloon) concept uses a dual gas methodology to produce a balloon design that has the advantages of both zero-pressure and super-pressure balloons. This dual gas balloon system allows for extended constant altitude flights, since the need for expendable ballast is eliminated, while maintaining a very low differential hull pressure and keeping the hull volume constant. The sealed, low pressure hull design is made of low cost, ductile polyethylene film filled with helium or hydrogen. It has an internal ballonet that can be filled with a refrigerant like ammonia, butane or propane. The refrigerant in the ballonet would be in a gas form, while reserve refrigerant would be stored in a liquid state. The balloon would be filled with just enough lifting gas to completely fill the hull at the maximum expected gas temperature at the target altitude. At night when the lifting gas cools and contracts, refrigerant gas would be released into the ballonet to maintain the volume of the balloon. Since the mass and the volume are unchanged the balloon system will not lose altitude during the night. In the morning when the lifting gas temperature starts to rise, the refrigerant gas is removed by condensing it to a

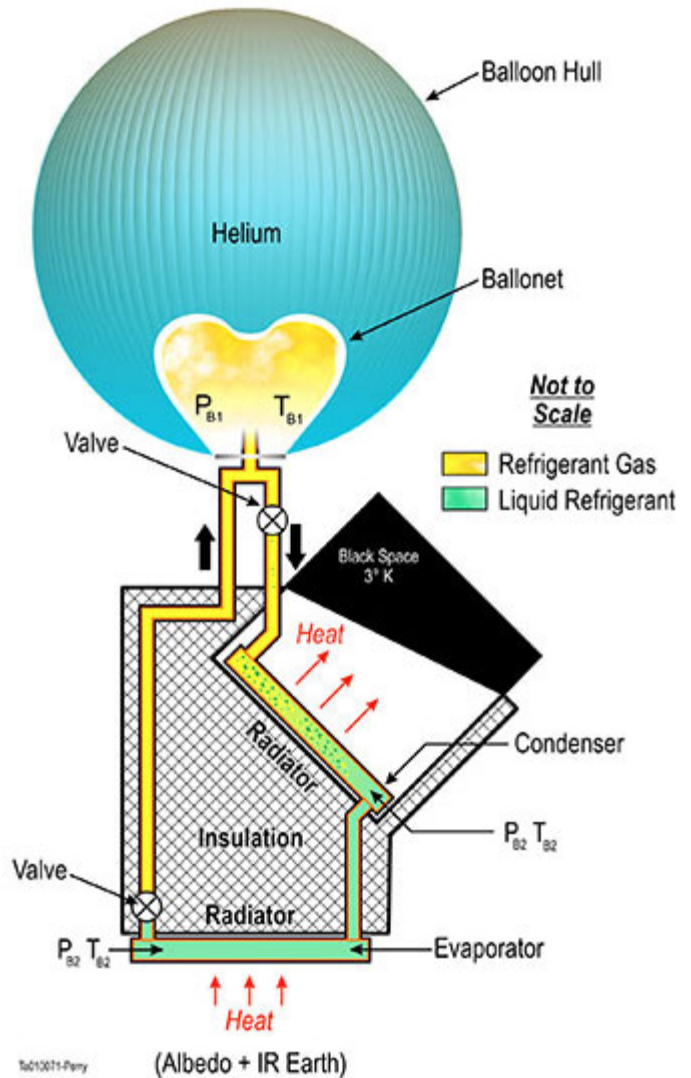


Figure 1: Constant pressure stratospheric balloon concept

liquid state. By using a combination of a condenser that radiates heat to "black space" and an evaporator that radiates to the "surface of the Earth," little or no electrical energy will be needed. The block diagram illustrates the concept configured to use butane as the refrigerant gas, which can be condensed without additional compression.

**Approach** — To achieve the project objectives, the following tasks were required:

- define the performance requirements for a CPSB
- develop a detailed thermal model of the proposed concept using Thermal Desktop® analysis software
- evaluate different refrigerant gases (ammonia, Freon, propane, etc.) and system configurations to determine which combination produces the optimum performance
- based on the thermal analysis results, determine the size of the condenser and evaporator radiators needed for a specific configuration and refrigerant gas to be used in the design of a prototype, suitable for demonstrating the concept.

**Accomplishments** — During Phase 1 of this project, the team defined the CPSB performance requirements and specifications, created a thermal model of the proposed system and evaluated a number of configurations using candidate refrigerant gases. Based on the results of this model, the size and mass of the required closed-loop refrigerant assembly was determined. Many candidate refrigerant gases were eliminated during this evaluation, but ethane, propane, and butane all proved to be feasible. This investigation found that a closed-loop refrigerant system using ethane as the refrigerant will have the lowest mass, resulting in a greater percentage of the CPSB total mass being available for the user payload.

The team evaluated several different possible design configurations for implementing the concept. While all appear to be achievable, a configuration using ethane was selected to be the basis for the prototype CPSB design planned for the second phase of this project. Based on the successful Phase 1 results, the team is proceeding with Phase 2, Design of a CPSB Prototype.

## 2016 IR&D Annual Report

---

### **Extension of SwRI's High Resolution Visible-Band Spectrometer into the Shortwave Infrared, 15-R8666**

#### **Principal Investigators**

[Peter W. A. Roming](#)

Michael W. Davis

Lindsay L. Fuller

Robert A. Klar

Christopher C. Mangels

Inclusive Dates: 06/13/16 – 10/13/16

**Background** — Methane is one of the most important greenhouse gases in the Earth's atmosphere. It is produced by both natural and anthropogenic sources, but it is uncertain how the contribution of these sources is changing over time. These uncertainties create challenges for developing strategies to deal with climate change. Because of its increasing abundance and strong warming potential, NASA has become more and more interested in small, lightweight instrumentation to make greenhouse gas measurements.

**Approach** — The overall objective of this project was to take our compact high-resolution visible-band spectrometer (CHiVeS) and outfit it with an infrared (IR) detector that is sensitive to the atmospheric spectral absorption wavelengths of methane and other greenhouse gases, and develop a tabletop version of our Hi-Resolution Infrared Spectroscopy Experiment (HiRISE) and determine performance.

**Accomplishments** — We divide our accomplishments into seven tasks that describe the logical progression of activities necessary to demonstrate the performance of HiRISE.

- We modified the optical design of our existing CHiVeS to use an IR instead of a visible detector. The modified design also accommodates the inclusion of a gas cell for greenhouse gas simulation.
- Modified our IR detector camera system to accommodate full spectral dispersion illumination of the IR detector.
- Used appropriate narrowband filters instead of a flight dichroic.
- Installed stray light covers, baffles and filters around/in the new optical path as needed to reduce background/photon noise.
- Measured the emission profile of various noble gases.

## 2016 IR&D Annual Report

---

### **Integrating SwRI Mass Memory Technology into a Focal Plane Array System, 15-R8669**

#### **Principal Investigators**

[Miles Darnell](#)

Mike Koets

Jennifer Alvarez

Inclusive Dates: 06/20/16 – 10/20/16

**Background** — A large aerospace company invited SwRI to participate in a strategic opportunity to showcase SwRI memory storage technologies for space applications. The company will be hosting an end-to-end demonstration of an all-digital, large-format focal plane array with imaging optics and back-end electronics to several clients. The demonstration will capture large-format focal plane data at video rates, store it to SwRI mass memory, and then play it back to visual displays for demonstration purposes. Such a demonstration will greatly retire technical risks in the minds of these customers and prove that the large aerospace company and SwRI have a proactive working relationship and compatible technology.

**Approach** — The technical activities of this project involved modifying an SwRI mass memory system to be compatible with a particular set of electronics for an imaging system. Upon detailed analysis of the imaging system electronics, changes to SwRI's system included data protocol, data rates, oscillator changes, and system hardware and firmware associated with oscillator changes.

**Accomplishments** — Each of the changes was implemented and successfully tested against jointly developed specifications. The next step, beyond the scope of this project due to the availability of the company's system, is to test with the imaging system electronics. The primary benefit of this project was to establish a collaborative relationship, not just a supplier-buyer relationship. Further, this project positioned SwRI to offer memory systems for space applications that are compatible with this hardware, which is a significant risk reduction activity for future proposals.

## 2016 IR&D Annual Report

---

### Testing Graphene Foils in a Space Plasma Instrument, 15-R8674

#### Principal Investigators

[Frédéric Allegrini](#)

Robert Ebert

Greg Dirks

Stephen Fuselier

Roman Gomez

Tim Orr

Paul Wilson

Inclusive Dates: 07/01/16 – 06/30/17

**Background** — In this project, we will test graphene foils in a space plasma instrument to increase their technology readiness level (TRL). Foils, until now made of amorphous carbon, are used for coincidence and time-of-flight (TOF) measurements. The interaction of particles with the foil results in multiple processes, which either enable or negatively affect the measurement. For example, the (1) particle-induced secondary electron emission enables coincidence and time-of-flight measurements, and (2) the particle charge state modification enables detection and measurement of energetic neutral atoms (ENAs). However, (3) the angular scattering perturbs the particle trajectory and may result in particle loss in the detector, and (4) the energy straggling reduces the particle energy. Processes 3 and 4 scale with foil thickness, while 1 and 2 are at most marginally affected by it. Thus, using the thinnest practical foil is always a goal. Current state-of-the-art carbon foils are upwards of about 9-nm thick.

Recently, the emergence of graphene (single atomic layer of carbon, 0.345-nm thick) has opened the possibility to reduce the foil thickness and, thus, tremendously advance foil performance by reducing angular scattering and energy straggling. In fact, we showed in recent studies (partially funded by SwRI and a NASA grant) that graphene foils outperform carbon foils in angular scattering by a factor of 2 to 3. Graphene foils could therefore replace carbon foils in future space plasma instruments.

**Approach** — We divided the project into three objectives:

- perform environmental tests on graphene and carbon foils by themselves
- compare the performance of graphene foils with carbon foils in an instrument with time-of-flight
- perform environmental tests on graphene and carbon foils in an instrument

**Accomplishments** — We manufactured and delivered our foil holders to Texas State University for the transfer of graphene foils. In parallel, we established a baseline of the performance of a space plasma instrument that contains carbon foils. Later, some of those foils will be replaced with graphene foils. We also designed and manufactured the fixtures.

## 2016 IR&D Annual Report

---

### Technology Development for Next-Generation Neutron Detector for Space Exploration, 15-R8675

#### Principal Investigators

[Bent Ehresmann](#)

Keiichi Ogasawara

Donald Hassler

Kelly Smith

Glenn Laurent

Inclusive Dates: 07/01/16 – Current

**Background** — The purpose of this project is to develop technology that allows us to reduce the mass and size of an existing SwRI-developed neutron detector for use in future lunar, near-Earth asteroid, and near-Mars space missions. One of the greatest risks associated with human space exploration remains the radiation doses astronauts are exposed to outside of Earth's protective atmosphere and magnetic field. A significant part of this radiation comes from neutrons that are created by interactions of high-energy Galactic Cosmic Rays (GCRs) and nuclei of the soil of extraterrestrial bodies, or spacecraft material. Neutrons, in particular, are of special concern because shielding against them is hard to accomplish with conventional shielding materials, and these neutrons can then interact with the human body.

In recent years, SwRI has developed and successfully flown state-of-the-art space radiation detectors, including the first-ever instrument to directly measure radiation on the surface of another planet – the Mars Science Laboratory/Radiation Assessment Detector (MSL/RAD). However, further improving these highly successful technologies is essential to maintain SwRI's status as one of the leaders in the field of space radiation detection. Volume and mass of an instrument are critical selection criteria for space missions. The research conducted in this project will help minimize the accommodation requirements of the instrument, and, thus, increase the chances of successfully proposing SwRI instrumentation for future human space exploration missions.

**Approach** — Our approach to minimize the instrumentation is to replace the comparatively large-sized read-out detector of our neutron detector with a smaller-sized read-out while maintaining the current neutron detection capabilities. We are analyzing if either Avalanche Photodiodes (APDs) or Multi-Pixel Photon Counters (MPPCs) can be used for this purpose. While these detectors have been previously proposed to and successfully flown in other spaceflight opportunities, they have not yet been tested with our neutron detection instrumentation. Thus, to raise the Technology Readiness Level (TRL) to an acceptable level – an important selection criterion for space agencies – we intend to test the new detector assembly in relevant neutron environments and assess its performance. Once successfully proven that the new assembly can maintain the existing neutron detection capabilities, we will optimize the mechanical design of the new package to minimize volume and mass.

**Accomplishments** — This project was only recently initiated (07/01/16) and is still in the first stages of the scheduled activities. Currently, the APDs and MPPCs are being prepared for a final evaluation that will allow us to decide between the two technologies.

## 2016 IR&D Annual Report

---

### Assessment of Thermal Fatigue in Light Water Reactor Feedwater Systems by Fluid-Structure Interaction Analyses, 20-R8434

#### Principal Investigators

[Debashis Basu](#)

Kaushik Das

Mohammed Hasan

Inclusive Dates: 12/13/14 – 12/15/15

**Background** — In a nuclear power reactor, thermal striping, stratification, and cycling take place as a result of mixing pressurized hot and cold water streams. The fluctuating thermal load generated by such unsteady mixing can result in fatigue damage of the associated structures. The mixing, which often is caused by faulty valves, potentially can affect safety related lines, such as the pressurizer surge line, emergency core cooling injection lines, reactor clean-up systems, and residual-heat removal systems. Generally, thermal fatigue is considered to be a long-term degradation mechanism in nuclear power plants. This is significant, especially for aging power plants. Therefore, improved screening criteria are needed to reduce risks of thermal fatigue and methods to determine the potential significance of fatigue. Although fluid mixing and thermal fatigue have been studied separately, a number of issues related to complex interaction between turbulent mixing and the mechanical structure of Light Water Reactors (LWRs) have not yet been resolved. Key uncertainties in this area include the effects of solid walls on variations in the thermal load amplitude and frequency (often referred to as filtering). These effects determine the temperature spectrum transmitted from the fluid to the structure. The primary objective of this project was to advance the use of numerical modeling techniques for reactor safety determination. This objective was achieved by developing a proof-of-concept benchmark simulation that demonstrates that computational methods can be used to resolve the turbulent mixing-induced thermal fatigue in the context of LWR operations.

**Approach** — The project used computational fluid dynamics (CFD) and numerical techniques to achieve the objectives. In particular, the modeling efforts primarily focused on:

- Using CFD tools to resolve the turbulent thermal mixing process to have accurate knowledge of the thermal processes in the fluid field
- Performing conjugate heat-transfer (CHT) calculations within the fluid and surrounding solid structure to obtain a realistic estimate of the fluctuating heat load to the solid and assess the effect of a solid wall on thermal load modification
- Evaluating thermal stresses
- Estimating the structural fatigue based on the calculated thermal stress using an analytical approach

The methodology comprises several steps. Initially, the flow field is calculated using a CFD solver. The flow solution is then compared against available experimental data for model confidence evaluation and benchmarking. Subsequently, temperature fluctuations on the structure are calculated using a CHT solver and the thermal stresses are calculated from the temperature fluctuations. The CHT analysis is used to predict fluid field and solid thermal fluctuation. The approach involves coupling the fluid and solid domains to predict the thermal stress generated by the thermal turbulence mixing phenomena. In this approach, the fluid field is modeled with the temperature dependent incompressible Navier-Stokes equations. Turbulence is simulated using the standard Smagorinsky sub grid scale large eddy simulation model. The heat

equation is used to model heat transfer in the piping system. For thermal fatigue analysis, the temperature, thermal stress, and stress intensity factor are calculated separately. These variables are used to find the structure degradation (number of cycles to failure and crack length propagation) by applying fatigue crack propagation correlation.

**Accomplishments** — Numerical simulations of the T-junction experiment carried out at the Älvkarleby Laboratory of Vattenfall Research and Development AB were performed to validate the numerical simulation results. Excellent agreement was achieved between the simulated results and the experimental data. A technical paper was presented in June 2015 at the American Nuclear Society annual meeting in San Antonio, and another paper was presented in November 2015 at the American Society of Mechanical Engineers International Mechanical Engineering Congress and Exposition conference in Houston. A MATLAB® code has been developed for the fatigue analysis. The project developed a robust integrated computational methodology to assess thermal fatigue damage in T-junction configurations that involve mixing of hot and cold fluids. Two reduced-order models, proper orthogonal decomposition (POD) and dynamic mode decomposition (DMD), were used to capture the coherent structures and turbulence scales. Two MATLAB codes were developed for the POD and DMD analyses.

## 2016 IR&D Annual Report

---

### Evaluate Atmospheric Microbiologically Influenced Corrosion Effects for Extended Storage of Spent Nuclear Fuel, 20-R8660

#### Principal Investigators

Xihua He

Amy De Los Santos

Inclusive Dates: 05/09/16 – 09/09/16

**Background** — The objective of this project was to develop methods to evaluate atmospheric microbiologically influenced corrosion (MIC) and its effects on dry storage systems (DSSs) during extended storage of spent nuclear fuel (SNF). At operating and decommissioned reactors in the United States, SNF can be stored in sealed DSS, where carbon steel and stainless steel are the commonly used materials. Under some atmospheric environmental conditions, an aqueous solution supporting microbial activity can develop on the DSS surface. It is uncertain, however, whether the microbial activity can lead to corrosion and if this corrosion mechanism can adversely affect any important-to-safety function during extended operation.

**Approach** — Experiments were conducted to evaluate MIC under low and high relative humidity (RH) conditions considering DSS relevant environments, defined by ranges of temperature, salt concentration, and RH of the surrounding air. Carbon steel and Type 304 stainless steel coupons and multielectrode array sensors loaded with different media were exposed to air in an environmental chamber, at controlled temperature and RH, to detect corrosion. Test media used were clean sand, field sand, simulated sea salt, soil, soil inoculated with aerobic bacteria, and a mixture of simulated sea salt with soil inoculated with aerobic bacteria. *Bacillus licheniformis*, a halotolerant, thermophilic bacterium, was selected for inoculation of some of the test media. All the tests were conducted at 50°C, and the dry and wet conditions were achieved by setting RHs to 35 and 90 percent, respectively. The bacterial strains in the media during and after tests were analyzed to obtain colony forming unit (CFU) counts and compared to the counts before tests. At the conclusion of the tests, the metal coupons were examined under a microscope for evidence of MIC.

**Accomplishments** — Bacteria CFU counts before and after tests show that bacteria survived and thrived at the test condition of elevated temperature and deliquescent brine, even at 35 percent RH. Sea salt may have stimulated the growth of bacteria and development of corrosion reactions. Extensive corrosion was observed on carbon steel at dry and wet conditions where bacteria were present. The elongated corrosion feature and patches of localized corrosion on carbon steel shown in Figure 1(a) were observed to correspond to high bacteria CFU counts in the test media and, consequently, may have been associated with MIC. Pitting of stainless steel was observed in simulated sea salt and other media with CFU counts on the order of  $10^6$  and  $10^7$ . Pitting of stainless steel was most severe in the media of soil mixed with sea salt inoculated with the selected bacteria as shown in Figure 1(b), suggesting synergism of sea salt and bacterial activity.

Localized corrosion activity also was monitored from carbon steel and stainless steel sensors loaded with soil inoculated with the selected bacteria. A combination of bacteria CFU counts before and after tests, microscopic evaluation of corrosion coupons, and sensor monitoring was effective in evaluating atmospheric MIC and its effects. Because of the ubiquitous nature of microbes and evidence of some MIC shown in this work, it is possible that aerobic microbes could exist in deliquescent solutions formed on DSS under atmospheric environments at elevated temperatures and enhance corrosion. The extent and

possible safety significance of MIC, however, would depend on the actual environmental conditions, especially the temperature, RH, radiation level, deposits on DSSs, and the variation of these conditions. Taking these observations into consideration, further study of the extent of corrosion associated with MIC is needed. Depending on the rate and extent of corrosion, consideration of MIC effects may be warranted for specific extended storage situations.

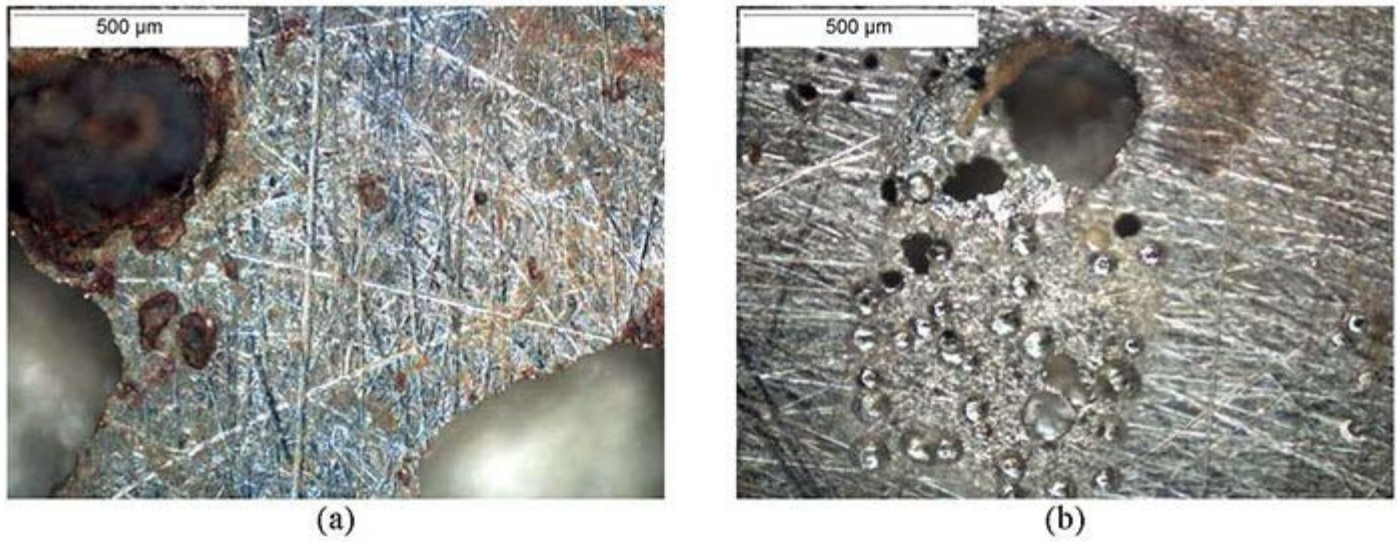


*Figure 1: Carbon (a) and (b) stainless steel specimens exposed to soil mixed with sea salt inoculated with bacillus licheniformis at 50 degrees C and 90 percent RH.*

## 2016 IR&D Annual Report

---

### Development of Computational Fluid Dynamics Framework for Characterization of High Energy Arcing Faults (HEAF) in Nuclear Power Plants, 20-R8680

#### Principal Investigators

Debashis Basu

Marc Janssens

Karen Carpenter

Inclusive Dates: 07/07/16 – Current

**Background** — A high energy arcing fault (HEAF) can occur in an electrical system or component through an arc path to ground or lower voltage, if sufficiently high voltage is present at a conductor with the capacity to release a large amount of energy in an extremely short time. Normally, HEAFs are caused by a failure within an electrical installation resulting from a defect, an exceptional service condition, or faulty operation. A HEAF is characterized by a sudden release of electrical energy through the air and the energy input from the arc to the air leads to a sudden pressure rise in electrical installations, followed by release of hot gases from the installations. This creates a hazard for the surrounding equipment, as well as nearby personnel. Because HEAF experiments are expensive, using computational fluid dynamics (CFD) to numerically simulate HEAFs is a viable and cost-effective analysis tool for determining the zone of influence (ZOI) of a HEAF for different types of high energy electrical cabinets. HEAF events initiate with an arc that heats and ionizes the surrounding environment to several thousand degrees, making it conductive; the temperature increases as a result of self heating induced by the current. Simulation of the HEAF phenomenon involves modeling the plasma-state gas as well as thermo-fluid analysis. The plasma-state gas has the electromagnetic force working on it, induced by the flowing current, in addition to the pressure and heat generation. The electromagnetic field significantly influences the overall flow and thermal field in the computational domain. This ongoing project is using existing commercially available CFD tools to develop a computational framework for numerically simulating the high-velocity mass and energy transport that occurs during HEAFs that pose a fire risk to nuclear power plants. The project also evaluates the feasibility of modifying existing CFD tools to accurately simulate the effects of selected HEAF events in nuclear power plants.

**Approach** — The project is using CFD and numerical techniques to achieve the objectives. In particular, the modeling efforts primarily are focused on:

- Set up a computational model framework to numerically simulate the pressure rise and energy flow of the hot gases due to a HEAF event in a high energy electrical enclosure.
- Determine how far the computational domain must be extended beyond the electrical cabinet to capture all targets that could potentially be damaged or ignited, and optimize the mesh to minimize impact on run time.
- Compute the thermal field within an enclosure with arc formation and also analyze the effect of arc on the temperature after the arc is extinguished.
- Compare two selected approaches for representing an electrical arc when simulating HEAF events. In the first approach, a simplified model based on experimental data will specify the open arc energy as a source term in the CFD calculations that calculate the pressure, velocity, and temperature responses. The more-detailed second approach involves coupled simulation of multi-physical fields related to the arc, using electromagnetic equations to calculate the Lorentz force, which in turn

provides a source term in the Navier Stokes fluid momentum equations. The two approaches are compared in terms of the predicted temperature and pressure within the compartment and the degree of agreement with the experimental results.

**Accomplishments** — Numerical simulations have been carried out for two geometries. The first geometry involved a box with an arc inside based on tests carried out at SwRI. The second geometry involved a distributed panel with bus bars. Excellent agreement was achieved between the simulated results and the experimental data for the thermal field and temperature. Project staff members were able to successfully couple the fluid dynamic solver with the electromagnetics solver to get an accurate estimation of the Lorentz force and electric field for realistic prediction of plasma characteristics. Preliminary results using this coupled model have been very promising and can be used to do detailed HEAF modeling in nuclear power plants.

## 2016 IR&D Annual Report

### Detecting Distracted Drivers Using Vehicle Data, 10-R8496

#### Principal Investigators

Adam K. Van Horn

David W. Vickers

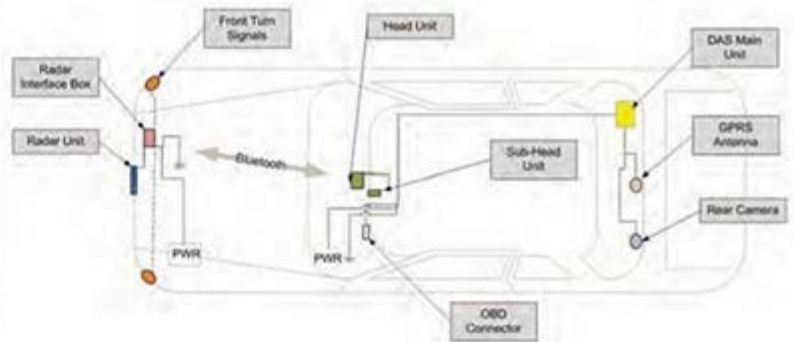
Michael A. Brown

Michael A. Dittmer

Inclusive Dates: 10/01/14 – 04/01/16

**Background** — The collection, refinement, manipulation, and analysis of large data sets are at the core of many business models today, with the increasing connectivity of people and devices. The rapid developments in active safety and connected and autonomous vehicles have greatly increased the volume of data produced on modern roadways. There are a number of organizations looking to leverage these new data sources in a myriad of ways, such as developing a deeper understanding of driver behavior. With an ever increasing rate of data generation, more and more organizations will be looking to employ data mining and machine learning to generate value from their data.

## SHRP2 Dataset



### Data Acquisition System Channels

- ◆ Multiple videos
- ◆ Machine vision
  - Eyes forward monitor
  - Lane tracker
- ◆ Accelerometer data (3 axis)
- ◆ Rate sensors (3 axis)
- ◆ GPS: latitude, longitude, elevation, time, velocity
- ◆ Forward radar
  - X and Y positions
  - X and Y velocities
- ◆ Cell phone
  - Automatic collision notification, health checks, location notification
  - Health checks, remote upgrades
- ◆ Illuminance sensor
- ◆ Infrared illumination
- ◆ Passive alcohol sensor
- ◆ Incident push button—audio (only on incident push button)
- ◆ Turn signals
- ◆ Vehicle network data
  - Accelerator
  - Brake pedal activation
  - Automatic braking system
  - Gear position
  - Steering wheel angle
  - Speed
  - Horn
  - Seat belt information
  - Airbag deployment
  - Many more variables

Figure 1: Example data streams of the second Strategic Highway Research Program (SHRP2).

**Approach** — The objective of this project was to evaluate the application of data analytic and machine learning techniques to vehicle behavior data sets to investigate the feasibility of detecting distracted driving. Data-driven methods are being investigated for predicting distracted driving using available data sources. This research focused on the case of an onboard diagnostic (OBD) and used internally generated data, such as on-board Global Positioning System (GPS), Inertial Measurement Unit (IMU) devices and video cameras. The data was analyzed in an automated fashion to detect events indicative of distracted driving. Patterns then were found in the data preceding these events using a variety of machine learning techniques. These techniques were first applied to high-level data sets to determine if there were any overall trends (e.g., standard statistical analysis) that indicated distraction.

Samples of data from individual vehicles and drivers were evaluated to determine more specific time-series-based indicators of distracted driving. This analysis included an evaluation of which sensors provided the most predictive power. The culmination of the previous research was the evaluation of data in streaming fashion. The focus of this stage was to evaluate whether it is feasible to detect, in real time, whether or not a particular vehicle is being driven by a distracted driver based on whether the vehicle is behaving in a way that usually precedes a distracted driving event.

**Accomplishments** — Time-series data consisting of both vehicle and driver, along with other pertinent data (i.e., event type, weather conditions, etc.) regarding 8,880 traffic events, was obtained from the Virginia Tech Transportation Institute from their second Strategic Highway Research Program (SHRP2), a naturalistic driving study (Figure 1). This raw data was cleaned, normalized, and loaded into a NoSQL data store. Initial analysis to determine those factors that are the strongest predictors of events was conducted leading to further exploration of the vehicle kinematic data and driver head position. Baseline models for driver gaze detection were established using data collected in SHRP2 and were evaluated for relative performance and accuracy. Additionally, clustering analysis (Partitioning Around Medoids) was used to determine if there were identifiable groups in the samples for the vehicles X, Y, and Z accelerations in the time-series data.

These analyses were combined to determine if the patterns discovered could be used to determine the near-future outcome of the vehicle (crash, near-crash, normal). Results indicated that these features alone were insufficient to predict whether a vehicle is about to be involved in the accident prior to driver intervention (e.g., application of brakes). Furthermore, issues were uncovered with the quality of the head position data generation algorithm, limiting the usefulness of this data. Further investigation is required with additional features to build a more complete and useful model of driver distraction.

## 2016 IR&D Annual Report

---

### LTE System Security Research, 10-R8505

#### Principal Investigator

[Brian Anderson](#)

Inclusive Dates: 10/20/14 – Current

**Background** — Cyber physical systems, which are expected to drive our future economy and to be critical to our national security, will need secure and reliable wireless communications. Cellular communications systems have very broad coverage and fourth-generation (4G) long-term evolution (LTE) cellular technology has excellent bandwidth and low latency. Localized or personal cellular access points that may be deployed inside a home, office building, or crowded event venue are expected to be very popular in the future as cellular operators work to extend coverage, allowing more users to take advantage of cellular services in a congested or closed space. Cellular connectivity may replace or co-exist with Wi-Fi access.

However, small cheap base stations probably won't be painstakingly designed with security in mind and they will likely be affordable to hobbyists and "hackers." A hacked base station could be used to intercept communications, track users, or prevent users from connecting to the desired operator network. System designers want to know whether the LTE user equipment they may be embedding in their systems could be vulnerable, so this research investigated one aspect of LTE system security, the "rogue" base station.

**Approach** — This research project developed and tested a methodology for identifying suspicious or rogue LTE base stations. A couple of commercially available systems for detecting a rogue base station were announced after this research project was initiated, but these were only effective against 3G systems and not LTE systems. This project was broken into two phases: 1) a study phase to investigate LTE signal and protocol parameters for detecting a suspicious system and 2) a development and test phase to demonstrate parameter usage in algorithms designed to identify a suspicious base station.

**Accomplishments** — A number of LTE signal and protocol parameters were identified and incorporated into algorithms that could be used to identify a suspicious LTE base station. Laboratory-scale cellular systems were created that exhibited some of the suspicious parameters. Algorithms were developed and tested to ensure they could differentiate suspicious base stations from normal cellular base stations, and a cell phone application that incorporated some of the algorithms was developed and demonstrated.

## 2016 IR&D Annual Report

---

### Platform-Independent Evolutionary-Agile Optimization, 10-R8536

#### Principal Investigators

[Phil Westhart](#)

Joel Allardyce

Inclusive Dates: 03/03/15 – 12/03/15

**Background** — GPUs have become more readily available as computational processors. Several languages and toolboxes have emerged to allow for the end user to migrate code execution onto a GPU. However, these coding frameworks change frequently to keep pace with the rapidly evolving field of GPU technologies. The more stable OpenCL, an open source version of CUDA that is not bound to NVIDIA GPU execution, has released two major versions and two minor versions since its initial release in 2008. A GPU-based solution has already been implemented in similar code and seen 30x speedup in execution. This empirically demonstrated performance surge makes a GPU solution attractive as the focus of the optimization effort.

In this solution, a broad range of optimization techniques will be defined and categorized. These techniques will include GPU solutions, compiler solutions, and other optimization techniques as discovered. The techniques will be applied to the target problem in various experimental setups until an ideal execution environment is established.

**Approach** — The objective of this approach aims to identify a set of optimization techniques with configurable settings that can be adjusted in response to the current execution environment, enabling the software solution to easily be ported to next-generation execution platforms. While our approach will cover a range of optimization techniques, the primary focus will be placed on GPU execution. The GPU implementation will be implemented in OpenCL, rather than CUDA. OpenCL does not have any restrictions on target platforms, making it ideal for an evolutionary-agile, platform-independent solution. Platform independence allows the code to execute on any brand GPU, as well as any brand CPU if desired.

The approach will also contemplate compiler optimizations, including potential compilation migration to other code languages. The various FORTRAN and C compilers each have their own strengths and weaknesses. Consideration will be given to compilers that compile to an intermediate language prior to final compilation to machine code. A multi-step compilation process such as this allows the original code to stay in its native form while still receiving the benefits that a different source code language would offer.

Noticeably absent from this approach are algorithmic optimizations. The implementation of the algorithm was performed by the scientists who understand the science behind the math. Gross modifications of the source code in the name of efficiency hurt the ability of the scientists to expand upon the algorithm if desired. Since the long-term maintenance code will likely fall back on these scientists, leaving the source code in its original state allows for easy extension and maintenance where necessary.

**Accomplishments** — A variety of techniques for computational optimization have been developed. These techniques include compiler optimization flags, compile-time source code optimization, and run-time parallelization using CPU and GPU techniques. These techniques have successfully been applied to the planetary formation simulation challenge problem to yield speedups ranging from 2 times to 26 times faster. The speedup obtained shows a wide variety that corresponds to the degree to which a particular test set can be parallelized. The development of the techniques was completed with generalization in mind. To this extent, templates for the OpenCL implementation have been generated.



## 2016 IR&D Annual Report

### Computational Performance Enhancements via Parallel Execution of Competing Implementations, 10-R8537

#### Principal Investigators

David Vickers

John Harwell

Robert Klar

Sue Baldor

Ben Abbott

Inclusive Dates: 03/10/15 – 12/04/15

**Background** — The Lattice-Boltzmann Method (LBM) facilitates the analysis of fluid flows. It represents physical systems in an idealized way where space and time are discrete. It provides less computationally demanding descriptions of macroscopic hydrodynamic problems. Many of our clients have problems that are amenable to solution using the LBM. However, ongoing work on these problems suffers from overly long computational times for the simulation runs. This research took advantage of the availability of large numbers of processors to evaluate a speculative space of optimization techniques during the execution of simulation runs. A genetic algorithm (GA) approach was evaluated for the dynamic selection of an optimum implementation that efficiently executes the LBM algorithm to efficiently adapt to temporal phase changes in the simulation.

**Approach** — The objective of the project was to use first the Lattice-Boltzmann Method problem and then the Symplectic N-body Algorithms with Close Approaches (SyMBA) problem to evaluate the applicability of a GA approach to optimizing the performance of computationally intensive simulation code. To evaluate the applicability, a framework, PARADYNE, was constructed to facilitate experiments with parallel, dynamically changing code. The original code provided by the problem presenters was first analyzed and optimized using a base set of transformations to produce a baseline suitable for the specialized GA-focused research. The code was then marked up to allow PARADYN to experiment with a variety of possible variations on the construction of the code, the organization of the data, and the flags used to compile the code. A set of genes (ways to vary the code, data, and flags) were defined and the set of alleles to be used (specific variations on the genes)



Figure 1: Non-thermal fluctuation base optimization

specified. The framework was then used to execute multiple versions of portions of the simulation in parallel and to evaluate the performance of those portions. The framework was used to create new variations based on the best performing versions. The continual evolution of the versions being run allowed the simulation to eventually perform better than the baseline solution (Figure 1) and to adapt to changes in the state of the simulation (Figure 2).

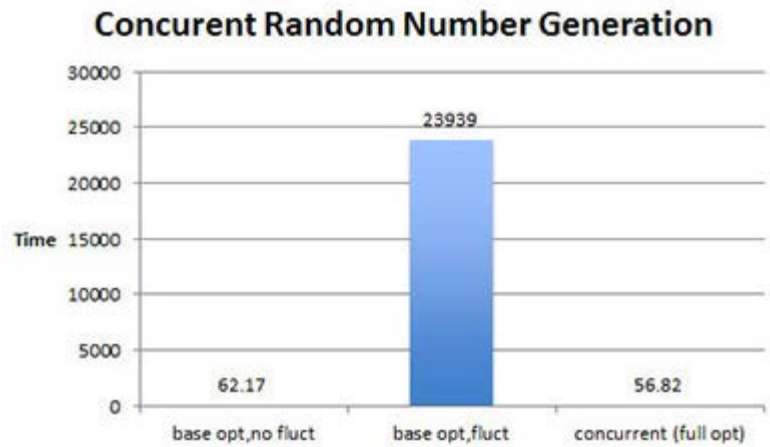


Figure 2: Thermal fluctuations and their optimization

**Accomplishments** — Baseline optimized versions of both the LBM code and the SyMBA code were created. Figures 1 and 2 show the improvements that were made during the base optimization phase of the LBM problem. As Figure 1 shows, up to ~2X speedup was achieved for non-thermal fluctuation problems. Figure 2 shows improvements made during the baseline phase for thermal fluctuation problems which in one case resulted in a speedup of more than 800X. Genes and alleles were defined for the LBM and the SyMBA code and the necessary plugins to the PARADYN framework were implemented. The LBM and SyMBA code was marked up for use by PARADYN. An example optimization run of the LBM code with PARADYN is shown in Figure 3. This figure demonstrates PARADYN's ability to dynamically adapt to changes in the simulation, as can be seen when the particles are released at  $t=10,000$ . Figure 4 illustrates PARADYN's ability to select increasingly optimized solutions as the simulation progresses, eventually reaching better performance than the baseline optimizations as evinced by the trend line. A comparison of the original code performance, along with the current PARADYN performance, is shown in Figure 5. A 5-8X speedup was achieved post base optimization for non-thermal fluctuation problems. The PARADYN framework was designed and implemented in a modular and reusable way that facilitated its use on both the LBM and the SyMBA projects.

### Benchmark Problem 2

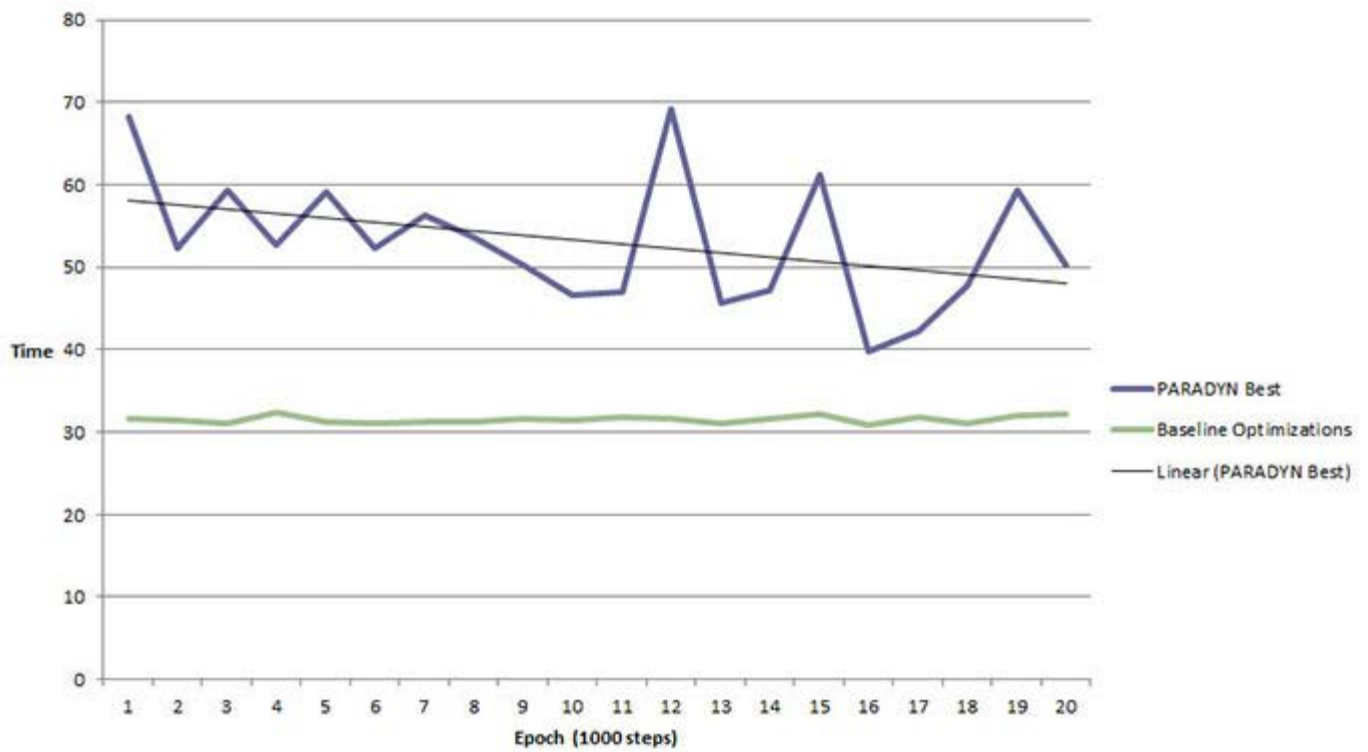


Figure 3: Responding to particle introduced in Epoch 11

### Benchmark Problem 2

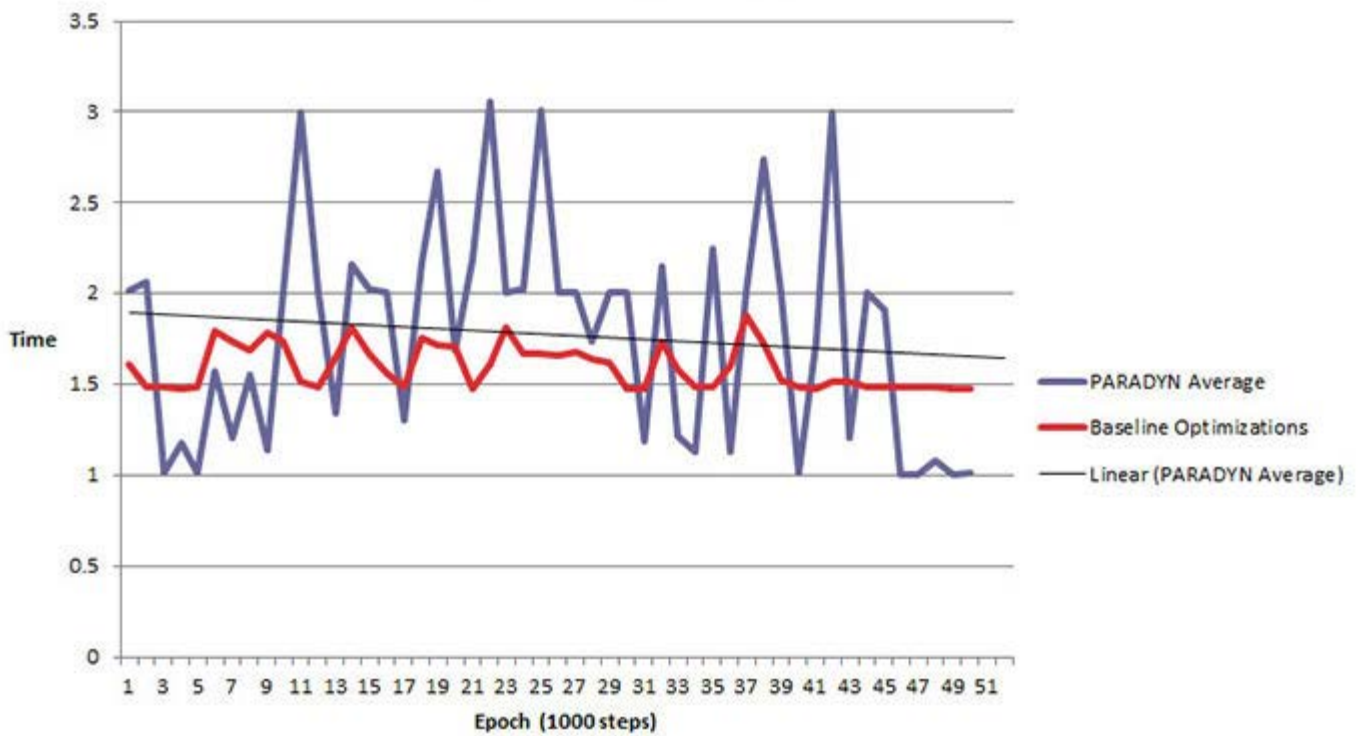


Figure 4: Finding better performance

## LBM Benchmark Times

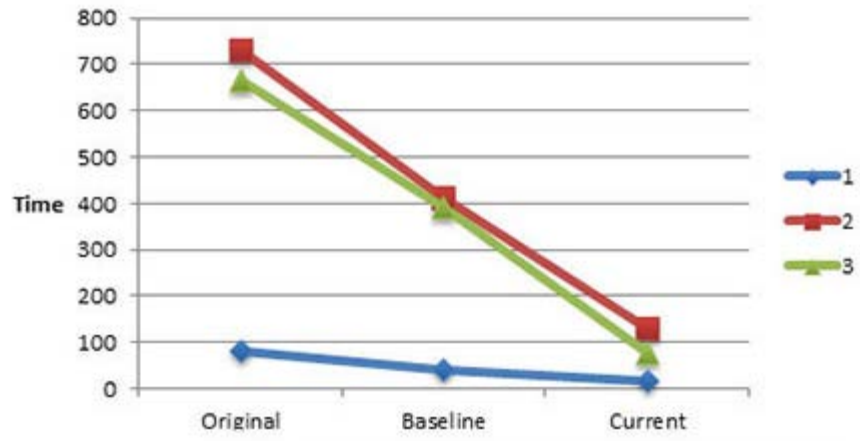


Figure 5: Baseline and GA-based improvement

## 2016 IR&D Annual Report

---

### **Code Generation and Planning Engine for Self-Tuning Runtime Optimization, Project 10-R8538**

#### **Principal Investigators**

[Sydney Whittington](#)

Adam Van Horn

Michael Dittmer

Paul Hoeper

Inclusive Dates: 03/10/15 – 12/04/15

**Background** — Faster computing opens new research areas as well as the potential for saving time and money. Programs can be "sped up" by enhancing hardware (clock speed, acceleration devices, etc.), software (better coding, compilers, etc.), algorithm choices (direct solution vs. approximation, etc.), or combinations of these three. High-performance computing has been used to model a large number of physical phenomena successfully: protein folding, ballistic simulations, cryptographic code breaking, etc. However, some problems remain intractable over reasonable time periods, such as modeling planetary formation over both short and long timescales with widely varying numbers of bodies, or 3D fluid flow modeling using the Lattice-Boltzmann method. SwRI has developed a solution to the planetary formation problem using symplectic N-body integration techniques. Additionally, SwRI has developed an implementation of this method for several fluid flow domains, biomedical and hydrological, at particle scales from nano to micro, and in both 2D and 3D. However, due to accuracy constraints and large dimensionality of the data, more complex simulations can take many months to run.

**Approach** — The techniques used in this research effort entailed the use of ROSE, a source-to-source compiler infrastructure, leveraging its Abstract Syntax Tree (AST) analysis and code translation capabilities. Using ROSE to apply a series of code transformations, the original source code is left untouched and new optimized source code is generated. A planning engine then evaluates the effectiveness of these transformations, allowing for the most-effective permutations on the current hardware to be used. Using the Intel Fortran compiler ifort, proven to generate the fastest executables, Profile Guided Optimization (PGO) capabilities were enabled, allowing the compiler to build on the transformations applied. Using these techniques, with their application to both the planetary formation problem and the Lattice-Boltzmann problem, average performance of the target problems has increased by approximately 2.5 times to 7 times.

**Accomplishments** — At the conclusion of the project, several tools have been acquired to better position SwRI for future optimization efforts. Compiler-based optimization techniques have been acquired, and avenues for further development efforts have been discovered. Expertise has been developed throughout the entire computational optimization process, including profiling applications, introducing compilation level optimizations, and exploiting specialized hardware for run-time execution optimizations. Investments in specialized optimization hardware on behalf of SwRI were undertaken. All of these combined result in a strong knowledge and resource foundation well-suited to further optimization projects.

## 2016 IR&D Annual Report

---

### **Automated Detection of Small Hazardous Liquid Pipeline Leaks, 10-R8552**

#### **Principal Investigators**

Maria S. Araujo

Daniel S. Davila

[Samantha G. Blaisdell](#)

Sue A. Baldor

Shane P. Siebenaler

Edmond M. DuPont

Inclusive Dates: 04/01/15 – 09/30/16

**Background** — The prevailing leak detection systems used today (e.g. computational pipeline monitoring) are unable to detect small leaks (<1 percent of the line throughput) or trigger a high number of false alarms. The latter is a major industry concern, as it leads to alarms being ignored, resulting in leak detection systems that are ultimately ineffective. The focus of this research was to detect small pipeline leaks while also characterizing and rejecting non-leak events to significantly reduce false positive rates.

**Approach** — The objective of this project was to develop and evaluate a technology that can be suitable to meet the goals set by the Pipeline Research Council International (PRCI) for small liquid leak detection:

Detect small leaks (1 percent of line throughput) in less than five minutes, with 95 percent confidence level, under all operating conditions (i.e. steady-state, pump start/stop, line pack, take-offs, etc.).

The approach focused on fusing input from different sensors in a variety of combinations (hyperspectral, infrared, and visual), and using feature extraction, classifier techniques, and deep machine learning to identify unique features that could provide a more reliable "fingerprint" of not only small liquid leaks, but also non-leak events in a variety of operating conditions to substantially reduce false positive rates. Leaks considered in this research included crude oil and refined products such as diesel, gasoline, and jet fuel, which covers a large percentage of hazardous liquid pipelines in the U.S. Leaks and non-leak events were simulated in various lighting and weather conditions to accurately characterize the signatures of leaks and non-leak events.

**Accomplishments** — Small leaks were simulated using various fluids (mineral oil, gasoline, diesel, crude oil, butane, nitrogen, methane, ethylene, and water) on a variety of representative surfaces (concrete, sod, gravel, and dirt). All imagers recorded data simultaneously to allow for constructing registered images using data from all or a subset of the sensors. Scenarios that could trigger false alarms (i.e. non-leak events) were also simulated and characterized. Focus was given to highly reflective and highly absorbent materials/conditions that are typically found near pipelines such as water pools, presence of highly-reflective surfaces (e.g. insulation sheeting on pipes), and concentrated zones of heat (e.g. from the sun and other warm fluids).

Feature extraction was performed using both spectral and spatial information which was then analyzed using algorithms including statistical features, local binary patterns (LBP), textons, and raw color features (RGB, HSI, and lab color spaces) based on the sensor type. Statistical classifiers such as State Vector Machine and Extreme Random Forest were applied, along with advanced deep learning neural network techniques, including the Convolutional Neural Network. The results demonstrated a set of technologies

and techniques that can be applied to successfully detect and identify hazardous liquids while also correctly defining non-leak events.

---

[2016 IR&D](#) | [IR&D Home](#)

## 2016 IR&D Annual Report

---

### Select Superoptimization of Finite Element Analysis Tools, 10-R8563

#### Principal Investigators

[Stephen A. Kilpatrick](#)

Alex G. Youngs

Joel B. Allardyce

Stephen R. Beissel

Ben A. Abbott

Inclusive Dates: 06/24/15 – 03/04/16

**Background** — Some of the following problems are most cost-effectively solved using Finite Element Analysis (FEA):

- Characterizing the ballistic limit of armored plating and composite fabrics
- Characterizing the performance of armored vehicles under blast and ballistic loads
- Characterizing the ballistic limit of materials with complex geometries

Ongoing work on these problems suffers from overly long computational times for the simulation runs. Significant additional project efforts would likely be funded if the simulation runtimes could be reduced by an order of magnitude. SwRI currently has two methods of modeling these problems: an externally available commercial software product and internally developed software. Due to processing limitations, both modeling methods can only be employed on panels of extremely limited size. The desire is to achieve significant optimization of both sets of software to enable the simulation of more realistic panel sizes.

**Approach** — Super-optimization is the task of finding the optimal code sequence for a single, loop-free sequence of instructions. This effort attempted to apply super-optimization techniques to specific functions to significantly increase the performance of the overall program. Initially, a set of basic optimization techniques were applied to the solution to provide a baseline set of performance enhancements. Once the baseline performance enhancements were made, the application of super-optimization was performed on selected hotspot functions in the code. Automated scripts were developed to benchmark and profile the two software products across a variety of input data sets.

**Accomplishments** — Several techniques were developed to better position SwRI for future optimization efforts. Expertise has been developed throughout the entire computational optimization process, including profiling applications, introducing compilation level optimizations, and exploiting super-optimization techniques. All of these combined resulted in a strong knowledge and resource foundation well-suited to optimization projects in the future.

## 2016 IR&D Annual Report

---

### Subtle Anomaly Detection in the Global Dynamics of Connected Vehicle Systems, 10-R8571

#### Principal Investigators

[Adam K. Van Horn](#)

Brian K. Anderson

Michael A. Brown

Paul A. Avery

Inclusive Dates: 01/01/16 – 07/01/16

**Background** — Increasing connectivity among vehicles, roadside devices, and traffic management systems under the U.S. Department of Transportation (USDOT) Connected Vehicle (CV) program creates the potential for both novel benefits to society as well as novel risks. The vulnerability of individual vehicles to targeted disruption has increased as their control systems and even their entertainment systems have shifted towards computer control. This is compounded as vehicles begin receiving and acting upon messages within a CV system.

The USDOT is actively funding research into the security algorithms, protocols, and procedures needed for the unique aspects of emerging vehicle and highway system technologies. The concept of security for automated vehicles, especially ones that are connected to other information sources via over-the-air (OTA) messages, must go beyond message *authentication* to consider the broader issue of message *trust* by using a multi-factored approach. The global dynamics of a system comprises individual and independent entities emerging as a result of the interaction of the individuals over time. This project investigated the algorithms and methods required to detect subtle anomalies in the behavior of a connected vehicle system at the system level.

**Approach** — The project team built and verified a traffic model using a commercially available traffic modeling and simulation software package and real-world data from vehicle detectors along a 21-mile stretch of Interstate 4 provided by the Florida Department of Transportation (FDOT). The simulation model was used to develop and train an anomaly classifier, which detects anomalous behavior in the global traffic system with CVs present in varying proportions.

**Accomplishments** — The project team used processes from SwRI's Automotive Consortium for Embedded Security (ACES) to develop a security risk modeling tool to evaluate a number of potential CV traffic system threat scenarios. This evaluation was used to identify the most suitable scenarios for further simulation and analysis, with the primary scenario being creation or emulation of a "ghost vehicle" with an incorrect speed or heading. The team evaluated real-world data to determine appropriate time-varying traffic volumes for the simulation and built the simulation using the traffic modeling software.

The simulation was configurable to allow for varying degrees of CV "saturation," or the number of vehicles equipped with CV technology [broadcasting basic safety message (BSM) data] compared to the global system. In the simulation scenarios tested, a subtle anomaly was introduced into a traffic network during a high concentration of traffic, similar to congestion that might coincide with the morning commute. Assuming appropriate available throughput for this scenario, all vehicles would be able to travel along the route with minimal delay. Since the traffic network is capable of handling this number of vehicles per hour, introducing an anomaly that affects enough vehicles will result in a self-sustaining jam.

To determine the necessary CV penetration for an anomaly to affect the traffic network, simulations were

executed at varying percentages of CV penetration, with a subtle anomaly introduced into each scenario. CV percentages at 5, 10, 15, 25, 75, and 100 were simulated and evaluated. The results from the testing provide evidence that introducing a subtle CV anomaly into the vehicular network at low percentage of CVs will not result in traffic jams; however, the transition is very sensitive to the CV mix and transitions quickly from "no-jam" to "jam" between 10 and 15 percent. The effect of the traffic jam then becomes more pronounced as the CV percentage increases, to where 100 percent CV system reacts immediately to the injected ghost vehicle, and very quickly results in a large and persistent traffic jam.

## 2016 IR&D Annual Report

---

### Construction Equipment Operator Training Simulators Technology Update, 10-R8572

#### Principal Investigators

[Rolan Tapia](#)

Steven Mann

Brian Chancellor

Warren Couvillion

Inclusive Dates: 07/01/15 – 01/04/16

**Background** — SwRI's simulator product line currently includes operator training simulators (OTS) for five of the most common machines in the construction industry. These simulators, which have been used to train hundreds of excavator, four-wheel drive loader, motor grader, crawler/dozer, and backhoe loader equipment operators, continue to be a source of revenue in this growing industry. These simulators form the basis for a rapidly increasing number of near-term opportunities in the construction and other related industries (e.g., mining, agriculture, roads and reformation, and crushing and screening applications). A technology update is required to maintain the competitive edge needed to capitalize on these opportunities.

**Approach** — The primary objective of this project is to enhance the existing simulator architecture framework for increased modularity and extensibility to reduce the cost of current and future OTS development efforts. These enhancements will be foundational for updating SwRI's product line to state-of-the-art software/hardware for increased marketability and an increased competitive advantage. The approach includes simulation architecture analysis and associated design modifications, conversion from SwRI's 3D graphics rendering engine (Grail™) to a state-of-the-art gaming engine (Unity), and implementation of these technology updates to the existing excavator OTS.

**Accomplishments** — An analysis of the existing simulation architecture/framework identified areas where the simulation architecture could be modified and/or enhanced to reduce future development costs and risks. Software modularity and reuse was increased through common controls and user interface development, machine model encapsulation, controls familiarization template development and transition to the Unity graphics engine. Acquisition and implementation of a Unity plugin now allows for rapid remapping of controls for new hardware. Machine models have been encapsulated to facilitate reuse in multiple scenes, lessons, and applications. Grail to Unity design modifications are providing enhanced operator menus, increased functionality and expandability, and improved physics (e.g., more realistic resistance when digging through dirt). Incorporation of these technology updates into the existing excavator OTS is complete.

## 2016 IR&D Annual Report

---

### Assessing the Feasibility of Ranger in Kit Form, 10-R8590

#### Principal Investigators

Kristopher C. Kozak

Edward S. Venator

Inclusive Dates: 09/14/15 – 01/14/16

**Background** — Ranger is a high-precision localization system that has been under development since September 2011. Ranger has proven to be a powerful enabling technology for automated vehicles, and has become attractive to external organizations that are working in the field. Although Ranger has been well tested and demonstrated, it has primarily existed as a series of prototypes that have been paired with engineering-grade software. As a result, the transfer of Ranger technology to other organizations has generally required significant customization of hardware and software, and on-going user training and support. Such large efforts and secondary costs slow the use and adoption of Ranger technology, which is attractive in large part due to its relatively low hardware costs. These issues motivated the establishment of this project to better understand the feasibility of creating a Ranger kit that could bridge the gap between the highly technical and ongoing development work on Ranger that occurs at SwRI, and the technically capable researchers and early adopters in the field of automated vehicles that would like to use Ranger now.

**Approach** — The research approach taken to assess the feasibility of creating a usable Ranger kit was to first identify the elements of the existing prototype system (hardware and software) that most significantly affected cost, complexity, and/or time to implement and deploy. These elements were then assessed for the viability and impact of improvements that could be made as part of this project. The power and control box, and the mapping software presented problems that could most reasonably be addressed as part of this project to reduce cost and complexity, improve usability of the system, and greatly reduce the time to deployment of new systems. A new LED and camera power and trigger system was designed that integrated the functions that were originally handled by discrete components into a single 4.25- x 2.875-inch printed circuit board (PCB). The map creation functions were aggregated into a single graphical user interface that controls and shares system configuration between the essential functions of map recording, map assembly, optimization (after data is recorded), and map-based localization.

**Accomplishments** — There were numerous goals accomplished during the course of this project. Most significantly, the size and cost of the required hardware was significantly reduced, and the software for building maps was simplified and made more intuitive. Some specific improvements to the hardware include replacing numerous, large discrete electronic components with a single, compact PCB; reducing the number of electronics enclosures from two to one; decreasing the total volume of the enclosures from approximately 1065 cm<sup>3</sup> + 3530 cm<sup>3</sup> (4595 cm<sup>3</sup> total) to 575 cm<sup>3</sup>; cutting the cost of the power and switching electronics by roughly half; reducing the assembly time (including assembly of the associated enclosures) from several days to several hours; and increasing the output voltage range to handle new and legacy LED modules. Some specific improvements made to the mapping software include streamlining software for recording data and building maps; implementing a graphical user interface to simplify the map creation process and eliminate the need for the user to set and modify numerous parameters for each new map; streamlining the multi-step map creation process; integrating both on-vehicle data recording and map creation functions into the same tool; and providing a range of options for map data processing, from a fully automated process to a guided, multi-step process that gives the user fine-grained control over the map creation steps. As a result of these improvements, the manual configuration time was reduced from nearly

10 minutes for the prototype software toolset (per map for a skilled user) to several seconds and it was proven feasible to create a kit form of the Ranger technology.

## 2016 IR&D Annual Report

### Deep Learning System for Robotic Pick Selection, 10-R8600

#### Principal Investigators

Michael Rigney

Alex Goins

Johnathan Meyer

David Chambers

Inclusive Dates: 10/01/15 – Current

**Background** — Robotic sorting operations are challenged by the task of interpreting 2D/3D image data to identify a pick point within a pile of mixed product types (boxes, widgets, parts, bags). Varying object colors, labels, sealing tapes, decoration, and occlusions contribute to scene complexity. Perception systems are typically developed by exploring and selecting engineered feature detectors and machine vision algorithms to interpret sensor data. High-level results from feature extraction operations may be input to a machine learning algorithm for classification or ranking.

Deep Convolutional Neural Networks (DCNN) have recently attained top performance scores among machine learning paradigms, in image-based object recognition competitions, and similar challenges. DCNNs are composed of several CNN layers followed by a traditional fully connected neural network (FCN). Through a progression of layers, CNNs implement low-level feature detectors and produce higher-level abstract representations of the input data. Importantly, CNNs are trained from example data, alleviating the feature engineering burden of traditional perception solution development.

**Approach** — A DCNN development environment has been integrated with a robotic parcel sorting testbed, which includes 2D and 3D vision sensors (Figure 1). Trained DCNN's select a pick location, which is scored by the accuracy of robotic parcel placement at the work cell output conveyor. A database of 12,000 pick observations is used for offline training. During work cell operation, pick performance is used for continuous adaptive DCNN training.



Figure 1: Parcel sorting work cell with ABB robot, vacuum

**Accomplishments** — Pick performance of a range of DCNN architectures has been evaluated. Baseline architectures mirrored those used for image-based object recognition. Improved pick performance has been achieved from architectures with reduced capacity (fewer convolutional kernels) and by adding a deconvolution layer before the FCN. Alternate network inputs (2D and 3D data encodings) have been tested. Initial architectures provided the position coordinates for a single pick location. Current architectures provide a map that can identify multiple potential pick locations (with confidence score) within the robot workspace.

## 2016 IR&D Annual Report

---

### **Focused Automated Discovery of Telemetry Device Constraints, Project 10-R8626**

#### **Principal Investigators**

[Sydney Whittington](#)

Alex Youngs

John Harwell

Inclusive Dates: 01/25/16 – 05/25/16

**Background** — Configuring typical devices in the telemetry community requires the creation of complex, device-specific configuration files. These devices use the Metadata Description Language (MDL), the emerging industry standard grammar that was defined by SwRI on the integrated Network Enhanced Telemetry (iNET) program. While the grammar of the configuration files is vendor-neutral, the device specific details are vendor-specific. Thus, a naïve approach to building these files is to construct a file, test it against a device, and then iterate. The specification sheets (and other documents) for the device can serve as a guide, but the details of flight test configuration possibilities are immense and, in this community, typically not fully documented. Thus, making use of trial and error and smart users familiar with the devices is the standard practice. Knowing this, we previously developed an SwRI-owned tool for constraint-based file generation, XFORGE 1.0. XFORGE supports melding of Department of Defense (DoD) technologies and commercial industry needs into configuration file generation frameworks.

**Approach** — The main idea of this research was to quickly create a functional experimental framework to evaluate the overall discovery concepts. To do this, we cross bred ideas from the artificial intelligence research community with automatic test and fuzzing concepts from the test and cyber security communities. Evaluation of our focused automated search techniques required a general ruleset capable of encapsulating the concepts of various classes of telemetry devices. The framework utilized this ruleset to generate and run tests on a device and collate their results, which led to evaluating the constraints on that device.

**Accomplishments** — This research has proven it is possible to build a tool that will allow us to decrease the entrance barrier into this form of standardized constraint grammar expression dramatically. That is, we created and evaluated an experimental tool that will lead to automatically generating a usable version of the standardized grammar for specific devices. By defining some basic observed rules from a device, we were able to iteratively determine the accuracy of these rules and build upon them, creating a ruleset which is used to test a significant portion of the configuration space of the device. This, in turn, led to a consolidated set of results that describes the apparent capabilities of the device and highlights any previously unknown capabilities or expected capabilities that do not exist.

## 2016 IR&D Annual Report

---

### Optimization of Advanced Lattice-Boltzmann Models, Project 10-R8629

#### Principal Investigators

[Phil Westhart](#)

John Harwell

Daniel Davila

Hakan Basagaoglu

Inclusive Dates: 02/08/16 – 06/08/16

**Background** — Many of SwRI's existing and potential clients have problems that are amenable to solutions using the Lattice-Boltzmann Method (LBM). However, the computational complexity and current long simulation times make use of these models for some of the applications in which our customers are heavily interested currently impractical. For LBM to be a viable approach in these applications, a 10X performance increase is needed in both the core LBM solver and the new modules.

**Approach** — Our approach was to adapt optimization techniques from previous internal research work (project 10-R8537) and attempt to apply them to the more complex 2D models and extend them to the 3D domain. Initially, the advanced 2D models were analyzed using industry-standard profiling software to determine which combinations of our existing optimization techniques might be successfully applied. Initial optimization efforts focused on code restructuring, compiler optimizations, data layout optimizations, data organization, instruction and data cache optimization, and concurrent models for random number generation. Further experiments building on the concurrent model developed on project 10-R8537 were conducted involving thread placement and generation methods (Box-Mueller vs. an approximate random generator) and compared for throughput and accuracy.

However, adaptation of existing permutations from 10-R8537 were not sufficient to achieve the desired performance increases for either the core LBM solver or the new modules, and the following additional optimization techniques were investigated.

- Parallelization: OpenMP directives were inserted into the code to parallelize loops wherever possible.
- Inter-processor Parallelization: The OpenMP runtime environment was configured to profitably utilize all cores on all available processors, rather than limiting to a single processor.
- Task Level Parallelism: Tasks within the current and next LBM timestep during simulation were scheduled and run as soon as their dataflow dependencies were met using Intel's Threading Building Blocks (TBB) C++ library.

**Accomplishments** — The overall performance increase achieved by our optimization approach on the 2D simulations is 15.2X/20.6X when considering the baseline to be the performance of the original code compiled with the Intel Fortran compiler. However, considering that only the PGI Fortran compiler was available on the target platform initially, it makes sense to use the PGI Fortran compiler execution times as the baseline of performance, which yields an average 21.2X/31X performance increase of the LBM code. This exceeds the goal of a 10X performance increase on the target hardware that was the objective for this project.

## 2016 IR&D Annual Report

---

### **Advanced Traffic Management Mapping Technologies: Linear Referencing, Vector Representation, and Multiple Raster Layers, 10-R8634**

#### **Principal Investigators**

[Adam Clauss](#)

Lynne Randolph

Dan Rossiter

Inclusive Dates: 02/10/16 – 06/10/16

**Background** — SwRI began observing an increase in requests for proposals (RFP) for Advanced Traffic Management Systems (ATMS) that referenced multiple requirements that the existing ATMS applications developed by SwRI had not previously attempted. These requirements included the ability to address toggling of different map features (roadways, water features, etc.), toggling of raster data such as weather radar and aerial imagery, and the ability to interact with and support linear reference system (LRS) data specified through the Federal Highway Administration (FHWA) All Roadway Network of Linear Referenced Data (ARNOLD) program.

To support LRS data, one of the goals of this project was to investigate methods of converting location data between LRS designations and latitude/longitude. The FHWA has mandated that information reported by agencies will use ARNOLD to designate positioning. The FHWA has not published a standard for this implementation but leaves this open to each state to determine the best method of providing the data. Because of this, states are looking to existing software to help provide this information. The ATMS developed by SwRI includes information which the states need to provide to the FHWA in the LRS format.

**Approach** — The research team requested and received permission from the Texas Department of Transportation (TxDOT) to utilize the mapping interface used by the TxDOT ATMS, developed by SwRI. This same mapping framework is also in use by existing projects for four other states.

This research project was divided into three distinct tasks: (1) identify available raster and vector data sources, including mechanisms for displaying them; (2) identify possible methods for integrating LRS/ARNOLD data; and (3) build a test harness to execute performance tests of the Lonestar Map Interface.

**Accomplishments** — The team expected some layers to behave measurably differently between raster and vector data formats. This was confirmed through testing when the water features and routes layers were effectively unusable as vector data due to their large number of points. More surprising was how quickly the raster data implementation outperformed the vector implementation, both in terms of time and memory consumption. The assumption was that holding the uncompressed raster images in memory for the different areas would far outweigh the costs of defining and drawing the individual data points for the vector data.

Despite the performance implications, vector implementations do have their advantages. Notably, because the user interface is aware of each data point, the user can interact with the data (such as hovering over an item to get a tooltip with additional information, including contact emails and phone numbers). For the raster implementations, the user interface is simply displaying an image — it is not functionally aware of the different data objects the image may be composed of.

With that in mind, a production implementation should consider a mix of raster and vector data. Data that

simply exists and needs to be displayed can be built into a raster layer to keep performance as high as possible, especially when using the larger datasets such as roadways and water features. Only data that the user needs to interact with — most likely points of interest of some kind — should be handled in vector form.

With regards to supporting ARNOLD, a process was identified through which commercial off-the-shelf (COTS) products could be used to perform the LRS conversion. While aided by the COTS tools, this method would also require human intervention in places where the tool may not always be able to identify the correct route on which to generate a linear reference. At this time, the ARNOLD requirements are not specifically defined by FHWA — they are only concepts, despite having been introduced years ago. It is hoped that if the ARNOLD requirements grow more detailed, this will help guide the LRS implementations the transportation agencies have and make it easier to convert between them.

## 2016 IR&D Annual Report

### Large-Scale Robotic Aircraft Painting Technology Research and Development, 10-R8640

#### Principal Investigators

Crystal Parrott

Steve Wiedmann

Carl Bargainer

Chris Lewis

Inclusive Dates: 03/20/16 – Current

**Background** — SwRI has been awarded an externally-funded large-scale laser repaint program for passenger-sized aircraft that initiated late in 2014. The system under development is being designed with the concept of extensibility for a variety of other large-scale aerospace processes. Aircraft painting represents the most significant process opportunity, with market potential estimated to exceed repaint. Multiple coatings will be applied during an aircraft's lifespan. In addition, coatings are re-applied due to branding and marketing positions by aircraft owners. Aircraft manufacturers and maintainers are actively seeking paint system solutions that reduce cost, improve quality, speed the process, and allow easy application of complex paint schemes such as logos and images for advertising and branding.

**Approach** — SwRI will use the large-scale robotic platform developed for laser repaint, and develop end effectors for painting and direct-print inkjet application. To meet industrial safety requirements, a custom robotic three-degree-of-freedom wrist will be designed that allows for paint fluids to be routed internal to the wrist. An end-of-arm-tool (EoAT) will be developed to support rotary bell paint spraying. SwRI will design and fabricate an inkjet EoAT with a printhead stabilization system to absorb vibrations induced by the large-scale robotic platform. To identify the effects of variable printhead orientation and the limits of key process parameters such as standoff distance, SwRI will integrate a commercial printhead with support systems and will test it in a lab setting. SwRI will integrate the two EoAT onto a robotic platform

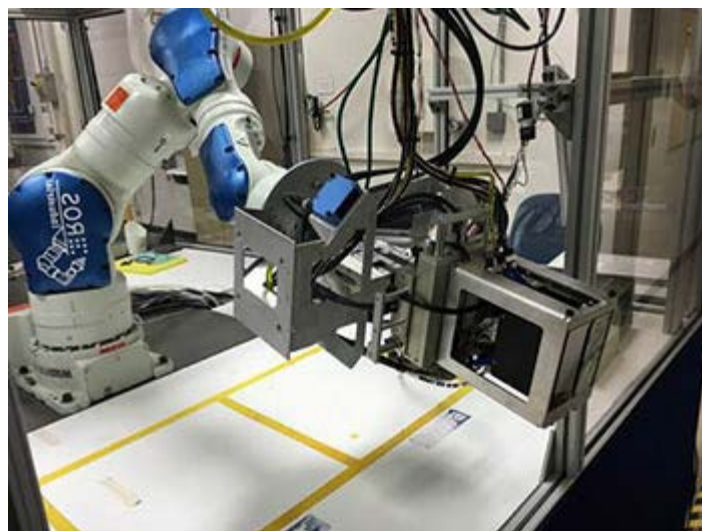


Figure 1: Inkjet EoAT on Laboratory Robot

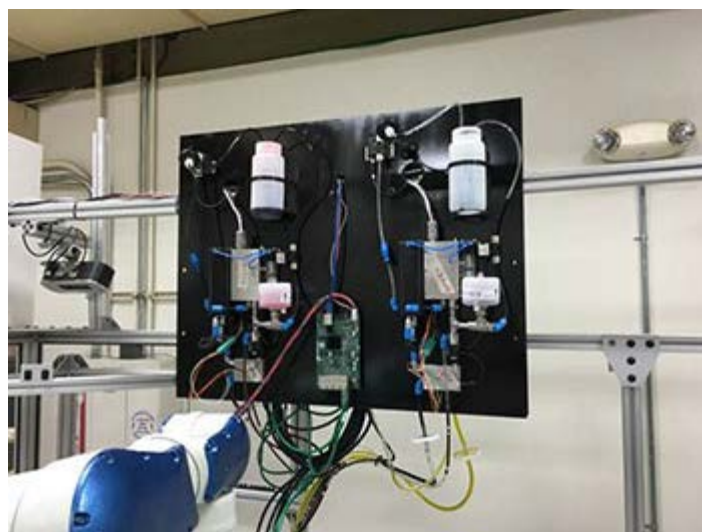


Figure 2: Inkjet Fluid Handling System

and demonstrate bulk paint application and direct inkjet printing.

**Accomplishments** — The robotic wrist, rotary bell painting EoAT, and inkjet EoAT were designed. A 3-axis printhead stabilization platform was assembled, and stabilization software is being developed. The inkjet printhead was selected and integrated with drive electronics, fluid handling system, and printing control software. The inkjet EoAT was fabricated and mounted to a six-degree-of-freedom laboratory robot for testing. Color images were printed with test fluid at varying angles and on curved surfaces. The effects of printing distance, ink inlet and outlet pressure, printhead orientation, and drive voltage waveform were investigated. Development of ink optimized for aircraft application was initiated. Future work will include fabrication of the robotic wrist and rotary bell painting EoAT for use on the large-scale robotic platform. Control software for the inkjet printhead stabilization platform will be completed and tested. Ink optimization parameters for aircraft application will be quantified, and any required changes to the ink handling system will be outlined. Demonstration of the inkjet EoAT will first be performed on a laboratory robot followed by demonstration of both the rotary bell painting EoAT and the inkjet EoAT on the large-scale robotic platform.

## 2016 IR&D Annual Report

---

### Automated Engine Hot-spot Detection at Standoff Distance, 10-R8644

#### Principal Investigators

Richard D. Garcia

Douglas A. Brooks

Inclusive Dates: 04/04/16 – 08/04/16

**Background** — It was recently brought to SwRI's attention that there was a strong need for automated hot spot detection of large-scale maritime diesel engines to support early warning of catastrophic engine failure. These failures present a very real threat to the operation and safety of the vessel, crew, and passengers. Additionally, any catastrophic engine failure on a passenger vessel that results in fire, explosion, excessive smoke, evacuation, or disabled vessel significantly impacts the public's perception of the entire industry.

Although modern engines on large maritime vessels employ in-engine sensing technology, these sensors only monitor key components, leaving the vast majority of the engine unmonitored. To account for this sensing deficiency, many maritime vessels assign a crew member to manually search for engine hot spots, an indicator of a possible failure location, with a handheld thermal camera. If a hot spot is located, the engineer can shut down the engine and address the overheating issue prior to a catastrophic failure. Unfortunately this type of intermediate spot-checking only provides small windows of evaluation and presents an inherent risk to the crew member performing the inspection.

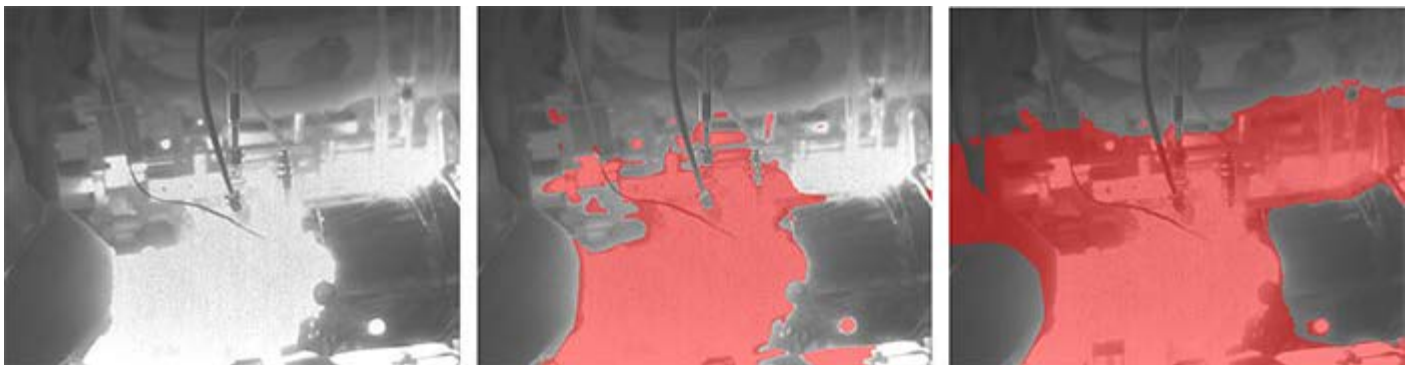


Figure 1: Illustration of the automated system's ability to classify a region that has exceeded its thermal threshold.

**Approach** — We leveraged SwRI's perception expertise to overcome the shortfalls of methods currently being used to detect engine hot spots. The theory was that SwRI's previously developed detection and classification architecture could be used to train a machine learning algorithm capable of autonomously detecting abnormal thermal conditions (i.e., hot spots) on a small-scale combustion engine using a thermal imager. This project also leveraged SwRI's extensive expertise in engine testing, data collection, and failure analysis.

For development, the project team used a forward-looking infrared radar (FLIR) A65 thermal camera to capture data of a small-scale combustion engine (2.0-L turbo charged). Following SwRI's prescribed safety guidelines, the engine was placed onto a dynamometer that can control fuel supply, oil temperature, coolant flow, and individual cylinder timing. This test setup allowed the team to capture nominal and abnormal engine conditions and provided the means to reliably create abnormal thermal conditions.

**Accomplishments** — For this effort, the team performed multiple experiments on four main engine states: non-running (cold) engine, recently started engine, steady-state running engine, and engine beginning to overheat. Through this testing, the team was able to demonstrate that it was indeed feasible to automate the process of accurately (within 2°F of ground truth) and consistently detecting when an area within an engine has exceeded a localized thermal threshold, see Figure 1. In addition to the aforementioned achievement, the team also equipped the system with the ability to automatically segment regions of the engine based on thermal and spatial information without any initial input from a user.

## 2016 IR&D Annual Report

---

### High Performance Streaming Data Processing, 10-R8677

#### Principal Investigators

[Stephen A. Kilpatrick](#)

Michael W. Timme

Todd A. Newton

Philip M. Westhart

Glen W. Mabey

Ben A. Abbott

Inclusive Dates: 07/01/16 – Current

**Background** — In 2004, as part of the Boeing 787 team, SwRI developed the first large-scale network-based data acquisition and telemetry flight test system. While our success in this arena continues today, the increasing momentum of standardized network technologies has led to unrealizable expectations. When technologies become commoditized, our customers expect the increased capabilities to smoothly and quickly be incorporated into their systems. While the core unifying technology, Internet Protocol (IP), eases this process, unique challenges unanticipated by our clients in the flight test telemetry domain are impeding the introduction of the next generation of high speed IP technologies. These challenges have led our competitors down the expensive path of attempting to develop special purpose hardware. While likely to create an expensive working solution for the short term, we believe a more open, commodity-driven approach is possible, which will have demand for the long term. This project evaluates the efficacy of utilizing commodity central processing unit (CPU) and general-purpose graphics processing unit (GPGPU) technologies to offload the processing challenges associated with the ever-increasing demands on network-based telemetry.

**Approach** — We have based our approach around the belief that the high packet rate nature of flight-test data systems offer a good opportunity for packet-level parallelism to be explored. The following methods have been explored initially.

- CPU-only approach: Create a simple application that reads incoming IP packets from a socket as fast as possible. Existing libraries and components claim that they have achieved acceptable results using this simple method; however, our experience with past data systems makes us skeptical that this approach will be successful once the test cases become more strenuous.
- Network Stack circumvention: direct memory access (DMA) incoming IP packets from the network interface controller (NIC) to an application on the CPU/GPU as fast as possible. We believe that the CPU alone will not be able to handle the high-throughput, low-latency packet processing that needs to be performed, so some amount of parallelized processing also will need to be accomplished on the GPU.

**Accomplishments** — Initial results have shown that through a combination of CPU and GPU processing, it is possible to receive, filter, and extract data at input rates upwards of 8 Gbit/s at latencies under 1 millisecond through the system. Our approach has been proven to be scalable enough to run on a high-performance computer and a smaller, ruggedized embedded computer. Research will continue to be carried out to generalize our approach across a variety of other test cases.

## 2016 IR&D Annual Report

### Using SequenceL Parallel Programming Language to Improve Performance of Complex Simulations, 16-R8540

#### Principal Investigator

Justin L. Blount

Inclusive Dates: 03/01/15 – 01/01/16

**Background** — This project was part of the Computational Optimization Focused Internal Research Program and was an offered solution to Call 1 challenge problem #2: "Desired Computational Enhancements for Our In-House Lattice-Boltzmann Method Based Numerical Model for Applications in Oil and Gas Exploration and Biomedical Fields."

**Approach** — The specific goals of this project were to:

- reduce the runtime of the in-house Lattice-Boltzmann method-based simulation by an order of magnitude of 10 or more
- evaluate the programming language SequenceL by comparing it with the existing implementation written in Fortran. This represents a bold and significant approach that uses a completely different technique to solving the computational problem as opposed to other approaches that focus on optimizing existing compiler environments or portions of the existing code base. As such, this approach presented a higher level of risk, but in the end, yielded greater performance gains.

Performance Results			
Benchmark	SequenceL Execution Time (s)	R8540 Fortran Execution Time (s)	Speedup Factor with R8540 baseline
1 (fluid only)	12.9	97.2	7.6
2 (one particle)	162.4	514.1	3.2
3 (two particles)	82.5	661.1	8.0
4 (thermal)	7,404.3	91,381.2	12.3
5 (50 particles) [1000 <sup>th</sup> scale]	161.1	2867.3	17.8

Figure 1: Performance results of SequenceL

**Accomplishments** — Significant reductions in simulation execution were achieved on all provided benchmark problems. The highest increase in performance was 17.8 times faster than the equivalent execution time of the existing code. Furthermore, this was achieved on the most scientifically relevant benchmark, which simulates 50 particles in a fluid flow, and thus it is significantly larger (more fluid and particles) than the other four benchmark problems. Given that we did not have adequate time to run this reference benchmark to completion using the Fortran baseline within the project schedule, we used a version of benchmark 5 that was shortened (1,000th scale) along the time dimension. Based on our experience on the project, we anticipate a similar speedup on the full length benchmark. The performance results are summarized in the table below, and were executed on a hardware platform established for this project to provide a valid comparison between existing Fortran code base and SequenceL code base executions.

To achieve these goals we reformulated the algorithms in SequenceL. SequenceL is a purely functional programming language with semantics that enable automatic compilation to parallel executables from function definitions. This is in contrast to methods, such as Open MP, which require the programmer to provide compiler directives on how to execute parallel instructions. Since SequenceL is a functional

language, the resulting program is 25 percent shorter and much more closely resembles the mathematical equations describing the Lattice-Boltzmann method-based simulation than the Fortran implementation. We first implemented the simulation of the fluid and then extended the program with the simulation of the particles. Our first attempt at simulating particles did not have the desired performance, but after a redesign we achieved our performance goals. Over the course of this project, we used a profiler to analyze the execution of the program and to direct efforts to improve the program.

The figure above "Employing SequenceL" and reengineering the modeling and simulation functions to run as optimized parallel algorithms achieved an increase in performance of 17.8 times faster than the equivalent execution time of the existing FORTRAN code.

In the final analysis, this approach was one of three employed separately against this problem, but the only one to achieve the desired order-of-magnitude performance improvements.

## 2016 IR&D Annual Report

---

### Investigation of Computational Methods for Modeling Bird Strike Impacts on Aircraft Structures, 18-R8477

#### Principal Investigators

[James Mathis](#)

Sidney Chocron

Joseph Bradley

Matthew Grimm

Nikki Scott

Inclusive Dates: 07/01/14 – 06/30/16

**Background** — Collisions involving birds and aircraft have been a problem since the beginning of aviation and have recently received more attention. A bird strike during flight can be a major threat to the aircraft depending on the size of the bird, speed of the aircraft and location of the strike. All aircraft components that are at risk for bird strike are required by regulating authorities to undergo a certification process aimed at demonstrating that a safe landing is possible after a bird strike event. Designers and manufacturers of these components rely heavily on experiments; however, costs to conduct research and development tests are substantial due to the destructive nature of the test and limited production prototypes. In recent years there has been a shift toward the use of computational tools to simulate the behavior of components during an impact event. Unfortunately, the simulations are not always accurate due to the complex composite materials that are often used on forward-facing surfaces in an effort to save weight. Clearly trends are shifting toward the use of numerical simulations for early design efforts and in some limited cases, full certification by analysis (CBA).

Based on our history in supporting many customers with quality bird strike testing, combined with our general expertise in computational modeling of ballistic impact and material response, SwRI has conducted a research project aimed at developing and demonstrating our capabilities to accurately model bird strike impact into aircraft structures using a dynamic finite element analysis (FEA) technique.

**Approach** — A combined experimental and computational approach was used to validate our bird strike modeling methodology. Material characterization experiments were carried out to determine the pressure vs. density response of the bird projectile to facilitate the accurate computation of impact loads. Common aerospace materials were then selected and tested against bird strike impacts to collect material response data including forces, dynamic deflections and strains. The data collected was directly compared to simulations of the impact tests that were conducted in parallel using the FEA code.

**Accomplishments** — A major focus of this project was the prediction of loads imparted onto rigid structures caused by bird impacts. Initial bird model impact simulations focused on determining impact pressure magnitude and distributions on rigid panels at various angles of attack. The bird material model that was used in our initial simulations was taken from literature and based on the equation of state for water. The initial simulation results correlated well with experimental data found in the literature but was later refined using data collected from our own material characterization experiments. Chickens were tested in confined compression experiments to determine the pressure vs. density relationship for implementation into an equation-of-state (EOS) model within the finite element software. New simulations were carried out, and demonstrated improved agreement with experimental data, especially for the non-normal impact conditions, as shown in Figure 1.

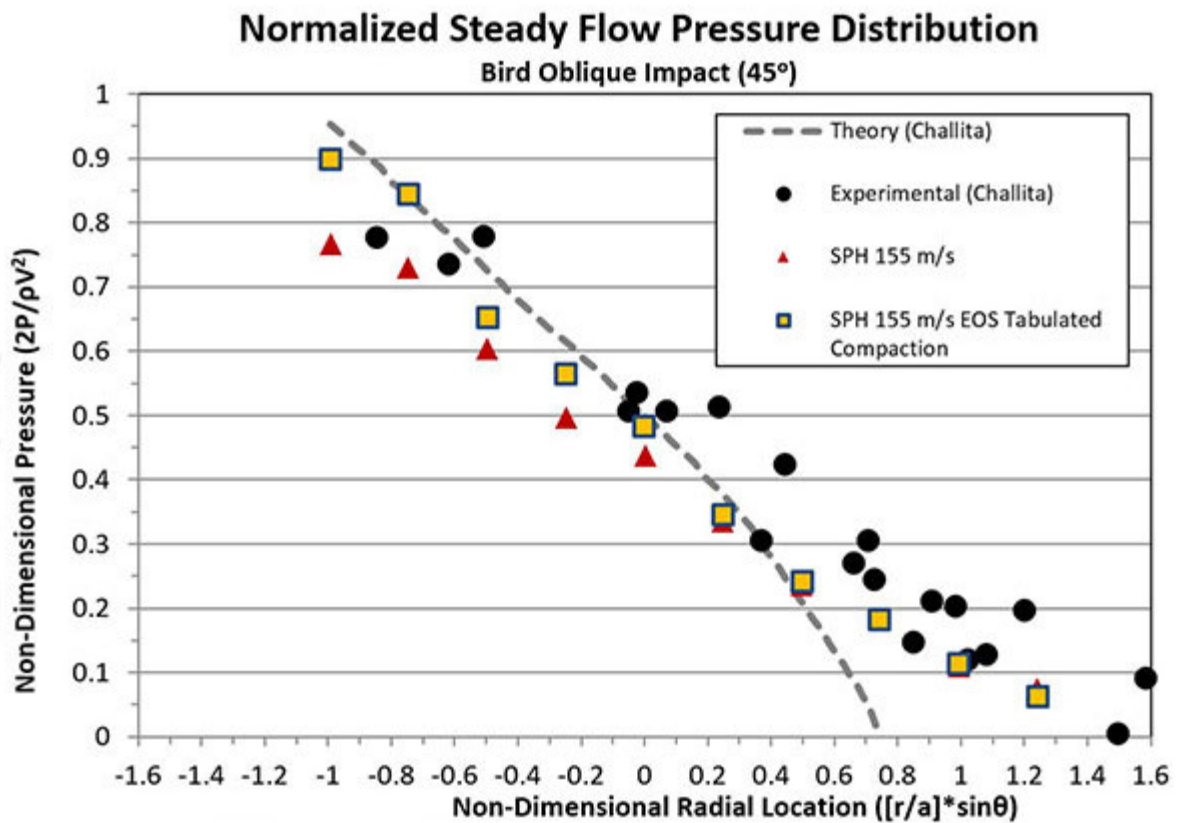


Figure 1: Steady flow pressure distribution for a 45-degree Impact.

Another key aspect of bird strike impact modeling is the accurate prediction of material response. Common aerospace materials including carbon-epoxy composite, 2024-T3 aluminum, and polycarbonate, were selected and subjected to bird impacts at the SwRI bird strike test facility. A series of 16 instrumented bird strike tests using real chicken projectiles were conducted against panels of the selected materials at 45-degree obliquity. During the tests, total reaction forces as well as strain and dynamic deflection of the panels were recorded. A digital image correlation system was used to capture dynamic strains and deflections over the entire back surface of the target panels during the tests.

The qualitative comparison of predicted damage showed excellent agreement as shown in Figure 2, and the experimental deflections and strains on the back surface of the panels showed excellent quantitative agreement as well, shown in Figure 3. These results indicated that both the bird model and target material models were performing well compared with experiments in both the failure and non-failure regimes.

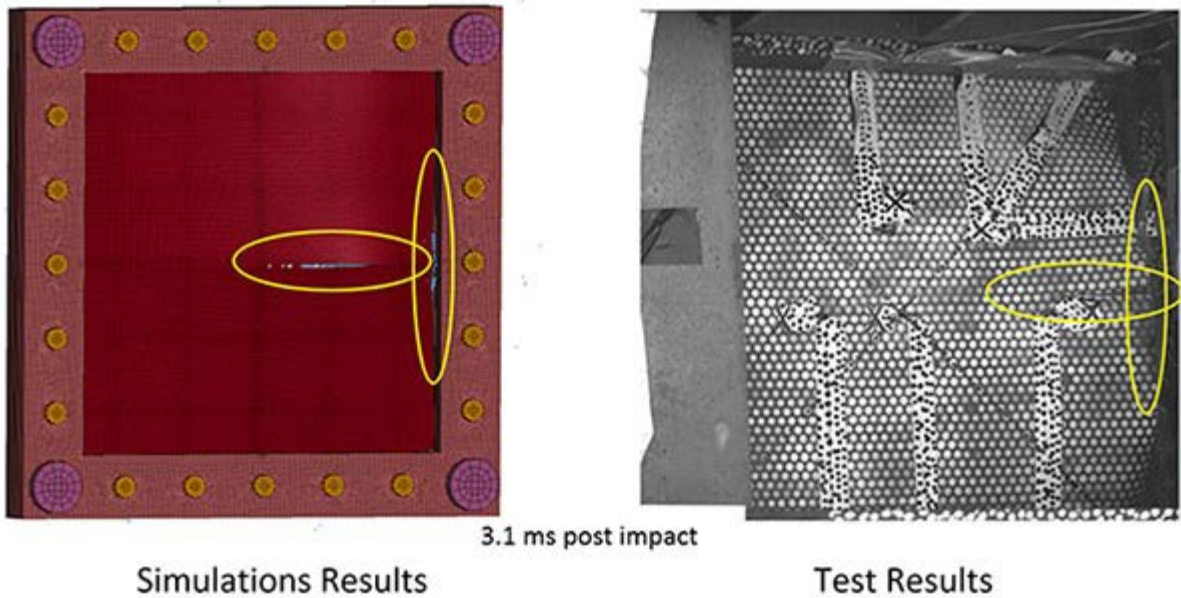


Figure 2: Qualitative comparison of damage predicted and observed on the back surface of the carbon-epoxy composite panel.

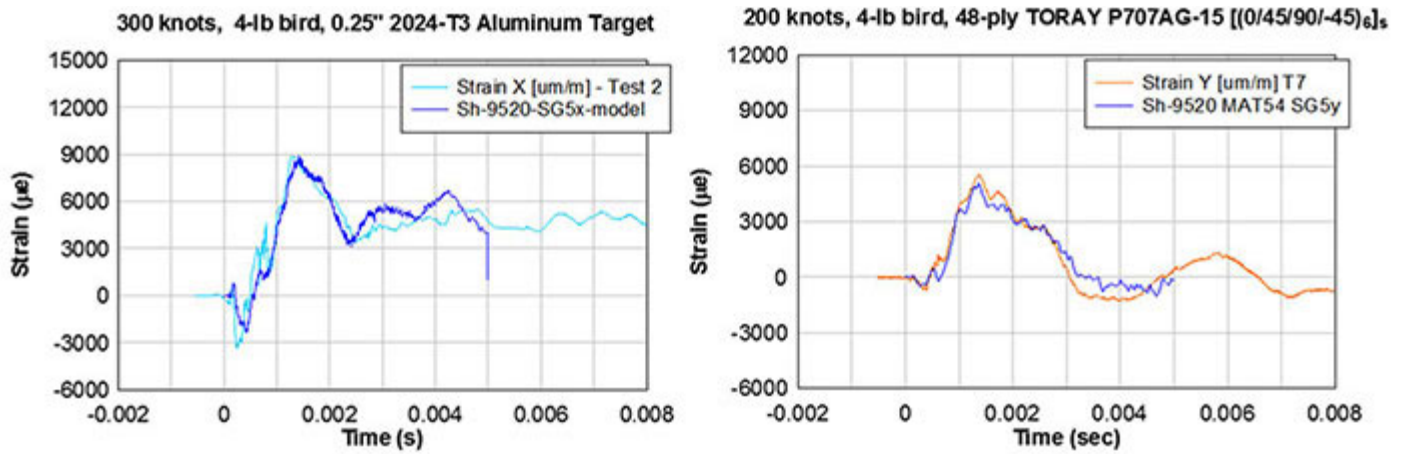


Figure 3: Comparison of experiment and simulation strain time-history response on back surface of the panel.

## 2016 IR&D Annual Report

---

### Algorithms to Improve the Speed of the Numerical Model Based on the Lattice-Boltzmann Method, 18-R8541

#### Principal Investigators

[Grant Musgrove](#)

Shane Coogan

Shahab Saleh

Inclusive Dates: 03/01/15 – 12/01/15

**Background** — This work solves the second problem of the first call of SwRI's Computational Optimization Focused Internal Research Program, "Desired Computational Enhancements for Our In-House Lattice-Boltzmann Method-Based Numerical Model for Applications in Oil and Gas Exploration and Biomedical Fields." Because the solver was developed through the solution of physical problems, computational efficiency was not a primary developmental concern. As the solver capability continues to expand with more complexity, computational efficiency is becoming increasingly important. The objective of the problem statement for this program is to improve the speed of the time-consuming computations of the Lattice-Boltzmann (LB) solver. In the posed problem, four computationally intensive issues are requested to be improved upon to shorten the solution time, namely:

- Reduce computation time for the streaming algorithm
- Reduce computation time to search for the particle boundary and nearby solid nodes
- Reduce computation time to generate normally distributed random numbers and predict an average nanoparticle trajectory from many simulations
- New methods to scale or run the code in parallel with CPUs, GPUs, or a combination of both

**Approach** — The work of this project is intended to solve the first three issues above by using efficient algorithms to speed up the computations of the current LB solver. The primary approach to improving the computation speed is eliminating repetitive computations in the code for which the result does not change or changes very little. Additionally, the solution approach to predict nanoparticle trajectories requires random number generation and uses a Monte Carlo sampling method, both of which are improved upon by using probabilistic methods.

**Accomplishments** — The work has increased the computational speed of the solver by up to a factor of two by reducing or eliminating the repetitive calculations within the code. Additionally, replacing the Monte Carlo sampling method with a discrete matched-moment method resulted in a speed up by a factor of five for simulations with random particle trajectories. A paper describing the matched-moment method, "Speed-Up of Colloidal Fluctuating Lattice-Boltzmann Simulations through Discrete Approximations of Probability Distributions," was presented to AIAA SciTech 2017.

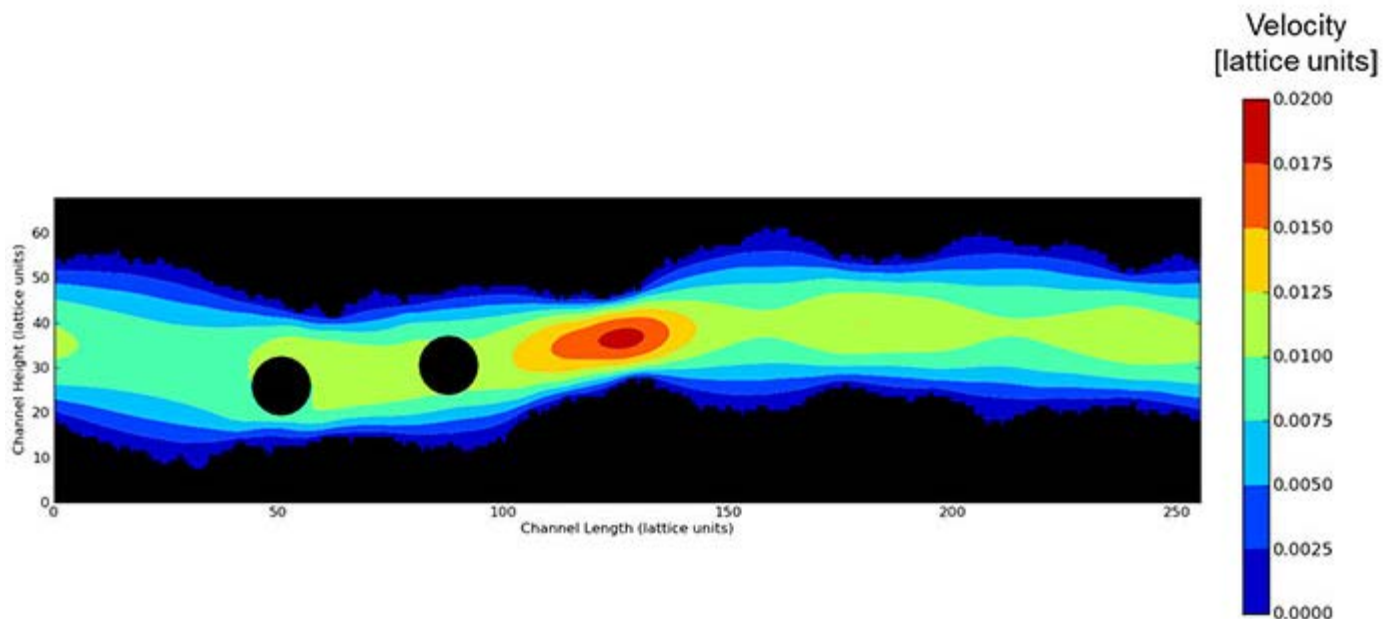


Figure 1: A core strength of the Lattice-Boltzmann solver is the ability to handle complex, arbitrary surfaces.

Benchmark	Baseline Wall Clock	Best Wall Clock	Speedup Estimate
1	1646 sec	842 sec	2.0x
2	120 sec	73 sec	1.6x
3	1483 sec	645 sec	2.3x
4*	3308 sec	780 sec	4.2x
5	165.3 hr	139.9 hr	1.2x
10*	16.2 hr	3.1 hr	5.3x
<i>All computations done on a single processor</i>			

Figure 2: Computations speeds were increased as much as a factor of five.

## 2016 IR&D Annual Report

---

### Improving the Efficiency of Computations Involving the Ballistic Impact of Full-Scale Structures of Composite Materials, 18-R8564

#### Principal Investigators

[Stephen Beissel](#)

Sidney Chocron

Warren Couvillion

Charles Gerlach

Inclusive Dates: 06/24/15 – 03/04/16

**Background** — Ballistic fabrics and their composites are essential components of various armor systems, including the body armor worn by soldiers and police officers. Computational modeling and simulation are gaining widespread use in the design of armor systems, as they provide both insight into the relevant physical processes and a means to reduce the cost and time of the design cycle. Accurate computational approaches to modeling ballistic fabrics and their composites have recently been developed by SwRI engineers using commercial finite-element software. These approaches explicitly model each yarn in the fabric, a level of refinement known as the meso-scale. Figure 1 shows the edge of a meso-scale model of a simply woven single ply of ballistic fabric. Simulations involving meso-scale models of multiple-ply armors consumed more computing time than that available during the design of a typical fabric armor system. This project therefore aimed to reduce the computing time required by meso-scale modeling of ballistic fabrics and their composites so that SwRI may effectively market these analyses to its clients in the Department of Defense and the defense industry.

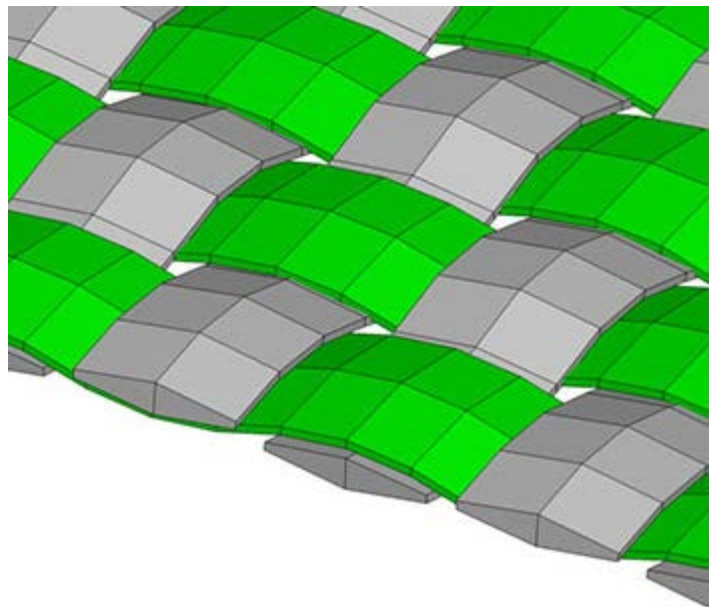


*Figure 1: The magnified edge of a meso-scale finite-element model of a single-ply ballistic fabric reveals the adjoining dual strands of hexahedral elements that comprise each yarn.*

**Approach** — The objective of this project was to reduce the computing time of the meso-scale fabric model to 10 percent of the time it consumed using commercial finite-element software on SwRI cluster computers. To do so, this project investigated multiple approaches. The first approach was to implement the model in finite-element software developed by SwRI engineers involved in this project. Unlike the commercial software, the SwRI software has been adapted for high-performance computing (HPC) hardware, which exploits the full power of parallel processing by maintaining efficiency to large numbers of distributed-memory processors. The speed of the meso-scale fabric model was then tested on off-site HPC hardware. Because the source code of the commercial software is not available, an additional advantage to this approach is the ability to modify the SwRI software as needed to improve the efficiency of the model.

The second approach involved subtle changes to the model itself. In its initial incarnation, the meso-scale model uses the most general form of the fundamental elements that comprise material. These elements are capable of developing stresses in all directions, as in a three-dimensional continuum. However, the yarns of a fabric develop stresses primarily along their lengths, with the exception of the yarns in contact with the projectile. This means that the yarns can be accurately represented by simplified elements that assume a reduced state of stress. One advantage of these elements is that they do not require the same small computational time steps of the more general continuum elements. As a result, significant reductions in computing times were expected. Because the model was modified in this approach, a necessary additional step was to demonstrate that the reduced-stress elements provide sufficient accuracy and robustness.

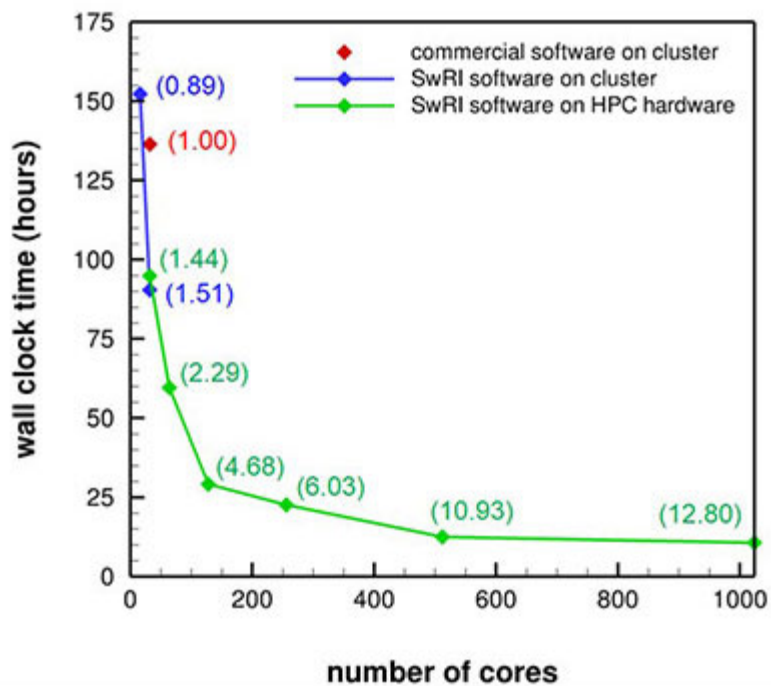


Figure 2: The wall-clock time from a benchmark computation using commercial software on a SwRI cluster (red datum) is compared to the times from computations using SwRI software on both cluster (blue data) and off-site HPC hardware (green data).

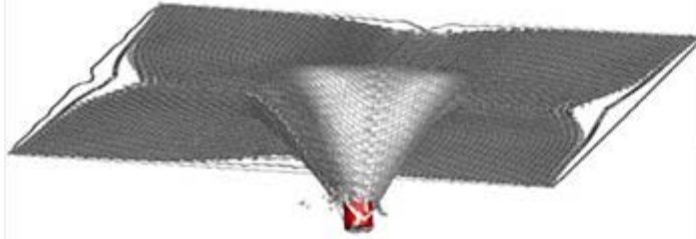
**Accomplishments** — The meso-scale fabric model was successfully implemented in the finite-element software developed by SwRI engineers, with model results very similar to those obtained by the commercial code in which it was developed. To evaluate relative performance, benchmark computations were conducted on the SwRI cluster where the meso-scale model was developed, and on HPC hardware maintained by the Department of Defense. Figure 2 compares the wall-clock times from these computations as a function of the number of parallel cores. The red data point represents the fastest run of the commercial code, occupying 32 cores of the SwRI cluster. Speed-ups were calculated relative to this run, and they are shown in parentheses next to each data point. The blue and green data were generated by the SwRI software on the cluster and HPC hardware, respectively. The project goal was attained by the computations using 512

and 1,024 cores on the HPC hardware, which resulted in speed-ups of 10.93 and 12.80, respectively.

For the second approach, the formulation of the reduced-stress elements in the SwRI finite-element software was modified to better represent elastic-plastic material behavior. Then a computer program was written to create finite-element meshes of woven fabrics composed of reduced-stress elements. These meshes matched in both refinement and physical detail the meshes of continuum elements initially created for the commercial software. Figure 3 compares the computed results of a cylindrical projectile impacting a single ply of fabric using the initial continuum elements on the left side, and the reduced-stress elements on the right side. When the benchmark problem was run on the cluster computer, the speed-up attained by the reduced-stress elements was 11.7.

In summary, two separate approaches pursued in this project each achieved the goal of reducing the run times to less than 10 percent of that consumed by the commercial code on the SwRI cluster.

yarns of continuum elements



yarns of reduced-stress elements

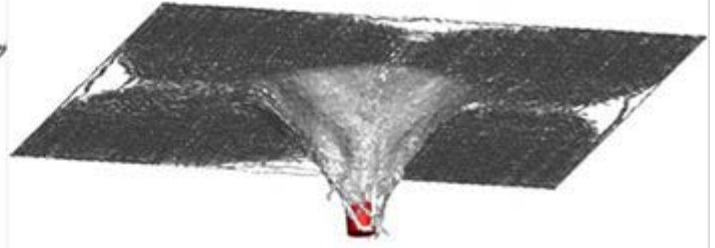


Figure 3: Results are shown from computations of a cylindrical projectile impacting a single ply of fabric composed of continuum elements (left) and reduced-stress elements (right).

## 2016 IR&D Annual Report

---

### **Development of a New Numerical Model to Simulate Chemotaxis-driven Bacterial Transport for Treatment of Tumor Cells and Mitigation of Bacterially-mediated Pipeline Corrosion Problems, 18-R8602**

#### **Principal Investigators**

[Hakan Başağaoğlu](#)

Alexander J. Carpenter

W. Kennedy Gauger

Miriam R. Juckett

Spring Cabiness

Inclusive Dates: 10/01/15 – Current

**Background** — The purpose of this project was to develop a new numerical model to simulate the directional motion of self-propelled, deformable chemotactic particles (e.g., live or engineered bacteria) in spatially- and temporarily-varying chemoattractant (e.g., nutrients) gradients in a non-Newtonian fluid in two- or three-dimensional geometrically-complex flow domains (e.g., tumor vasculature). To our knowledge, there is no current numerical model containing all of these capabilities. The model has potential uses in diverse biomedical fields and in the oil and gas industry. The model is intended to be validated or tested with microfluidic experiments to be conducted as part of this project.

**Approach** — A RapidCell (RC) model and our in-house Lattice-Boltzmann (LB) model was dynamically coupled through a set of new equations we derived to calculate the position of receptor clusters on the chemotactic particle surfaces through which the chemotactic particle would detect and orient itself toward the time-variant steepest chemoattractant gradients. The new coupled model is a multi-scale numerical model that can simulate cell-scale adaptation dynamics and protein signaling, and particle-scale bacterium-fluid hydrodynamics. A new module to simulate non-Newtonian fluid flows was developed by describing the local kinematic viscosity of the fluid as a function of the second invariant of the rate of strain tensor. A new module to simulate the motility of arbitrary-shape particles was developed using trigonometric, geometrical, and topological identities. A new module to simulate advective-diffusive distribution of substrates was developed using a new LB approach, in which the relaxation parameter was described in terms of the diffusion coefficient and the equilibrium distribution was formulated as a function of substrate concentrations. We implemented various optimization techniques (e.g., maximization of compiler-time determinism and optimization of array memory layout) and parallelized the code through the implementation of OpenMP directives to accomplish computationally enhanced large-scale simulations. As for the experimental tasks, we conducted microfluidic experiments with *E. Coli* to analyze their tumbling and direct run motions in response to chemoattractants in an initially stagnant fluid in a confined microfluidic channel.

**Accomplishments** — A combined RC-LB model was developed successfully to simulate multi-scale processes governing chemotactic motility of particles (e.g., bacteria) in stagnant or flowing fluids in geometrically complex flow domains. The non-Newtonian fluid flow module was successfully developed and validated against the analytical solutions available for pressure-driven pseudoplastic and dilatant fluid flows in a smooth-walled channel. The advective-diffusive fluid flow module was successfully developed and validated against analytical solutions derived for spatial-temporal distributions of a pulse injection of a substrate from a point source into a Couette flow. The arbitrary-shape particle fluid module was developed and successfully simulated the trajectories of circular, ellipsoid, rectangular, triangular, hexagonal,

boomerang-shaped, and star-shaped particles in confined channels (validation tests are in progress). The optimized and parallelized codes accomplished an average of 21-fold computational performance improvement. Microfluidic experiments with E.Coli captured chemotactic motility of bacteria, involving their tumbling motion in search of food source (substrates) and direct run motions toward the nutrient source, but the quality of the images was not good for model validations.

[Click for media and references.](#)

---

**[2016 IR&D | IR&D Home](#)**

## 2016 IR&D Annual Report

---

### **Computational Model Development and Validation for Additive Manufacturing Simulation, 18-R8650**

#### **Principal Investigators**

[Christopher J. Freitas](#)

Nathan F. Andrews

Inclusive Dates: 04/01/16 – Current

**Background** — Additive manufacturing (AM) is a revolutionary development for manufacturing complex parts and components. Traditional subtractive manufacturing in which stock materials are cut or tooled to reveal the part inside have dominated manufacturing for more than 100 years. However, as the need for added complexity in manufactured parts has increased, Subtractive manufacturing has proven to be fundamentally handicapped by the limitations of the equipment used in the manufacturing process. Parts with internal structures, overlapping curved elements, and internal chambers or voids are difficult if not impossible to manufacture by subtractive processes. Additive manufacturing processes, however, are not constrained by geometric complexity, in that the part is built up by depositing raw materials in layers and in locations only where the materials are required based on the part design. Thus, geometrically complex parts can be built using a wide range of materials such as plastics to composites to ceramics to metals (and alloys). However, one of the critical hurdles to the broad adoption of AM is the qualification of additively manufactured parts.

What is needed is a physical understanding of the raw material fusion process and the dynamic interaction between deposited layers, which can provide insights into performance margins, uncertainties in those margins, and their sensitivities to process parameters. Modeling and simulation provides a mechanism to develop this understanding. To date, limited progress has been made in the simulation of AM processes, with some investigators focusing on the particle melt processes leading to material microstructure characterization, while others focus on part build and thermal deformation. The field of modeling and simulation is immature in support of AM build processing and is open to new approaches in modeling and simulation to support AM workflows and part builds. This research will fill this technology gap.

**Approach** — The research proposed in this work is to develop and demonstrate a complete workflow through the AM process, using a new computational simulation tool to support a "design by analysis" methodology. There are three key research elements to this effort. First, develop and validate a computational tool that can simulate the part build process in a way that avoids the current failures of other AM modeling approaches. The specific new model features include a fully unstructured Lagrangian grid system for ease of problem setup with dynamic re-gridding using paving methods cast in a finite volume method, a preprocessor step using the discrete element method for modeling of powder scale material through a melting/freezing phase change and nucleation and growth model, and an element-by-element time-dependent nonlinear solution method for improved efficiency. The second element is the design and fabrication of a new reference standard part that addresses the full design complexity available in AM and provides a common framework for simulation validation and comparison of different AM processes. The third element is the use of CT imaging technology and metrology tools to collect as-built part data (dimensions, deformation, and material characteristics) for use in simulation validation.

**Accomplishments** — The research to date has focused on developing the discrete element method (DEM) computer code for simulation of: (1) powder bed deposition accounting for gravity, electrostatic forces, particle shape and size distributions, and surface characteristics, (2) laser-powder interaction

resulting in melt pool formation, (3) melt pool solidification based on nucleation/growth processes, and (4) secondary thermal annealing of solidified melt pools due to melting of adjacent new powder layers.

## 2016 IR&D Annual Report

---

### **Dynamic Response of Steel-Plate and Concrete Composite Small Modular Reactor Structures Under Explosive and Seismic Loads, 20-R8433**

#### **Principal Investigators**

[Kevin J. Smart](#)

Asad Chowdhury

John Stamatakos

Carl Weiss

Inclusive Dates: 12/13/13 – 12/13/15

**Background** — The overarching objective of this project was to develop a modeling approach that would provide a better understanding of dynamic behavior and responses of shallowly buried steel concrete small modular reactor (SMR) containment dome structures subjected to dynamic loads (e.g., explosive loads). This objective was achieved by starting with an existing constitutive relationship [concrete damaged plasticity (CDP)] and explicitly modeling concrete and steel key components (surface plates, intervening concrete, and steel stud bolts).

**Approach** — A three step approach was used:

- Conduct numerical simulations of experiments of steel-concrete (SC) structures with explicit inclusion of concrete and steel components, and compare the simulation results with those from the experiments.
- Repeat the simulations using the CDP constitutive relationship with a simplified ABAQUS model to capture the overall behavior of the SC structure without explicitly simulating the internal steel components (stud bolts), which provide a rational and efficient method to analyze SC structures and constitute the major contribution of this research project.
- Test the simplified ABAQUS model against an independent set of experiments to gain confidence in the model validity. The simplified ABAQUS modeling technique would then be used to study the response of hypothetical underground SC SMR containment structures subjected to selected dynamic loads (e.g., surface explosions) without explicitly modeling each steel and concrete constituent of the SC SMR containment structures.

**Accomplishments** — Numerical simulations were conducted for both in-plane and out-of-plane shear test specimens as well as an unconfined compression test. Load versus strain curves from the numerical simulations were compared to experimental results with a focus on matching specific load-strain points (i.e., concrete cracking strength, steel yield strength, maximum strength). The SMR containment structure was analyzed without explicitly modeling the steel stud bolts. The temporally and spatially varying pressure load produced strongly nonuniform deformation of the containment structure with maximum induced displacement in the range of 9 to 11 cm. The complexity of the pressure loading history is manifest as oscillatory deformation of the containment structure, as well as induced horizontal accelerations. Despite the induced displacements and accelerations, the model results suggest that for the cases studied plastic strain (failure) of the steel and concrete components is quite small (less than 2 percent in outer steel plate) and is focused near the model base.

---



## 2016 IR&D Annual Report

### Investigation into Engine Wear Map Development with Radioactive Tracer Testing, 03-R8479

#### Principal Investigators

Craig Wileman

Peter Lee

Mike Moneer

Inclusive Dates: 07/01/14 – 03/31/16

**Background** — Stoichiometric natural gas engines are becoming more widely used in on-highway transport applications. With reduced natural gas prices, fleet operators may find a move from diesel fuel to natural gas advantageous. Compressed natural gas is a cheaper alternative to diesel and a more energy-dense fuel on a mass basis. With U.S. national averages for diesel and compressed natural gas around \$3.89 per gallon and \$2.11 per diesel gallon equivalent, the upfront vehicle premium of the natural gas-fueled engine can be regained in fuel costs. With radioactive tracer testing, there exist a means of quickly evaluating wear rates in these new powertrain units. Development of a testing method for engine wear rate mapping will afford SwRI the opportunity to respond to a growing product segment through efficient, short duration wear testing. To evaluate long-term durability using currently available methods would require multiple engines to be run over some designed test cycle for hundreds of hours, followed by a complete engine teardown with post-test part metrology to determine the wear incurred on the critical engine parts over the operational period. Even with the current number of manufacturers producing stoichiometric natural gas engines for on-highway usage, a proven method and equipment capable of mapping wear severity across the operating range is a marketable technology.

**Approach** — The goal of the project was to create a wear map for the Cummins ISX 12G, with the steady state wear rates collected through a 21-point run matrix across the operating range of the engine. To achieve the

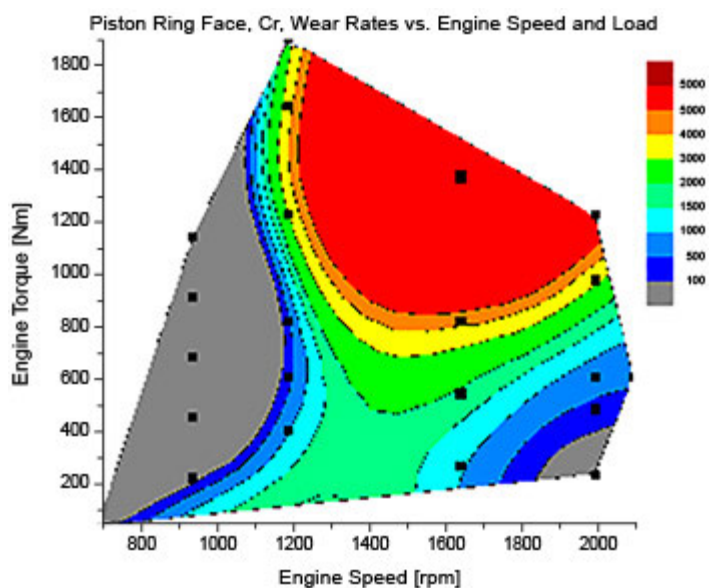


Figure 1: Piston ring face, Cr, wear rates versus engine speed and load.

goal, a two-stage approach utilizing a Plint Te-77 reciprocating, sliding contact tribometer was employed prior to full-scale engine testing. The tribometer testing allowed for the systematic separation and combination of operating inputs that affect part wear rates. The results from the Te-77 tribometer work were applied to construct a method for gathering and interpreting wear rates in the fired engine testing such that the normalized steady state wear rate observed at one set of conditions is repeatable regardless of the preceding engine condition or day acquired. The Te-77 was adapted for use with a gamma ray detector intended to monitor the accumulation of radioactive markers in the system while the rig is operational. The inclusion of the gamma detector in the system permitted monitoring the wear rate response of the parts while altering single inputs such as the applied load and/or reciprocating speed. Through the simplified loading of ring segments running on liner segments in the Te-77 rig, the project examined the repeatability of wear rates on single sets of test pieces across varied but controlled and repeatable parameters such as load, speed, lubricating oil flow rate, and lubricating oil temperature. The fired engine work including 21 operating conditions was completed over four weeks of operation using two reference conditions and two test conditions per day. The reference conditions were tracked over the duration of the program to normalize the daily test condition wear rates against the ever-changing wear state of the engine. Contour plots were created to illustrate the operating condition sensitivity of each of the three radioactive isotopes created to study the piston ring and rod bearing wear within the engine.

**Accomplishments** — The work within the current project resulted in experimental data that defines an operational and statistical approach to engine wear rate mapping. SwRI is currently working on several natural gas engine projects, and has several proposals or pre-proposals for natural gas engine design and/or development. The market for natural gas on-highway engines, and thus for their design and development, has been expanding for the last few years. The knowledge and experience obtained from this testing will support current and future natural gas engine projects. There is a potential for intellectual

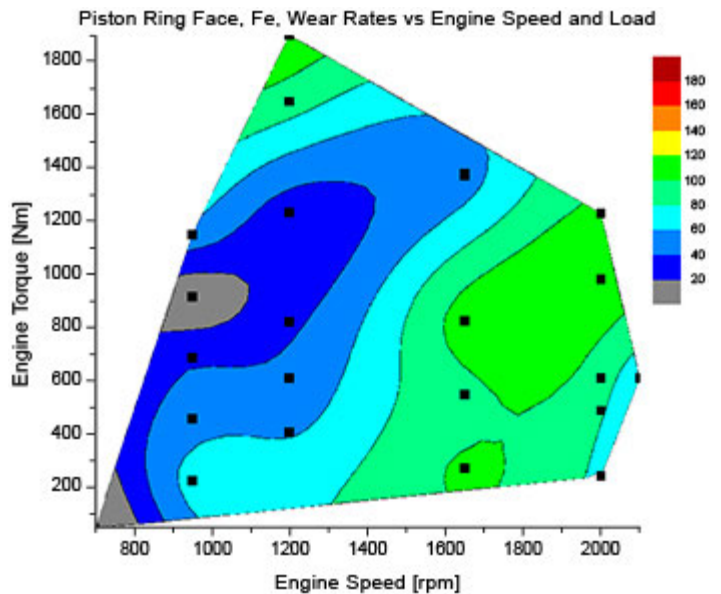


Figure 2: Piston ring side, Fe, wear rates versus engine speed and load.

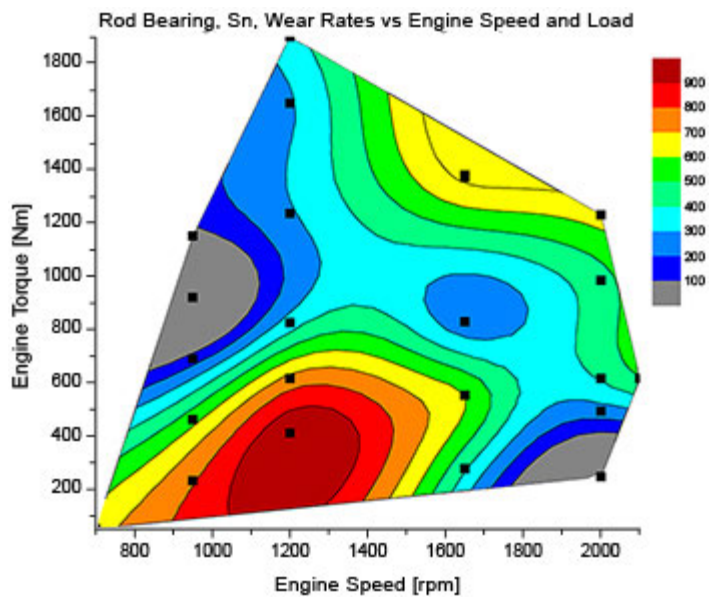


Figure 3: Rod bearing, Sn, wear rates versus engine speed and load.

property on prediction of high wear operating conditions and subsequent control strategies or features to avoid those conditions.

The project offers other significant benefits that include:

- Developing a real-time radioactive wear testing on a Te-77 reciprocating test rig
- Investigating a correlation between a Te-77 wear test rig and an operating engine
- Demonstrating the use of radioactive tracer wear testing on a stoichiometric spark ignited natural gas engine
- Developing a test methodology to evaluate wear measurement across a range of operating conditions and under a continually changing engine "state of wear."

## 2016 IR&D Annual Report

### Lubricant Impact on Fuel Economy — Correlation between Measured Engine Component Friction and Vehicle Fuel Economy, 03-R8502

#### Principal Investigator

Peter Morgan

Inclusive Dates: 10/01/14 – Current

**Background** — Friction reduction is one of the primary methods to improve vehicle fuel economy with future lubricants. Many lubricant manufacturers are targeting low viscosity lubricant formulations in combination with friction modifier (FM) additive chemistry to reduce friction losses in modern engines. Low viscosity formulations can reduce friction losses in areas where hydrodynamic lubrication is prevalent, such as crankshaft or camshaft main bearings, as well as components that operate with hydraulic pressure, e.g., camshaft phaser actuators. Friction modifier additives often serve as a means to reduce friction losses in components that encounter various lubrication regimes due to rapid changes in the directions and speeds of the two sliding surfaces, e.g., interaction between piston or piston rings and cylinder liner surfaces.

**Approach** — SwRI has been working with many lubricant manufacturers to quantify the effects of lubricant formulations on engine and component friction or vehicle fuel economy. However, data that clearly correlates how specific lubricant properties or compounds impact engine component friction (e.g., piston-liner friction) and vehicle fuel economy measurements have not been generated. By utilizing these two established test methods (engine motoring friction measurement and vehicle fuel economy measurement), SwRI is able to demonstrate how specific lubricant properties or additive chemistries impact the friction of various engine components and how those impacts translate into changes in vehicle fuel economy.

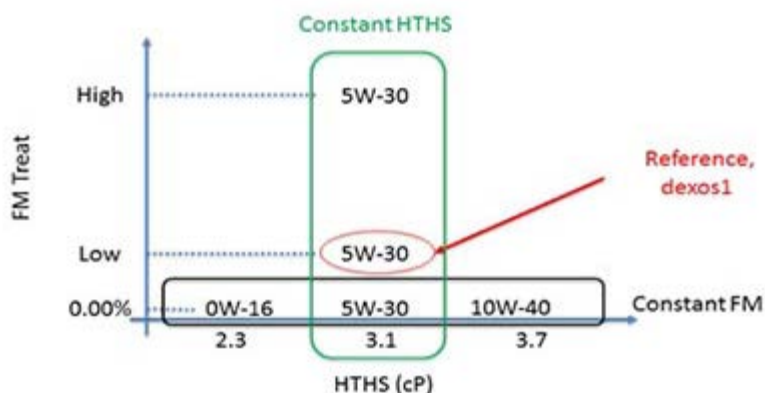


Figure 1: HTHS vs. FM treat.

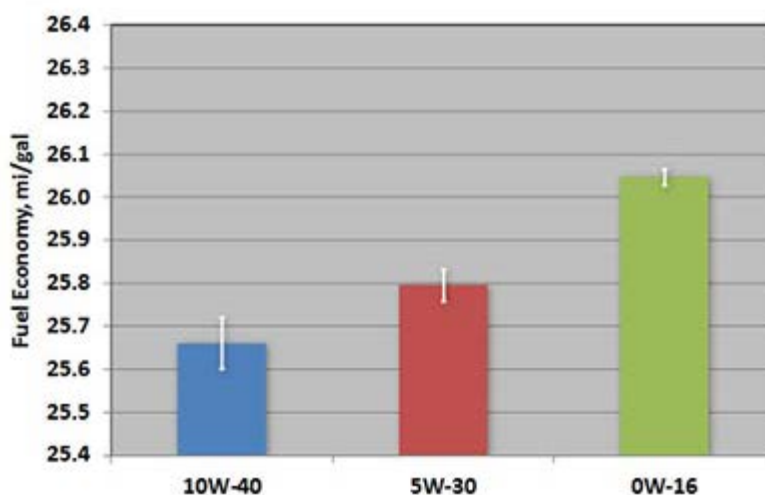


Figure 2: Lubricant viscosity impact on combined vehicle fuel economy.

The five test lubricants illustrated in Figure 1 were identified by SwRI and prepared by Lubrizol. This matrix

of lubricants allows us to look at both the effect of viscosity and FM on the vehicle fuel economy.

The lubricants were tested in a 2012 Chevy Malibu to determine gaseous exhaust emissions and fuel economy. The vehicle was installed in SwRI's light-duty vehicle chassis dynamometer test facility and operated over the Federal Test Procedure (FTP-75) and Highway Fuel Economy Test (HwFET).

Following the vehicle fuel economy measurements, the engine was removed from the vehicle and used for the engine motored friction measurement. Detailed information about engine and engine component friction were obtained from the motoring friction testing.

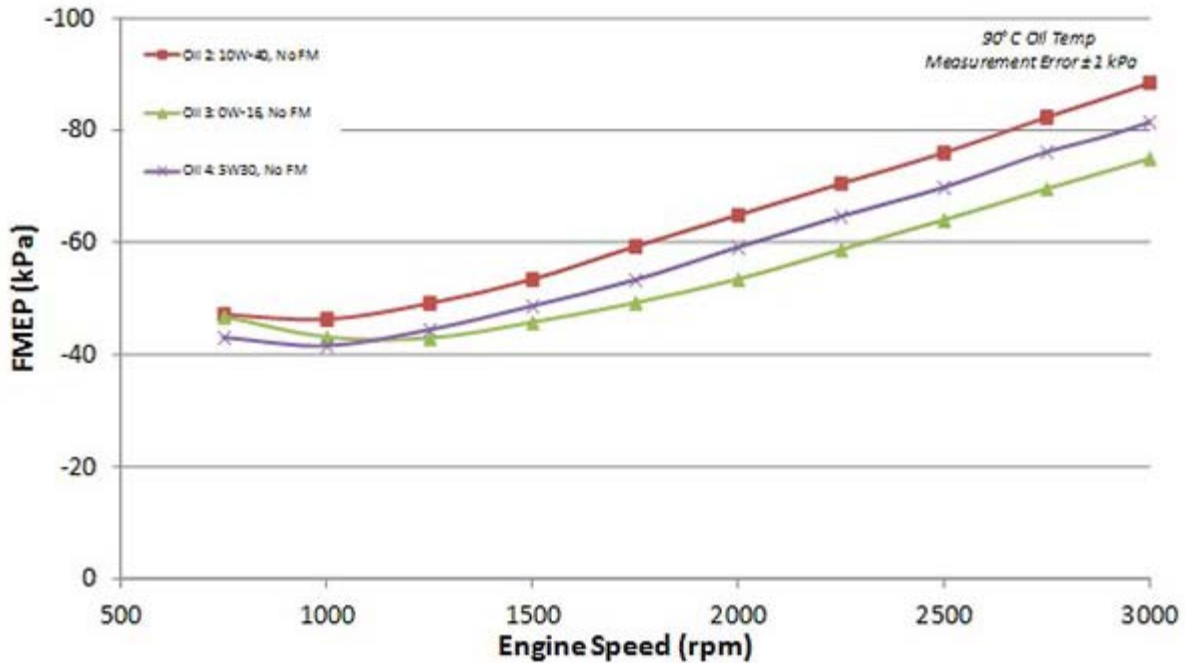


Figure 3: Lubricant viscosity impact on motorized friction test.

**Accomplishments** — With the help of SwRI's Direct Electronic Vehicle Control (DEVCon), the vehicle testing was able to demonstrate our leadership in test repeatability. This repeatability allowed us to see the impact of both viscosity- and friction-modified lubricants.

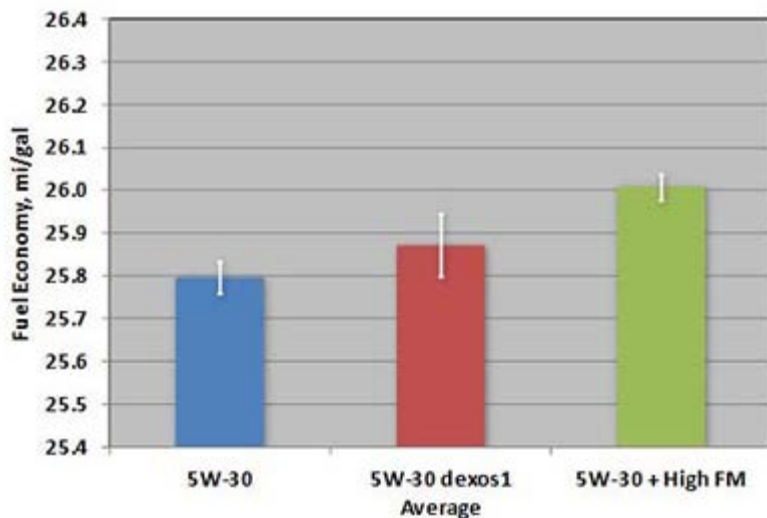


Figure 4: Impact of FM treat rate on combined vehicle fuel economy.

Figure 2 shows the viscosity impact on combined fuel economy from the three lubricants (10W-40, 5W-40, and 0W-16) with no FM. As expected, operating the engine with high viscosity lubricant showed a decrease in vehicle fuel economy and low viscosity lubricant showed an increase in vehicle fuel economy. This change in fuel economy is primarily evident for drive cycle conditions that include significant amounts of low load engine operation and/or cold operating temperatures (e.g. cold start) since the impact of lubricant viscosity on friction is amplified at those conditions.

These operations were verified during the motored friction test. Figure 3 shows the clear difference in viscosities across

almost the entire engine speed range. However at low engine speeds, we were able to see 0W-16 increase in friction due to a loss of hydrodynamic lubrication with this low-viscosity lubricant. This friction increase wasn't enough to offset the benefit over the rest of the engine speed range.

Figure 4 shows the change in combined fuel economy on the three lubricants (no FM, commercial FM dose, and large FM dose) with the same viscosity. The lubricants allow us to look at the impact of operating the engine with differing levels of FM treat rates in the lubricant. As expected, operating the engine with increased levels of FM in the lubricant showed an improvement in vehicle fuel economy. This same improvement can be seen in the motored friction test, Figure 5.

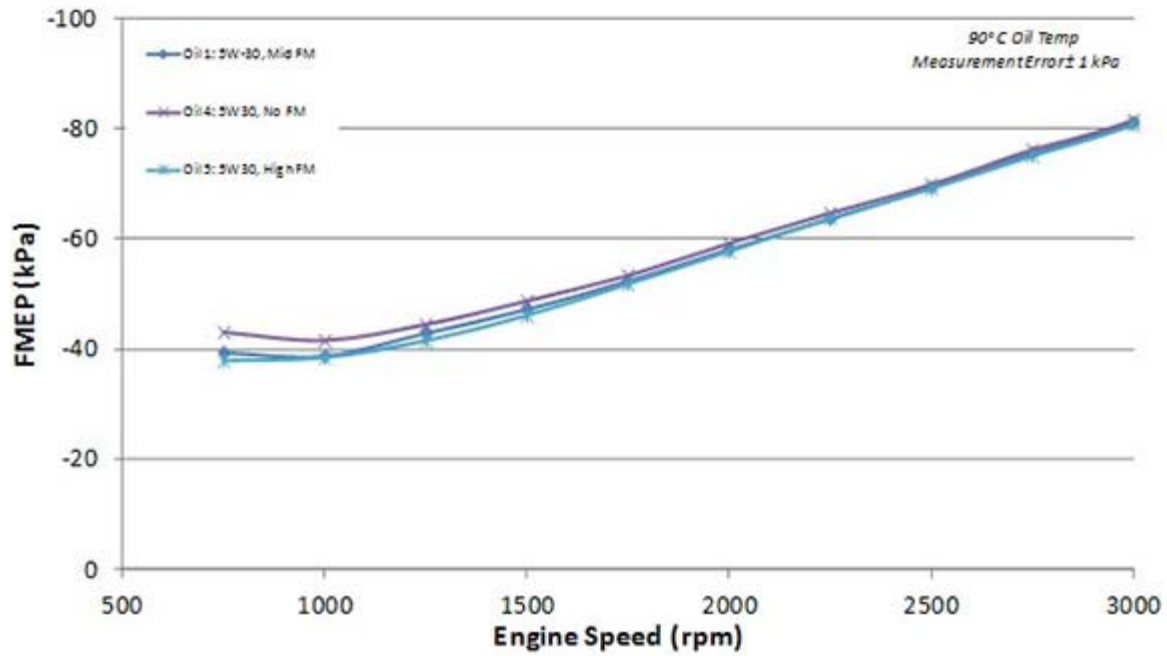


Figure 5: Impact of FM treat rate on motorized friction test.

## 2016 IR&D Annual Report

### Experimental Investigation of Co-direct Injection of Natural Gas and Diesel in a Heavy-duty Engine, 03-R8522

#### Principal Investigator

Gary Neely

Inclusive Dates: 01/01/15 – 12/31/16

**Background** — For the U.S. market, an abundant supply of natural gas (NG) coupled with recent greenhouse gas (GHG) regulations have spurred renewed interest in dual-fuel combustion regimes that utilize NG for the heavy-duty truck market. The GHG regulations stipulate that by 2017, truck engines shall emit 6 percent lower CO<sub>2</sub> emissions than the reference 2010 engines with an additional 6 percent reduction required by 2027. Combustion of methane (CH<sub>4</sub>), the main constituent of NG, produces up to 20 percent lower CO<sub>2</sub> emissions due to its higher hydrogen content compared to diesel. However, because the NG is injected into the intake manifold, a homogeneous NG and air charge are subject to the compression process, packing some of the charge into piston crevice regions that are difficult to oxidize during the combustion process. These crevice losses lead to reduced engine efficiency and unburned CH<sub>4</sub> emissions that essentially offset the benefit of reduced CO<sub>2</sub> emissions of NG combustion, as methane is thought to have a strong global warming potential.

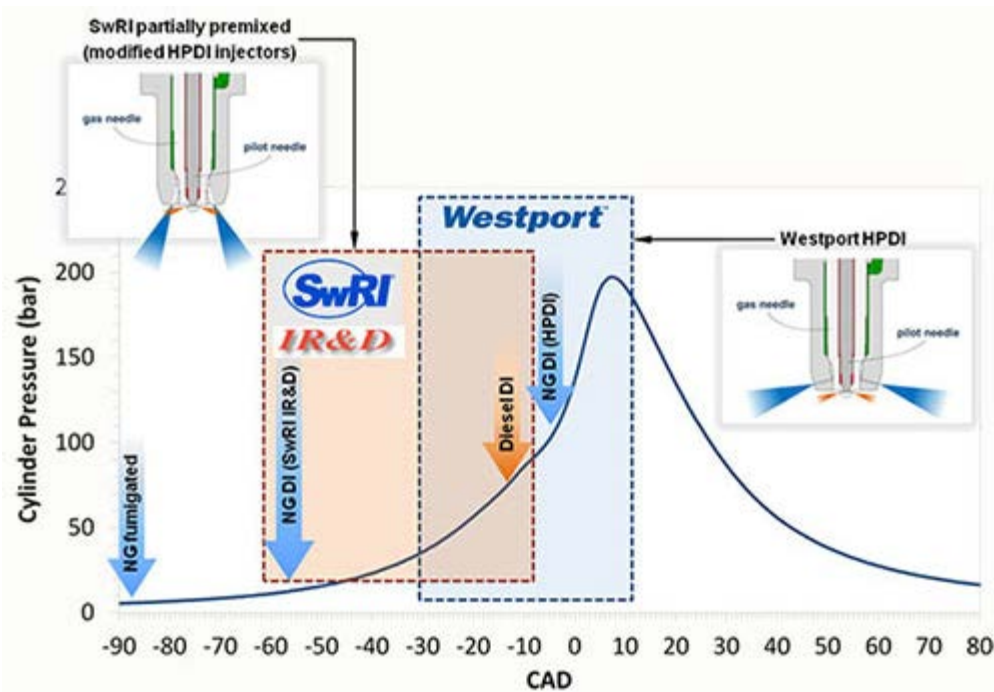


Figure 1: Dual-fuel Injection strategies. HPDI is production strategy while DI<sup>2</sup> is the strategy studied in this project.

**Approach** — This project was aimed at leveraging the unique co-direct-injection capability of the Westport™ High Pressure Direct Injection (HPDI) system to reduce the fuel penalty and methane

emissions associated with traditional introduction of natural gas (NG) in dual-fuel engines. The HPDI system was used to control the amount of NG pre-mixing by injecting NG during the compression stroke, which reduced the crevice packing issue of fumigated NG. The injection strategy investigated in this project, called DI<sup>2</sup>, differed from the production HPDI strategy, as illustrated in Figure 1.

**Accomplishments** — By operating in the DI<sup>2</sup> combustion mode with the baseline injection nozzles, the engine efficiency was improved by more than 2.5 brake thermal efficiency points compared to the most efficient operation using the HPDI combustion strategy. At the same time, the measured combustion efficiency was improved to 98.6 percent, up from 97.1 percent measured for an equivalent fumigated combustion strategy. The improved combustion efficiency led to a 50 percent reduction in unburned CH<sub>4</sub> emissions compared to fumigated engine operation. In addition, modified injection nozzles with a narrower NG spray angle than the baseline injector (see Figure 2) were procured and evaluated on the engine to determine if further combustion loss reductions were available. As shown in Figure 3, the modified nozzles provided an additional 50 percent reduction in combustion losses at the engine condition tested.

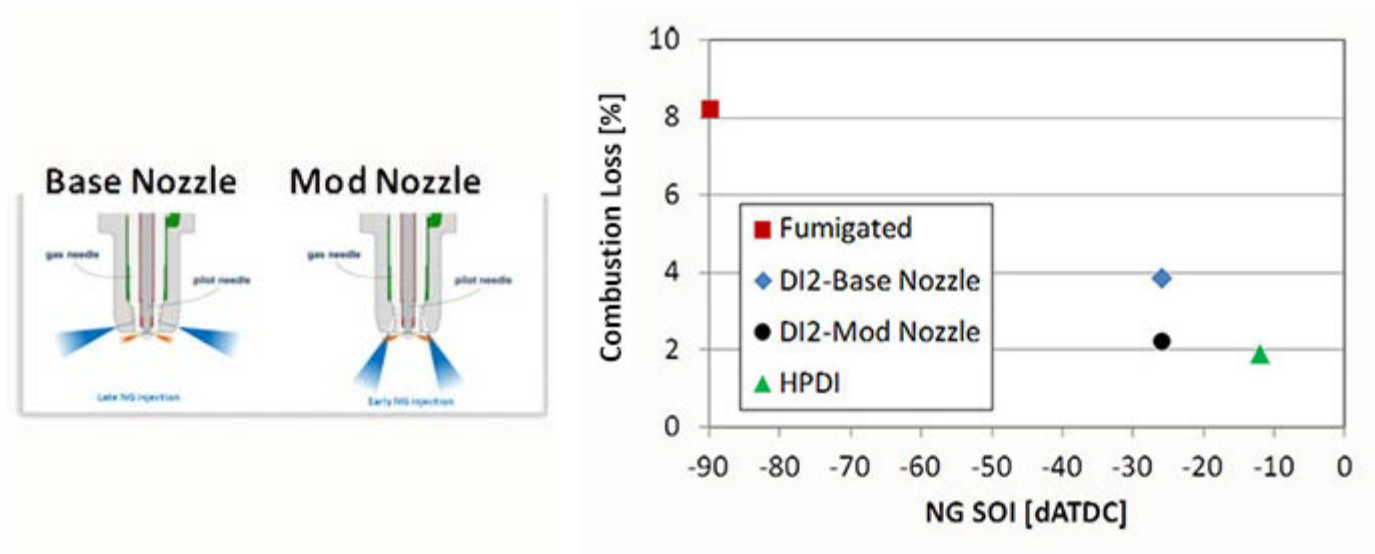


Figure 2: Baseline and modified injection nozzles. Figure 3: Combustion losses for various dual-fuel combustion strategies at 1,500 rpm/9 bar BMEP: Fumigated, HPDI, and DI<sup>2</sup> with baseline and modified nozzles.

The results confirm that significant reductions in unburned CH<sub>4</sub> emissions can be achieved for dual-fuel combustion with advanced injection technologies, positioning the dual-fuel engine well for meeting future GHG regulations.

## 2016 IR&D Annual Report

---

### Combustion Chamber Design Optimization for Advanced Spark-Ignition Engines, 03-R8551

#### Principal Investigators

Kevin Hoag

Inclusive Dates: 04/01/15 – 03/31/16

**Background** — Among the first questions to be addressed in laying out a new engine are those of total displacement and the number of cylinders. Immediately following from the resulting displacement per cylinder, is bore-to-stroke ratio optimization. While these two dimensions can be simultaneously adjusted over a wide range at constant displacement, there is an optimum bore-to-stroke ratio for any particular application. For many years, the optimum bore-to-stroke ratio for fuel-efficient automobile engines has been just below 1.0. With the objective of improved thermal efficiency and reduced fuel consumption, trends in new automobile engine development have included reduced displacement, reduced engine speed, and turbocharging. Another recent trend for optimum fuel efficiency is to increase the tumble air motion during each intake stroke as a means of enhancing turbulence at the start of combustion and increasing flame speed. These trends have led engine developers to revisit the question of bore-to-stroke ratio optimization. Reduced engine speed allows longer stroke engines while maintaining acceptable piston speeds. The combination of reduced engine speed and boosted intake manifold pressure allows acceptable engine breathing with a smaller bore. Increasing the stroke may result in increased turbulence while reducing intake port restriction.

**Approach** — The adjustable deck height feature of the new SwRI single-cylinder research engine shown in Figure 1 provided a unique opportunity to change the engine's stroke while holding all other parameters constant. This allowed an experimental assessment of the effect of bore-to-stroke ratio on combustion performance and engine efficiency. Three crankshafts were machined to provide bore-to-stroke ratios of 1:1, 0.88:1, and 0.75:1. With each crankshaft the deck height was adjusted to maintain a constant compression ratio, and boost pressure and exhaust gas recirculation (EGR) rates were controlled, simulating conditions of a turbocharged engine. The engine was tested at 2,000 rpm from zero EGR to the maximum amount tolerable before the onset of auto-ignition. Tests were done with ignition timing optimized for maximum efficiency, and then repeated with retarded timing for maximum torque output. A reduced test matrix was repeated at 4,000 rpm.



Figure 1: SwRI single-cylinder research engine with adjustable deck height feature.

Ideally the engine bore would be reduced with each stroke increase to maintain constant displacement. This was not possible while holding all other design parameters constant, so scaling of the final results was done to estimate the effects of bore-to-stroke ratio at constant displacement.

**Accomplishments** — A fuel efficiency improvement of three to

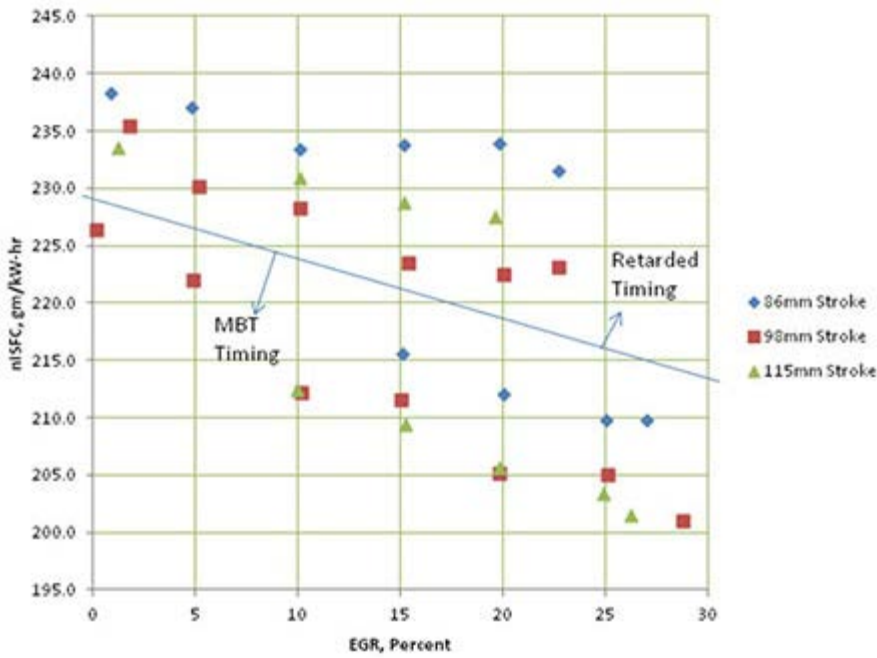


Figure 2: Fuel efficiency improvement with reduced bore-to-stroke ratio.

eight percent, or increase the compression ratio by about one (from 9.5:1 to 10.5:1 for example).

The results were presented at the SAE Fuels & Lubricants conference in October 2016, and the paper was selected for the SAE International Journal.

five percent was found as the bore-to-stroke ratio was reduced from 1:1 to 0.88:1. No further benefit was found in reducing the bore-to-stroke ratio to 0.75:1, and in some cases this was detrimental. Figure 2 provides an example of these findings. Reducing the bore-to-stroke ratio was also effective in increasing the flame speed, accounting for a portion of the efficiency improvement. A scaling exercise based on flame speed and flame travel length allowed the effects to be estimated at constant displacement. It was estimated that the increased stroke and reduced bore could be used to increase full-load EGR by about

## 2016 IR&D Annual Report

### Transient Durability Analysis of Aluminum Cylinder Heads, 03-R8611

#### Principal Investigators

Anthony Megel

Inclusive Dates: 12/14/15 – 04/14/16

**Background** — The purpose of this project was to develop initial methods and procedures and investigate potential challenges to performing transient analysis of aluminum cylinder heads verified by temperature differences on an engine during steady-state versus transient operation and produce data that can be shown to potential clients to win project work and gain members for the Aluminum Head Evaluation, Analysis and Durability (AHEAD) Consortium. Manufacturers have recently realized that damage can occur due to temporary deformations that occur as the operating condition of the engine changes. When the power level in an engine is increased, the combustion chamber faces of the cylinder head are subjected to the higher levels of combustion heat, which causes increased deformation until the heat flow becomes developed into the water jacket. Similarly, when the power level and engine speed are suddenly decreased, the coolant flow is being reduced at a different rate compared to the heat input the cylinder head. Researchers classify this as a long-term response phenomenon with effects that only occur and can be observed during engine transient operation.

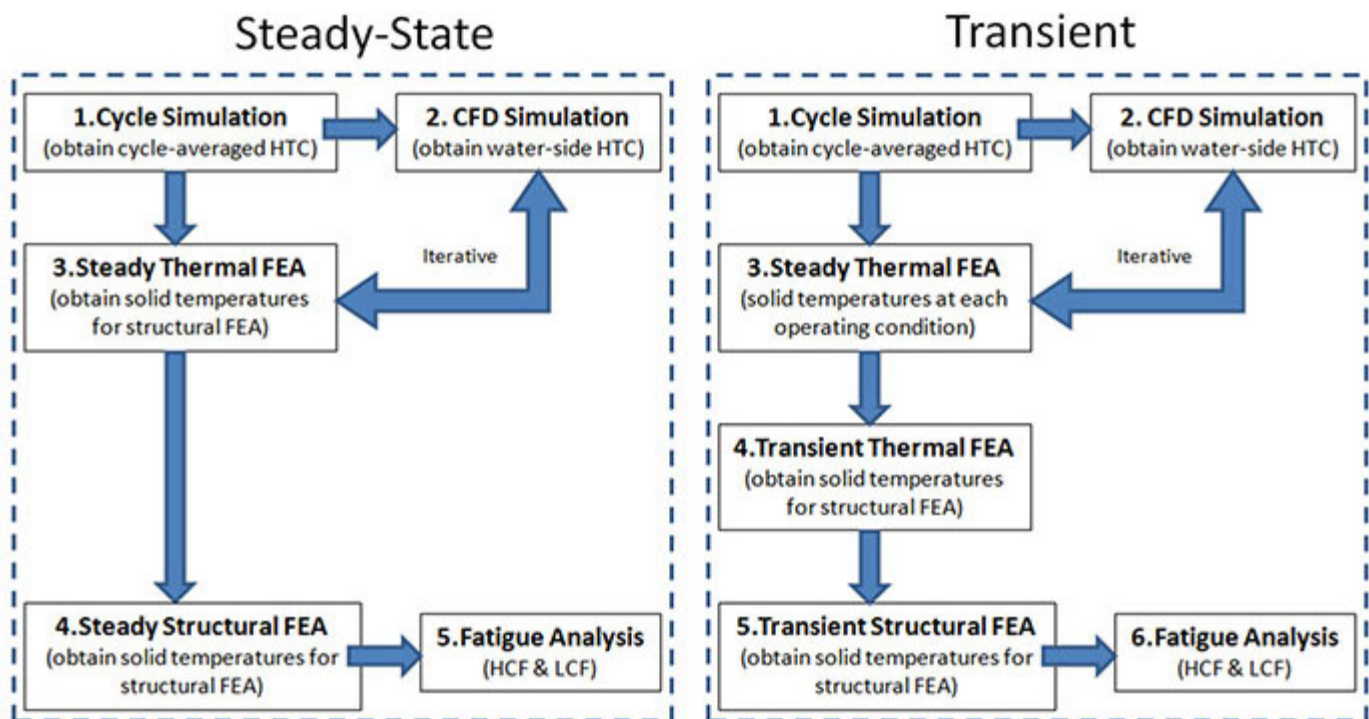


Figure 1: Simplified steady-state (left) and transient (right) cylinder head analyses

**Approach** — A transient thermal finite element analysis model was calculated for the transient cycle from (1) low-speed, low-load, to (2) low-speed, high-load, to (3) high-speed, high load. The water jacket heat transfer coefficients were determined for steady state at each of these conditions and scaled linearly with engine speed during the transient thermal analysis. The model was calibrated to the steady operating

temperature fields measured on a test engine by adjusting the heat transfer coefficients as required.

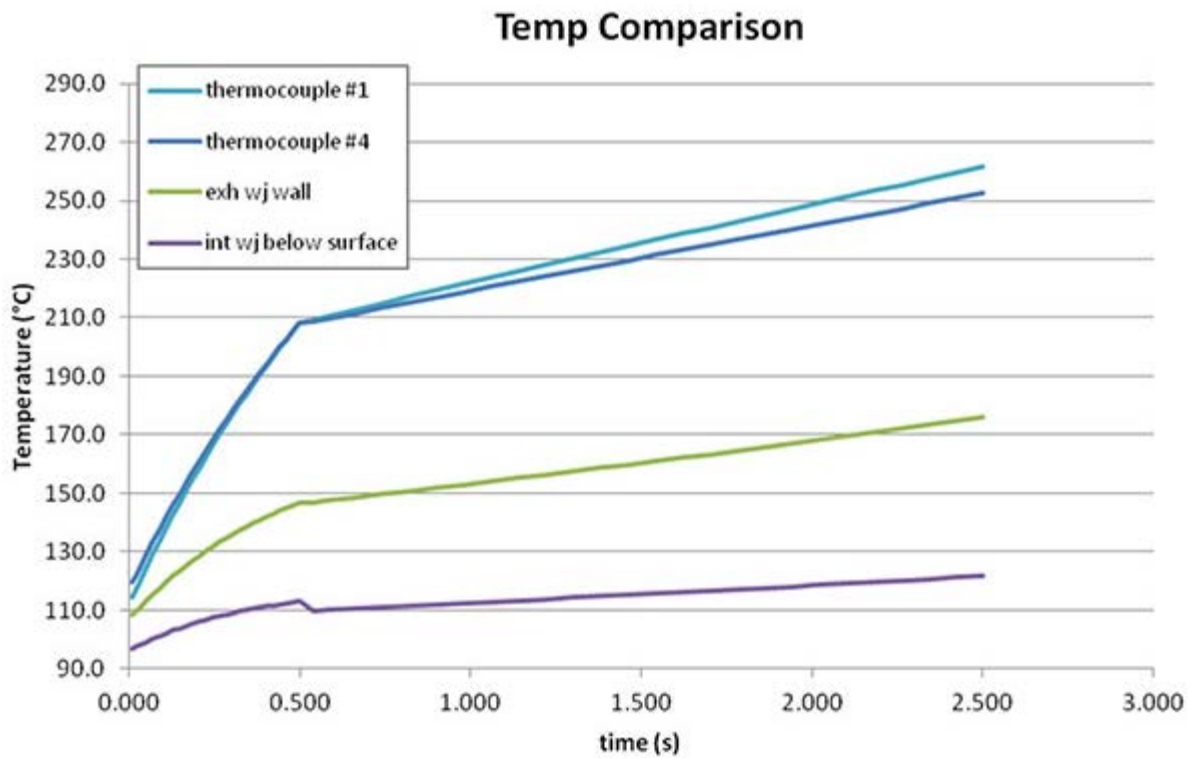


Figure 2: Transient temperature comparison of various nodal locations

**Accomplishments** — The maximum thermal gradient in the engine occurs within the intake valve bridge near the valve seat. At the low-speed, high-load condition, the thermal gradient at this location was three times greater for the transient analysis than the steady-state analysis. The temperature change behavior in the cylinder head also shows the transient effects that would not be recorded with steady-state simulation and validates that structural analysis will produce different stress results in steady versus transient simulations.

## 2016 IR&D Annual Report

### Low Cost, High Brake Mean Effective Pressure, High Power Density Diesel Engine, 03-R8617

#### Principal Investigators

Chris Bitsis

Inclusive Dates: 01/01/16 – 12/31/16

**Background** — For most global markets, small displacement diesel engines used in light duty on-road and off-road applications are facing increased challenges in meeting emissions, cost and packaging constraints as well as competition from turbocharged, gasoline direct injection (GDI) engines. Recent disruptions in the United States light duty on-road market has caused increased uncertainty for the small diesel engine. An opportunity exists for a lower cost, reduced complexity small diesel engine. Reducing some of the cost and complexity of diesel engines could improve the market penetration of these engines.

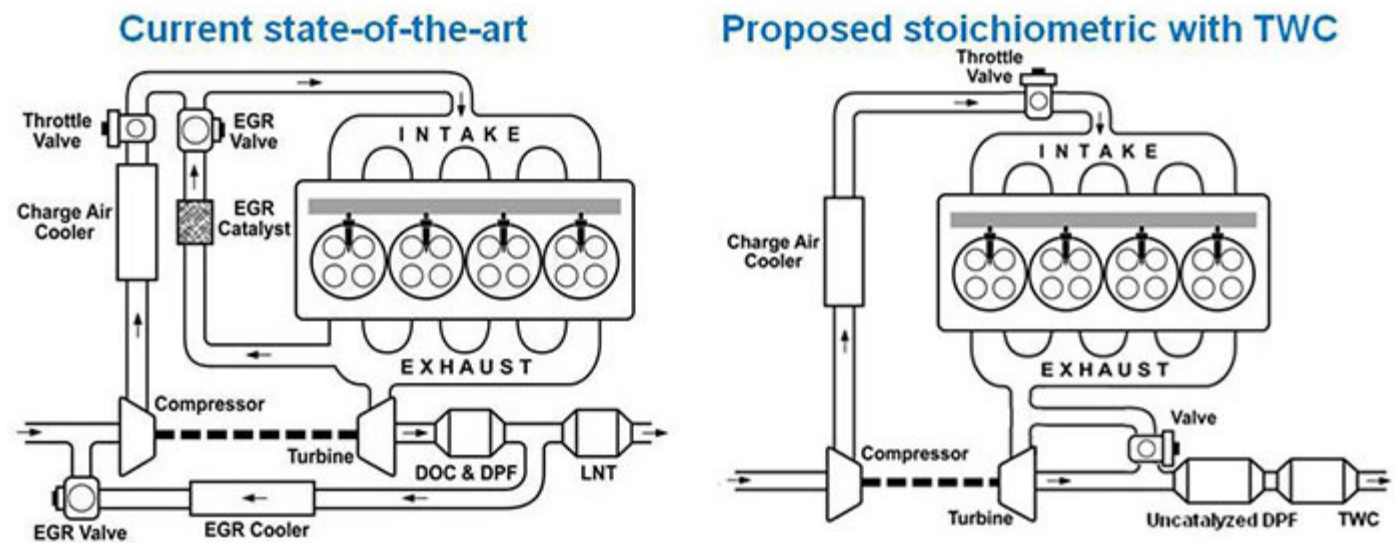


Figure 1: Comparing complex traditional diesel engine arrangement vs. simplified arrangement for stoichiometric diesel

**Approach** — This project will create a low-cost demonstrator diesel engine that can be directly applied to future light-duty or small non-road engine applications. This will be accomplished by utilizing an aftertreatment system with reduced complexity and lower cost, yet still has the potential to meet United States and European Union (US/EU) on-road and non-road emissions regulations. Specifically, it is proposed that a highly downsized, high BMEP diesel engine can be built to operate at stoichiometric conditions such that a modern low-cost 3-way catalyst (TWC) emission control system could be successfully deployed. The major cost-savings of the proposed strategy comes through simplification of the EGR and emissions aftertreatment systems. The cost savings is balanced slightly by the increase in structural requirements of the base engine. A comparison of the complexity of a traditional diesel engine vs. a stoichiometric diesel engine is shown schematically in Figure 1.

**Accomplishments** — This project has only recently completed baseline data collection and simulations for new hardware. Two newly designed pistons have been acquired to reduce engine out particulate matter

(PM) emissions. A rematched turbocharger has been ordered with an increased temperature range, more typical of a gasoline engine. This hardware is expected to be evaluated soon with goals of increasing engine efficiency and decreasing PM emissions.

## 2016 IR&D Annual Report

### Fast Catalyst Light-Off on a Heavy-Duty Natural Gas Engine, 03-R8620

#### Principal Investigator

Tom Briggs

Inclusive Dates: 01/01/16 – 12/31/16

**Background** — The purpose of this project is to develop methods for achieving faster light-off of the emissions catalyst on a heavy-duty natural gas engine, with less fuel consumption penalty than is possible with conventional engine controls. For emissions certification in the U.S., a heavy-duty engine is tested on the heavy duty federal test procedures (HD-FTP) test cycle, as shown in Figure 1. In this test procedure, it is critical to get the catalyst temperature up to 400°C as quickly as possible to control the emissions or the engine will not pass the test. In a demonstration project that SwRI has been executing for the California Air Resources Board (CARB), the tailpipe emissions from a 12-liter displacement natural gas engine have been reduced from the current requirement of 0.2 g/bhp-hr to 0.02 g/bhp-hr. In the process of achieving this reduction, the fuel consumption over the HD-FTP test cycle had to be increased by 2 percent to heat the catalyst quickly enough. This increased fuel consumption is not acceptable in a production system as the U.S. EPA is now targeting a 5 percent reduction in engine fuel consumption as part of new CO<sub>2</sub> standards. As most of the additional fuel consumption is in the first 20 seconds of the test cycle in order to heat the catalyst, this research was undertaken to develop other approaches to heating the catalyst that would have less or no fuel consumption penalty.

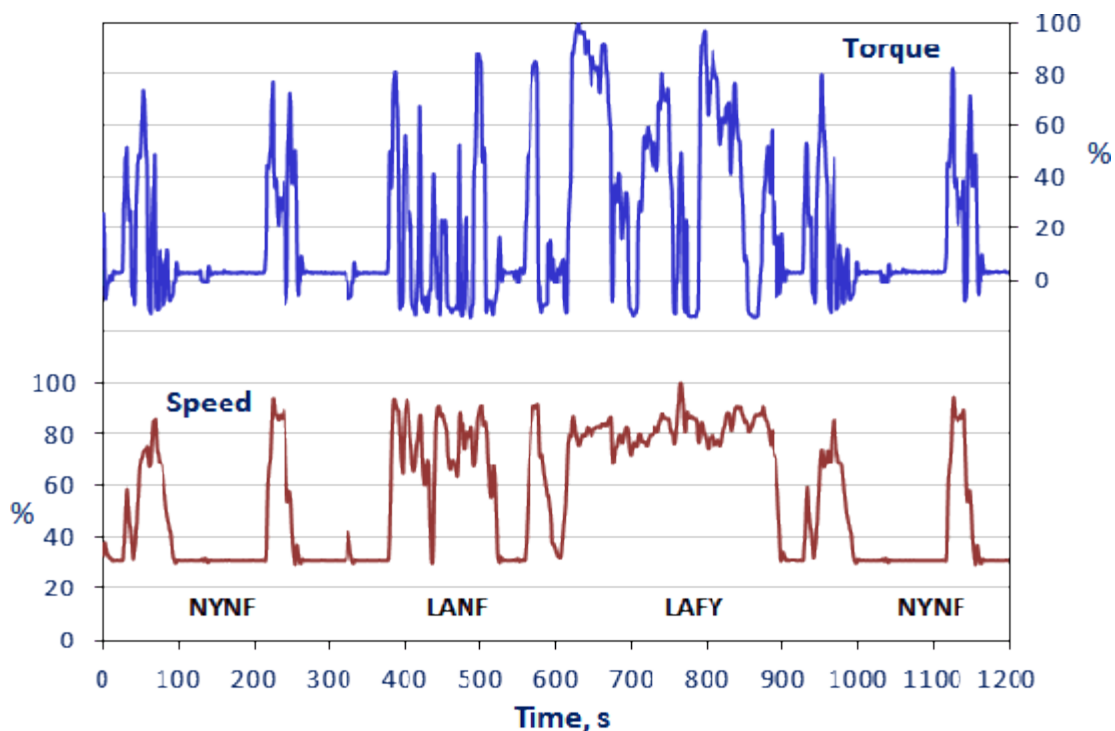


Figure 1: Heavy-duty engine Federal Test Procedure test cycle.

**Approach** — It is already known that most three-way catalyst formulations will allow the oxidation of H<sub>2</sub>

and O<sub>2</sub> at very low temperatures (<100°C). Under normal circumstances an engine produces very little H<sub>2</sub> in the exhaust, but the Dedicated EGR development at SwRI has shown that significant H<sub>2</sub> production is possible under rich combustion. The first stage of the research is to characterize the catalyst response to these rich combustion products. This will provide guidance as to how the engine needs to be run to achieve fast catalyst heating. The next phase of the project is demonstrating methods for providing the rich products of combustion to the catalyst with less fuel consumption penalty. One strategy is to run the engine rich, but to use an air pump to supply additional air to the catalyst where it can react with the rich combustion products. This solution has been used in the light-duty gasoline engine industry before, but is relatively untested for heavy-duty engines. The other approach is to run the engine with three cylinders lean and three rich. This is expected to provide both H<sub>2</sub> and O<sub>2</sub> to the catalyst with minimal fuel consumption penalty and is expected to provide a path to extremely low engine emissions with good fuel consumption.

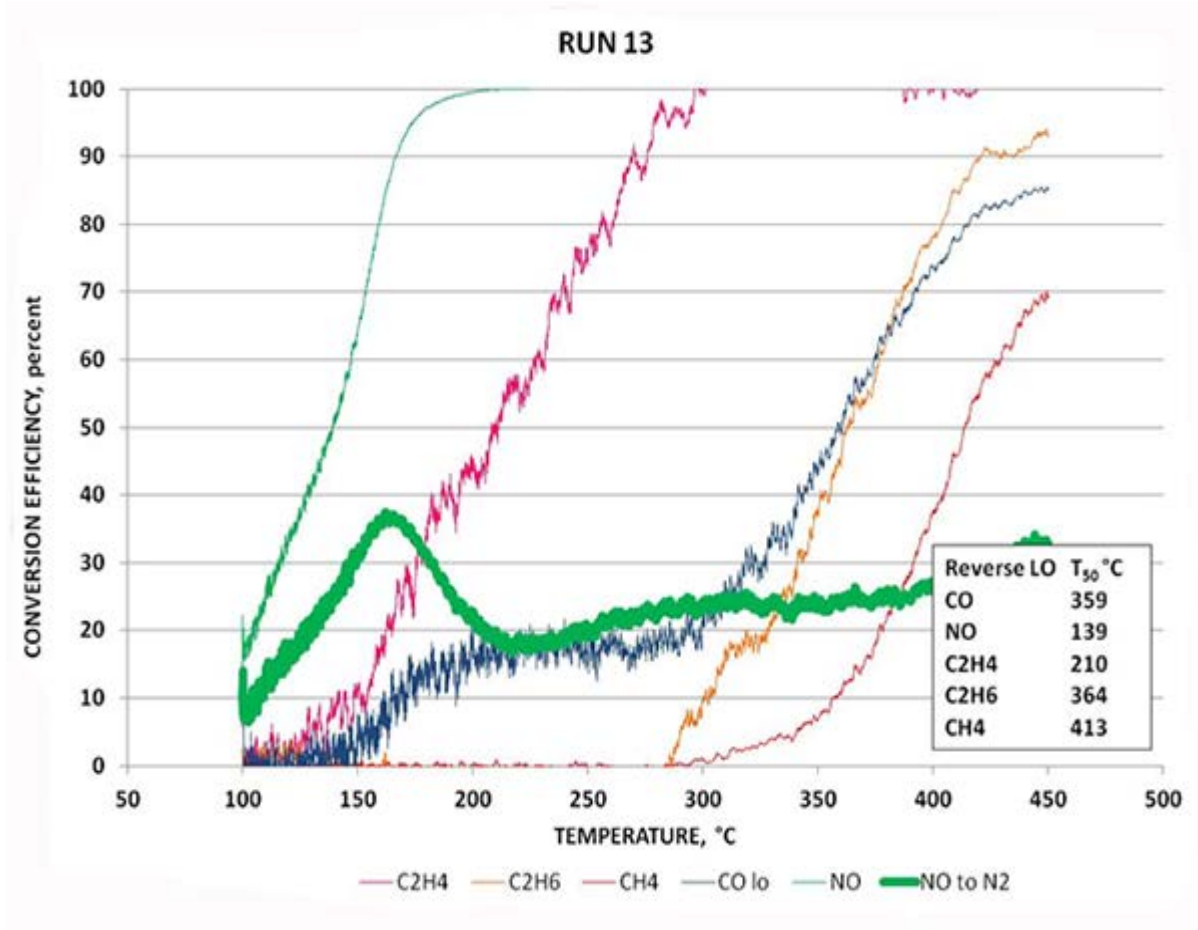


Figure 2: Catalyst bench testing.

**Accomplishments** — The catalyst bench testing has been completed, with suitable engine-out gas compositions identified. An example result is shown in Figure 2, which simulates operation at the rich combustion end of the intended study. It can be seen that the NO reduction begins at 139°C, which is significantly lower than for non-rich conditions. This result will guide our work to demonstrate on-engine solutions that can help achieve future emissions and fuel economy goals.

## 2016 IR&D Annual Report

### Dilute Combustion Assessment in Large Bore, Low Speed Engines, 03-R8633

#### Principal Investigators

Kevin Hoag

Zainal Abidin

Nick Badain, Powertrain Technologies, Ltd.

Inclusive Dates: 03/01/16 – 07/29/16

**Background** — Promising dedicated exhaust gas recirculation (D-EGR) engine results have been achieved in test cells and in a vehicle demonstration. This has led to exploration of further possible applications. A previous project (03-R8534) explored the use of D-EGR engines as a lower cost replacement for medium duty diesel engines in trucks and construction equipment. However, medium duty engines have larger displacement, and tend to require higher torque at lower engine speeds than their automobile counterparts. Transmission and final drive gearing can be used to operate the engine at higher speeds, but this penalizes life-to-overhaul. It is therefore important to ensure that D-EGR combustion system performance can be maintained with a larger cylinder bore, and with high specific output at relatively low engine speeds.

**Approach** — Based on application projections studied in the previous project, an engine having a 107-mm bore and 124-mm stroke, operating at 2,000 rpm at 17 bar brake mean effective pressure (BMEP) was selected as representative. The objective of this project was to use combustion modeling to make an initial assessment of combustion performance under the conditions identified as representative for a medium duty D-EGR application. Beginning from a validated 2-liter, 86-mm bore by 86-mm stroke D-EGR automobile engine, the objective was to scale this engine to one having a 107-mm bore and 124-mm stroke. A 3D computational fluids model of the combustion system (Figure 1) was used along with a previously developed D-EGR auto-ignition model in a 0D engine cycle simulation to predict the onset of auto-ignition. Combustion performance was then assessed at 2,000 rpm, and loads in the range of 15 to 17 bar BMEP. Higher engine speeds and load increases were also assessed to further bracket the findings.

**Accomplishments** — The increased bore diameter results in longer unburned mixture residence time, and this would be expected to increase the problem of auto-ignition. However,

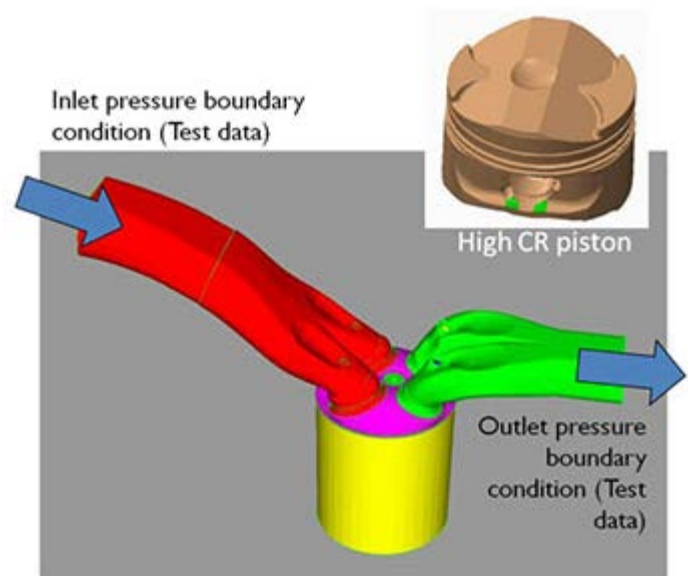


Figure 1: 3D computational fluids model of the combustion system.

the increased bore diameter also increases the flame travel time, reducing the rate of energy release, and resulting unburned mixture pressure and temperature. Under the longer stroke conditions of the medium duty engine, the higher piston speed at a given engine speed increases the turbulent kinetic energy and heat release rate. While this increases flame speed and reduces unburned mixture residence time it also increases pressure and temperature. The result is an increased tendency to auto-ignite, and the need for aggressive timing retard. Predicted results were that sufficient timing retard could be achieved, but with a resulting fuel efficiency penalty. An example is shown in Figure 2, where temperature ahead of the flame is plotted versus crank angle, at 2,000 rpm and 17 bar BMEP. The sudden temperature jump is indicative of auto-ignition, and the curves represent incremental timing retard. As the ignition timing moves later from 24.25 degrees before top dead center to 18.25 degrees, auto-ignition occurs later. As the timing is retarded still further, there is no evidence of auto-ignition. It was concluded that high-load, low-speed conditions can be achieved, but will require the fuel efficiency penalty of retarded ignition timing.

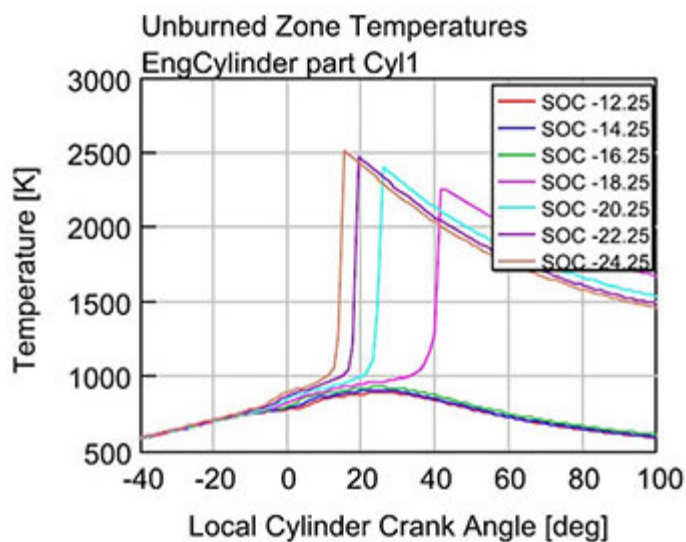


Figure 2: Increased bore diameter results, where temperature ahead of the flame is plotted versus crank angle.

## 2016 IR&D Annual Report

---

### Fuel Economy Effect of Advanced Vehicle Hardware, 03-R8649

#### Principal Investigators

[Matt Blanks](#)

Jianliang Lin

Brent Shoffner

Kevin Whitney

Inclusive Dates: 04/01/16 – 11/03/16

**Background** — Aggressive greenhouse gas and fuel economy regulations require that automakers continually improve the fuel economy of new vehicles. Consequently, automakers are requiring their suppliers to develop advanced vehicle hardware that contributes to these fuel economy goals. The objective of this research is to investigate the possible fuel economy gains that can be achieved through the use of low-friction coatings on engine piston rings, as shown in Figure 1. For this program, a high-precision measurement technique is used to determine a vehicle's fuel economy both before and after a low-friction coating is applied to piston rings. This measurement technique yields results that relate directly to global fuel-economy regulations without the need to extrapolate from bench-style friction testing.

**Approach** — The technique for evaluating the low-friction coating is the implementation of SwRI's Direct Electronic Vehicle Control (DEVCon) system combined with a high-precision chassis dynamometer. DEVCon is used to apply an electronic accelerator pedal position (APP) signal directly to the vehicle's engine control unit (ECU) and eliminates the variation normally introduced by a human driver. Figure 2 shows an example of continuous fuel flow that was measured from three repeat tests using both a human driver and DEVCon for vehicle control.



*Figure 1: Engine piston rings after removal from engine*

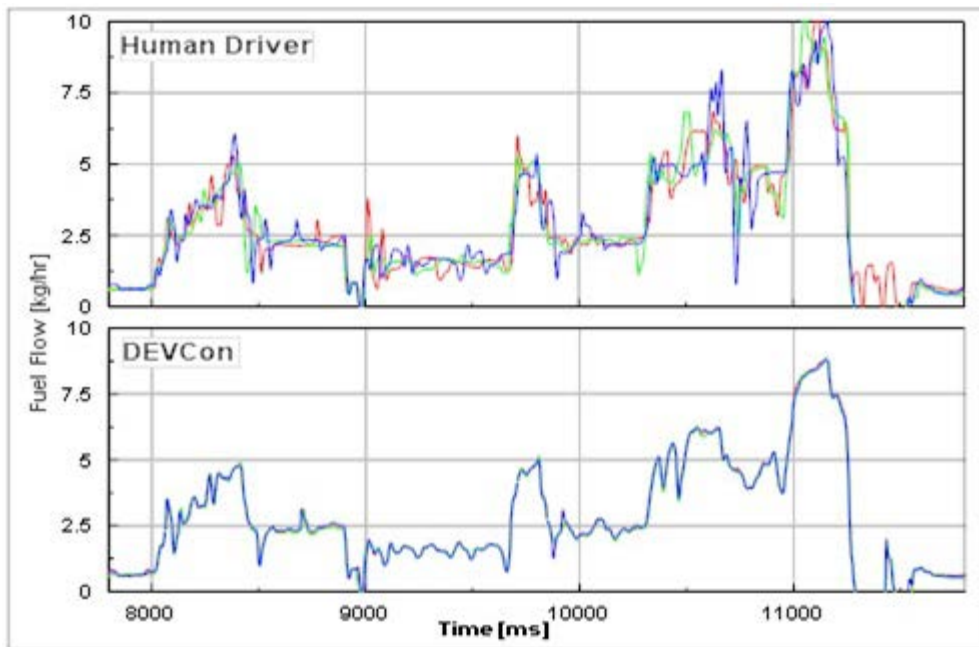
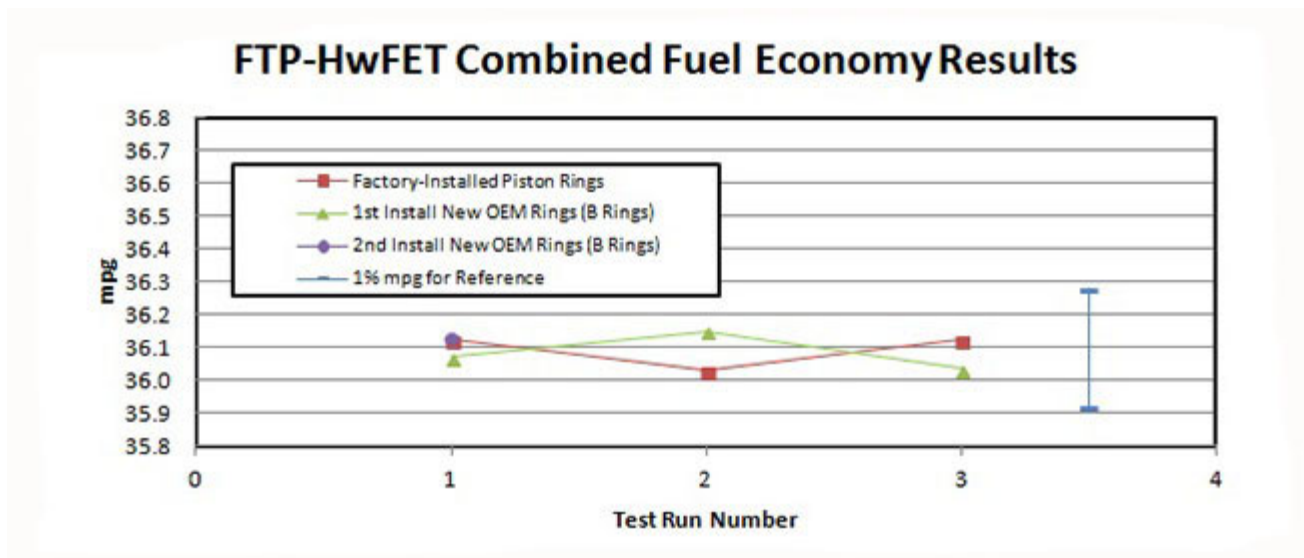


Figure 2: Continuous fuel flow measurement with a human driver and DEVCon

**Accomplishments** — The test vehicle's fuel economy has been measured in three configurations using the Federal Test Procedure (FTP-75) and Highway Fuel Economy Test (HwFET) vehicle certification cycles. The first configuration was tested using the factory-installed piston rings. The second configuration used new original equipment manufacturer (OEM) piston rings (B rings) and the third configuration is currently being tested after removing and reinstalling the same exact B rings. Figure 3 gives the available FTP-HwFET combined cycle test results for each configuration.

A major goal of this project was to determine the "engine rebuild" effect on fuel economy. These initial results indicate that an engine can be completely disassembled and reassembled without causing a major shift in fuel economy. This finding is significant and indicates that the fuel economy effect of a low-friction coating or other advanced hardware can be measured using the entire vehicle. Future vehicle configurations will be tested using low-friction coated piston rings bracketed by repeat tests with B rings to monitor drift.



\*Only one test result for the third vehicle configuration was available at the time of this report.

*Figure 3: Vehicle fuel economy results with factory-installed and new OEM piston rings*

## 2016 IR&D Annual Report

### Validating Using Laser Scan Micrometry to Measure Surface Changes on Non-Concave Surfaces, 08-R8562

#### Principal Investigators

Eric Liu

Sean C. Mitchem

Kerry J. McCubbin

Inclusive Dates: 06/22/15 – 11/04/15

**Background** — Contact stylus profilometry is a staple instrument in the field of surface metrology due to its high sensitivity to detect sub-micron level surface deviations in the vertical plane. To evaluate changes in surface topography caused by wear phenomena, contact stylus profilometry requires accurate overlays of the worn surface profile relative to that of the original unworn surface profile using common unworn surface features that are present in both worn and unworn surface profiles. This limits the articles that can be measured and is not applicable to newer engine technology, where previous parts designs only had partial contact between two surfaces but now involve contact that causes wear across the entire surface and eliminates the unworn reference edges that were previously available. SwRI developed a method documented in U.S. Patent Application 14-620,020 utilizing laser scan micrometry (LSM) to measure wear on cylindrical objects that have no unworn features on the surface. The focus of this research involved proving equivalency of the SwRI-developed technique LSM method with the industry-accepted technique of contact stylus profilometry for measuring wear on camshafts that have undergone lubricant testing. For clients to feel comfortable with our new measurement technique, it was important to produce data and demonstrable testing results that showed a level of equivalency in wear measurement results.

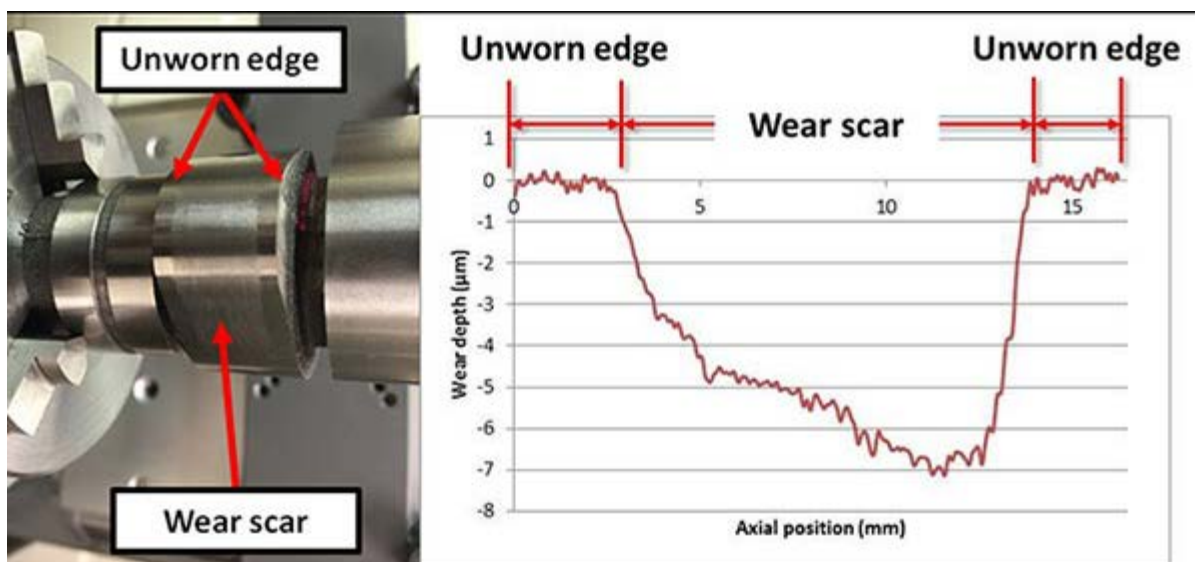


Figure 1: Worn cam lobe test specimen (left) and example of surface profile obtained by contact stylus profilometer (right)

**Approach** — Our approach involved measuring wear on cam lobes with different wear severities using both methods and then comparing the wear measurement results to determine equivalency (see Figure 1).

To validate the accuracy of our method, we needed to improve the angular positioning accuracy over our existing proof-of-concept system (see Figure 2). This was accomplished by integrating an absolute encoder on the rotational axis and developing motor drive algorithms that use encoder feedback to provide precise and repeatable angular positioning. By being able to validate the accuracy of our angular positioning at each measurement point, we were able to compare the measurement data with data collected from measuring the same part on the contact stylus profilometer.

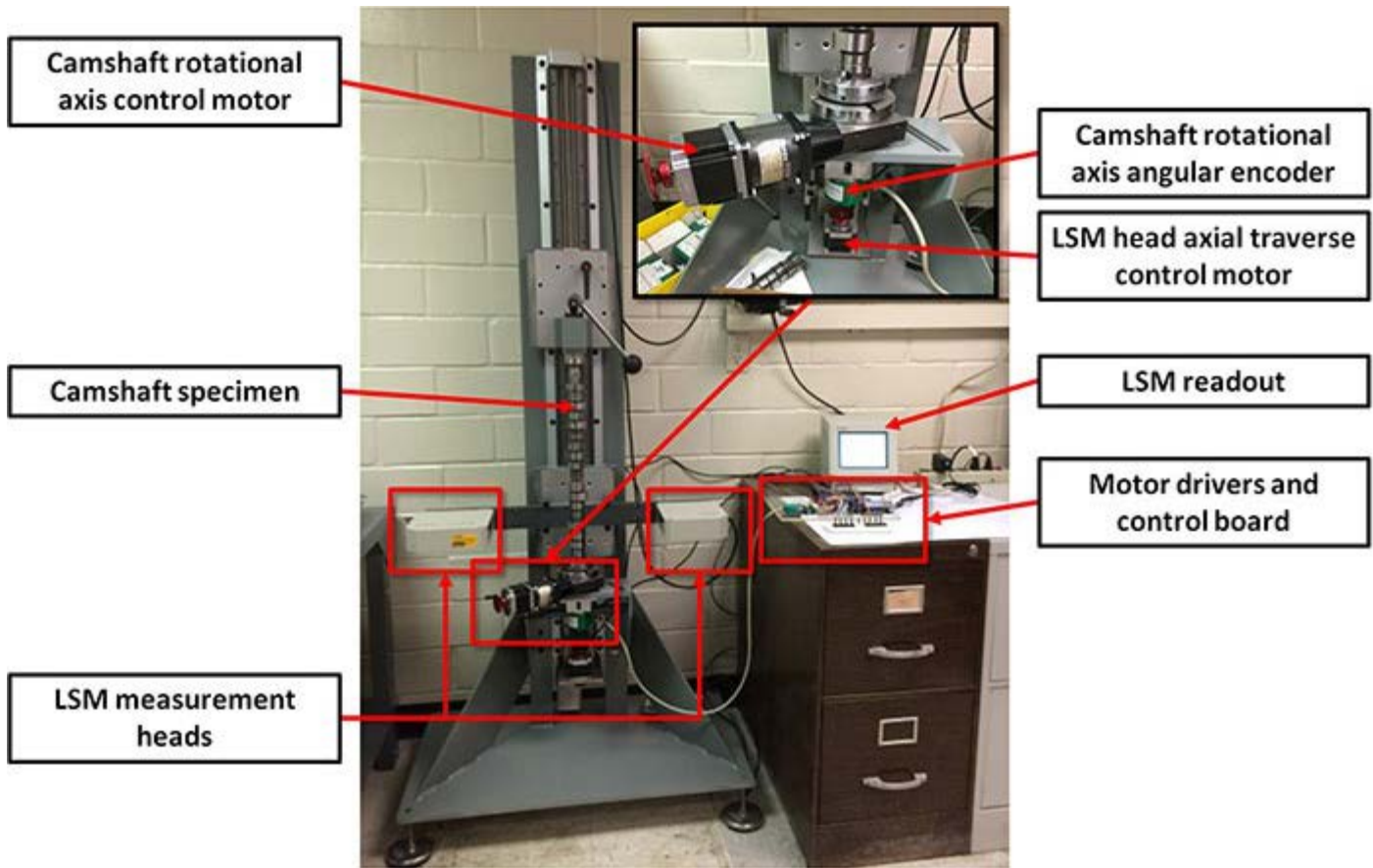


Figure 2: Components of LSM measurement apparatus

**Accomplishments** — Our results in achieving precise angular positioning by using the encoder feedback were 100 percent. We were also able to improve the motor controls to eliminate any potential issues with backlash or partial steps. Measurement results showed that we were able to achieve a measurement equivalency of 81.4 percent on a 10 $\mu$ m-deep wear scar, and 76.5 percent on a 20 $\mu$ m-deep wear scar, well within what would be acceptable to our client base (see Figure 3). Additionally, we were able to validate that we can achieve a 93.4 percent repeatability of  $\pm 2\mu$ m between two separate measurements of the same test sample, a major goal of the research. With the additional capability to measure surfaces that have worn reference surfaces, which contact stylus profilometry cannot measure, we feel confident that we now have a measurement technique that our clients will seek to use in their testing needs.

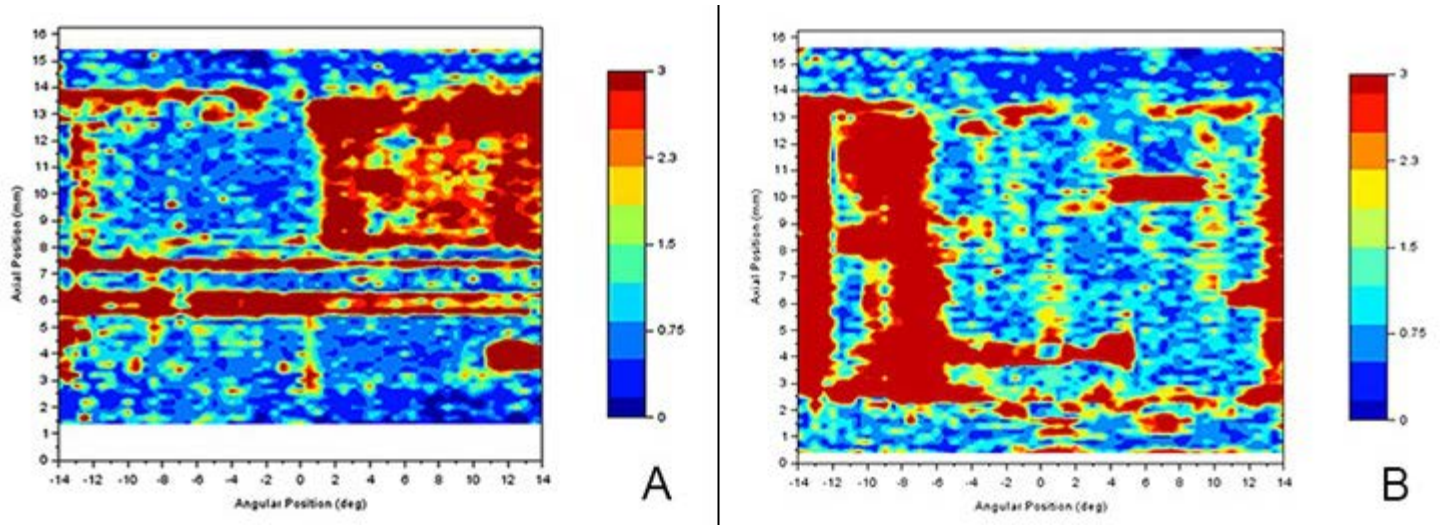


Figure 3: Map of difference between contact stylus profilometer and LSM measurements of cam lobe surface with approximately 10 $\mu$ m-deep (A) and 20 $\mu$ m-deep (B) wear scars within range of -14° to +14° of the zero point

## 2016 IR&D Annual Report

---

### Development of a New PAH Method for Process Oils, 08-R8625

#### Principal Investigators

[Joseph C. Pan](#)

Gillian Soane

Inclusive Dates: 01/25/16 – 05/25/16

**Background** — In 2006, the European Commission of European Union (EU/EC) issued a standard that required all process oils going into tires made or to be imported into the EU must contain benzo(a)pyrene, BaP, less than 1.0 ppm, and "sum of 8 specified PAHs" (polycyclic aromatic hydrocarbons) less than 10 ppm. The official method chosen was IP346, which did not produce data for BaP or "sum of 8 specified PAHs" with which one can evaluate whether or not an oil meets the EU's original standard for PAHs. In 2013, EU/EC published a new PAH method, EN 16143:2013, which was a GC/MS-based method (gas chromatography/mass spectrometry) and produced data for BaP and "sum of 8 PAHs." Unfortunately, this new EU PAH method calls for using a double LC (liquid chromatography) column cleanup for sample preparation, which is very time consuming and labor-intensive. It also loses naphthalene, acenaphthylene, and acenaphthene in the sample preparation part of the process, unfortunate for labs that try to analyze oils to meet not only the EU/EC standards but also the German PAH standard, which calls for monitoring 18 PAHs.

**Approach** — Our approach was three-fold:

- To apply a liquid-liquid partition cleanup method for sample preparation, which involves partition of PAHs and non-PAH hydrocarbons between a polar (example, DMF, N,N'-dimethylformamide, and NMP, N-Methyl-2-pyrrolidone) and a non-polar (such as pentane, hexane, and cyclohexane) organic immiscible solvents.
- To add a silica gel column cleanup procedure for sample preparation
- To use six PAH ISs (internal standards) instead of just three for PAH quantification on GC/MS.

**Accomplishments** — The liquid-liquid partition procedure sped up the sample cleanup process by at least five fold compared with the double LC cleanup method described in the EN 16143:2013 method. The liquid-liquid partition procedure produces sample extracts at least three times cleaner (i.e. less hydrocarbon background noise) than the double LC cleanup procedure. The additional PAH ISs help produce better data qualitatively and quantitatively. For example, without Dibenz(a,h)anthracene-d14, a junk peak in a client's oil samples would have been misidentified as Dibenz(a,h)anthracene.

## 2016 IR&D Annual Report

---

### Investigation of Drought Intensity and Periodicity in South Texas Using Chemical Records in Bat Guano Cores, 20-R8519

#### Principal Investigators

[F. Paul Bertetti](#)

Ronald T. Green

Leanne Stepchinski

Nathaniel Toll

Inclusive Dates: 12/04/15 – Current

**Background** — The purpose of this work is to examine the potential use of guano deposits to develop a robust proxy for climate change and drought history in south Texas. Should sampled guano deposits exhibit chemical and isotopic variations that can be correlated with periods of known drought, this record could be used to model regional changes in recharge to groundwater systems. Results of the project will strengthen SwRI's position as a leader in innovative arid and semi-arid recharge and water resource assessment and will enable pursuing external funding to develop an extended climate record for south Texas, developing longer-term drought frequency, duration, and intensity models, and developing a new market area for assessing longer-term drought history in the arid southwest, where there is no other comparable technology.

**Approach** — The approach of this project is to ascertain whether the frequency, severity, and longevity of droughts can be identified using anion, cation, and isotopic chemical markers sampled from guano cores extracted from the Bracken Bat Cave. Chemical marker data from bat guano cores samples may provide the basis for determining historical climatic cycles in central Texas. Radiocarbon ( $^{14}\text{C}$ ) and stable isotopic ratios ( $^2\text{H}/^1\text{H}$ ,  $^{13}\text{C}/^{12}\text{C}$ ,  $^{15}\text{N}/^{14}\text{N}$ , and  $^{18}\text{O}/^{16}\text{O}$ ) along with other supporting chemical data will be used to establish age and chemical signatures associated with core sample depths. Using other climatic proxies (such as speleothem isotopic data and tree ring data), the data will be correlated to climatic variations. Past recharge will be estimated using the inferred climatic cycle and the empirical relationships between precipitation and recharge developed by SwRI staff. Future recharge predictions will be predicated on the inferred climatic cycle, precipitation/recharge empirical relationships, and published global climate change predictions.

**Accomplishments** — Approximately 24 feet of guano core samples was collected from the Bracken Bat Cave during three sampling events in early 2016. The individual 12-inch core sample tubes were packaged and stored under refrigeration to minimize potential changes due to microbial or other biologic activity until they were processed for detailed characterization and subsampling. Collection of guano from the thickest and presumed oldest part of the cave deposits was not fruitful due to groundwater saturation and associated fluid behavior of the guano, but distinct stratification of the guano was observed in the sampled areas. Upon opening and subsampling, the guano cores revealed distinct physical and compositional layering. For example, guano pellets along with insect and bone detritus enabled identification of more than 20 layer sequences within a nine-foot vertical section. The core subsamples are currently being processed to isolate fractions for specific analyses. Chemical, isotopic, and mineralogical analyses will be conducted once preparation of the isolates is complete. Contrary to initial expectations, the sampled areas appear to represent more recent guano deposition over the course of a few decades rather than centuries. While the relatively recent and short time frame of the guano record will likely preclude determination of longer-term climate trends, it will be extremely useful for calibrating the guano chemical and isotopic

markers with known climate and regional precipitation data. This calibration will be a powerful proof-of-concept tool in the pursuit of funding to extend the climate record using guano cores from other south Texas caves.

## 2016 IR&D Annual Report

---

### Distinguished Lecture Series and Invited Review Paper, 20-R8588

#### Principal Investigators

[David A. Ferrill](#)

Inclusive Dates: 09/14/15 – 07/14/16

**Background** — Unexpected invitations were received inviting the investigator to serve as a 2015-2016 American Association of Petroleum Geologists (AAPG) distinguished lecturer, and prepare and submit an invited review article on mechanical stratigraphy and normal faulting to the *Journal of Structural Geology*. This project was awarded to develop two presentations for an American Association of Petroleum Geologists (AAPG) distinguished lecture series, give these talks during distinguished lecture tours across North America to be arranged by the AAPG, and prepare an invited review article on "Mechanical Stratigraphy and Normal Faulting" for publication in the *Journal of Structural Geology*.

**Approach** — The project was organized into two tasks: "Distinguished Lecture Series" to develop two presentations and cover staff time for two AAPG Distinguished Lecture tours and "Invited Review Paper" to develop the invited review article.

**Accomplishments** — Accomplishments included developing abstracts and presentations on two lecture topics: "Mechanical Stratigraphy and Normal Faulting" and "Mechanical Stratigraphic Controls on Fracturing (Jointing) and Normal Faulting in the Eagle Ford Formation, South Central Texas, U.S.A." Two distinguished lecture tours were advertised by AAPG as the eastern North America tour and the western North America tour. During the eastern tour, lectures were given at four locations in the upper mid-western and northeastern United States. During the western tour, lectures were given at three locations in the western United States and one location in Alberta, Canada. In addition, invited lectures were given in San Antonio to two different geoscience organizations. The Task 2 goal was accomplished by separating the originally planned single manuscript into two separate but related manuscripts. One paper, "Myths About Normal Faulting," was published in a Special Publication of the Geological Society of London titled "Geometry and Growth of Normal Faults." The invited review paper, "Mechanical Stratigraphy and Normal Faulting" for the *Journal of Structural Geology* was completed and submitted to the journal at the end of the project performance period. The project accomplished broader objectives of enhancing understanding of the interplay between mechanical stratigraphy and deformation processes in rock strata, with particular relevance to petroleum exploration and production, and establishing a benchmark of the current state of knowledge of mechanical stratigraphy and normal faulting in the peer-reviewed literature.

## 2016 IR&D Annual Report

---

### **Mechanical Stratigraphy and Natural Deformation in the Austin Chalk, 20-R8637**

#### **Principal Investigators**

[David A. Ferrill](#)

Kevin J. Smart

Ronald N. McGinnis

Alan P. Morris

Kirk Gulliver

Inclusive Dates: 04/11/16 – 08/11/16

**Background** — The purpose of this project was to develop the technical basis to propose and secure future commercial project work for oil industry clients, including a new joint industry project focused on the Austin Chalk, field seminars, and other proprietary analyses for clients related to mechanical stratigraphy, *in situ* stress conditions, geomechanical modeling, and natural deformation (fracturing, faulting, folding) in the Austin Chalk.

**Approach** — The objectives of this project were to identify outcrops that could be studied to understand mechanical stratigraphic character and variability of the Austin Chalk, identify the best analogs for structural styles (extension fractures, faults, folds) that may influence the Austin Chalk reservoir behavior, and perform outcrop characterization of mechanical stratigraphy and geologic structures to represent key aspects of geomechanical behavior of Austin Chalk during hydraulic fracture stimulation. Outcrops of Austin Chalk in south-central Texas (San Antonio area) were investigated, including the upper, middle, and lower portions of the formation. This area represents the nearest outcrop exposure of the Austin Chalk to much of the active drilling and production from the Eagle Ford Formation and overlying Austin Chalk, and provides relevant exposures for understanding deformation within the area of exploration and production interest. The structural style of the exposed Austin Chalk in this region is within the Balcones Fault system, which is the up-dip portion of the Gulf of Mexico marginal fault system. Extensional faulting influences the structural style of the Austin Chalk throughout the exploration and production area of south Texas.

**Accomplishments** — Results of reconnaissance field investigations document significant variability in failure modes (extension fracture versus shear), fracture orientations, and fracture intensity (or spacing) within a 200 km<sup>2</sup> area. Our work documents that incompetent beds within the Austin Chalk localize fracture terminations and in some cases caused fault (shear fracture) dip change (refraction). These results led us to conclude that fracture network characteristics are related to mechanical rock properties and structural position. These differences are potentially important factors for hydrocarbon production from the Austin Chalk, and are particularly important for exploitation of the Austin Chalk as a self-sourced reservoir. Identification and analysis of a diverse array of natural and man-made exposures provided excellent examples for use in future field seminars and the basis for developing additional research. We plan to expand these results by developing training for oil and gas companies exploring and producing in the Austin Chalk, developing and marketing proposals for new oil industry funded consortium project work, and supporting client-specific proposals for structural analysis and geomechanical modeling of induced hydraulic fracturing in the Austin Chalk.

## 2016 IR&D Annual Report

---

### Developing an Integrated Methodology to Estimate Geologic Stress States, 20-R8654

#### Principal Investigators

[Alan P. Morris](#)

David A. Ferrill

Kevin J. Smart

Inclusive Dates: 04/01/16 – Current

**Background** — The *in situ* geologic stress state is an important factor in drilling and completing (including hydraulic fracturing) wells in all hydrocarbon production settings, especially so in unconventional hydrocarbon ("shale" oil and gas) plays. Production from mature resource plays requires refracking existing wells, and drilling and hydraulic fracturing new in-fill wells. Initial production has altered the *in situ* stress state in these mature fields, and new strategies are needed to maintain economic production. Robust predictions of the stress state are required to develop these strategies. In concert with the shale oil and gas revolution has been the remarkable increase in earthquake activity associated with energy production, either as a result of the disposal of fracking waste water or directly from hydraulic fracturing itself. Prediction and evaluation of induced seismicity depends on accurate characterization of *in situ* stress states.

**Approach** — The objective of this project is to develop a methodology that will incorporate a range of geological observations into a robust *in situ* geologic stress estimate. Such observations can include microseismic events and discernable natural deformation features such as faults, extension fractures, pressure solution seams, and folds. We are using existing datasets from field (outcrop) and subsurface examples to develop workflows and analytical tools to estimate stress states. In this process, two new approaches to microseismicity analysis will be implemented.

**Accomplishments** — To date, the project has significantly modified and improved on the existing stress inversion algorithm patented by SwRI. The new algorithm searches a wider range of possible solutions to fit the input data, and provides output to a potential user for quantitative and qualitative evaluation of results. Tests of the new algorithm against well-constrained datasets indicate that further refinement is required to fully utilize the concept of "null data points" — points that represent slip planes that are unlikely to ever have developed, and that can be used to condition the minimization algorithm to avoid spurious solutions.

## 2016 IR&D Annual Report

---

### **Integrated Use of Structural Geologic Framework and Unstructured Numerical Models of Groundwater Flow, 20-R8659**

#### **Principal Investigators**

Nathaniel J. Toll

[Ronald McGinnis](#)

Kevin Smart

Inclusive Dates: 03/12/16 – 09/12/16

**Background** — Numerical models of groundwater flow and solute transport have been advancing in complexity since hydrogeologists began using them. Despite these advances, the ability to represent complex geologic features in three dimensions has eluded hydrologic modelers. As a result, simplifications of geology are made when a conceptual model is translated into a numerical mesh or grid for simulation. Within the geologic community, the ability to model complex three-dimensional solids has existed for over a decade. However, until recently, hydrologic modeling codes have required that geologic strata be represented as continuous layers. Building realistic process models requires cooperation between structural geologic modelers and numerical modelers. The real-world geologic model must be translated into an unstructured grid/mesh and parameterized.

**Approach** — In the course of this study, we investigated workflows to convert complex geologic models to unstructured numerical meshes and grids. Attempts were made to create numerical meshes/grids for the application of unstructured numerical codes to simulate a portion of the Edwards Aquifer that has historically introduced errors to regional aquifer models due to the oversimplification of its geology. The project was organized into four tasks:

- Creating two geologic framework models
- Converting geologic framework models into unstructured meshes and grids using groundwater modeling software packages FEFLOW™ and GMS™/MODFLOW-USG
- Simulating groundwater flow in a cropped portion of the Edwards Aquifer using the unstructured mesh/grid
- Converting the geologic framework models into an unstructured mesh suitable for use in the finite-element modeling software ABAQUS for subsequent geomechanical analysis

**Accomplishments** — A viable workflow to convert structural geological models has been developed for groundwater flow and geomechanical models. The theoretical capability of unstructured mesh models diverges from the practical ability to translate all geologic complexity into a mesh. Using unstructured mesh or grid frameworks for numerical models includes the following potential benefits: the ability to model horizontally discontinuous stratigraphic layers, reduction in model elements because the mesh discretization or refinement can be variable horizontally and vertically, and the ability to represent subvertical faults and offsets of stratigraphic layers due to faulting. The workflows developed in the course of this study provide confidence to market these advances to existing and new clients in the water resources, and energy exploration and production programs.

## 2016 IR&D Annual Report

---

### **Mission Data Selection and Digital Terrain Modeling for Assessing Seasonal Flows on Mars, 20-R8662**

#### **Principal Investigators**

[Cynthia L. Dinwiddie](#)

Brian L. Enke

D. Marius Necsoiu

David A. Stillman

Inclusive Dates: 05/23/16 – 09/23/16

**Background** — High-resolution digital terrain models and orthorectified images are fundamental tools for conducting small-scale investigations of dynamic surface processes on Mars, such as recurring slope lineae and dark dune spot seasonal flows. Highly accurate, but low-resolution Martian topographic data first became available with returns from the Mars Orbiter Laser Altimeter, ultimately resulting in global gridded data sets. The arrival of Mars Reconnaissance Orbiter in 2006 might have revolutionized high-resolution stereo photogrammetry through use of stereo image pairs obtained from the High Resolution Imaging Science Experiment and Context cameras, but production of Martian terrain models from these images remains bottlenecked due to a general lack of community access to state-of-the-art photogrammetric workstations, peripheral hardware, software, and accompanying skillset.

**Approach** — The objective of this project was to rapidly develop SwRI staff capability to select appropriate Mars mission stereo image data and process these data into digital terrain models and orthorectified into products ideally suited for SwRI's Mars science research. The objective was achieved using a suite of free and open-source stereo photogrammetry and automated geodesy tools.

**Accomplishments** — We developed and quantitatively assessed the quality of new terrain models and orthorectified images from both Gale and Russell craters. These are sites of equatorial recurring slope lineae and mid-latitude, seasonally frost-affected sand dunes (including the Russell megadune, the largest sand dune in the solar system), respectively. Knowledge gained through this project can be transferred to terrain model production for planetary bodies other than Mars, as well, using the same suite of software tools. Therefore, new staff capabilities gained from completing this project will support multiple planetary research and data analysis grants and mission team proposals.

## 2016 IR&D Annual Report

### Proof-of-Concept Development of a Traversing Hot-wire Anemometer for Natural Gas Applications, 18-R8593

#### Principal Investigator

[Christopher L. Grant](#)

Inclusive Dates: 09/21/15 – 01/28/16

**Background** — In the natural gas industry, pulsating flow may occur when rotating machinery, such as a compressor, or particular piping geometry produces flow with periodic pressure and velocity fluctuations. When flow is measured in the presence of pulsations, significant measurement errors can result, regardless of the type of flow metering device. Velocity pulsations typically occur at frequencies higher than what is resolvable for most flow meter types and the pulsations can produce flow field distortions that may also contribute to the measurement error. For example, the error mechanism introduced by pulsating flow is not well understood in ultrasonic flow meters that depend heavily on an axisymmetric, swirl-free, fully-developed, turbulent velocity profile at the meter cross section to produce accurate measurement.

In the subject project, in which pulsation effects on flow measurement were studied in a high-pressure natural gas pipeline, a hot-wire anemometer (Figure 1) was chosen to directly measure and map velocity shifts in the flow due to pulsations because the hot-wire anemometer is capable of rapid dynamic response. However, hot-wire anemometers are fragile, involve an unshielded electrified wire, and are typically used for atmospheric air experiments. Therefore, the application of this method to natural gas at high-pressure was unique. The goals of this project were to (1) develop a traversing hot-wire anemometer tool that could measure the local flow velocity throughout the cross section of a pipe in an elevated-pressure natural gas flow and (2) use the anemometer tool to collect meaningful data in a pulsating natural gas flow.

**Approach** — The low-pressure loop (LPL) at SwRI's Metering Research Facility (MRF) was used to develop and test the proof-of-concept hot-wire anemometer tool. The LPL allowed for control of the flow rate, pressure, and temperature of flowing natural gas in an 8-inch diameter line. Additionally, the LPL was



*Figure 1: Hot-wire anemometer traversing system installed in a pressurized natural gas pipeline and a close-up view of a hot-wire measurement probe.*

equipped with a pulsation generator that allowed for the control of pulsation frequency and, to some extent, pulsation amplitude. The prototype hot-wire anemometer tool constructed during this project and a donated ultrasonic flow meter were installed in the LPL downstream of the pulsation generator (Figure 2). The length of the test section was determined by calculating the length of a standing wave at 43 Hz. Without using the pulsation generator, the hot-wire anemometer tool was calibrated *in situ*. Afterward, sweeps of pulsation frequencies between 5 Hz and 45 Hz, typical of the range of pulsation frequencies produced by reciprocating compressors in field installations, were tested at two flow rates. Data from the ultrasonic flow meter, the hot-wire anemometer tool, and additionally installed piezoelectric pressure transducers were recorded for analysis and comparison.

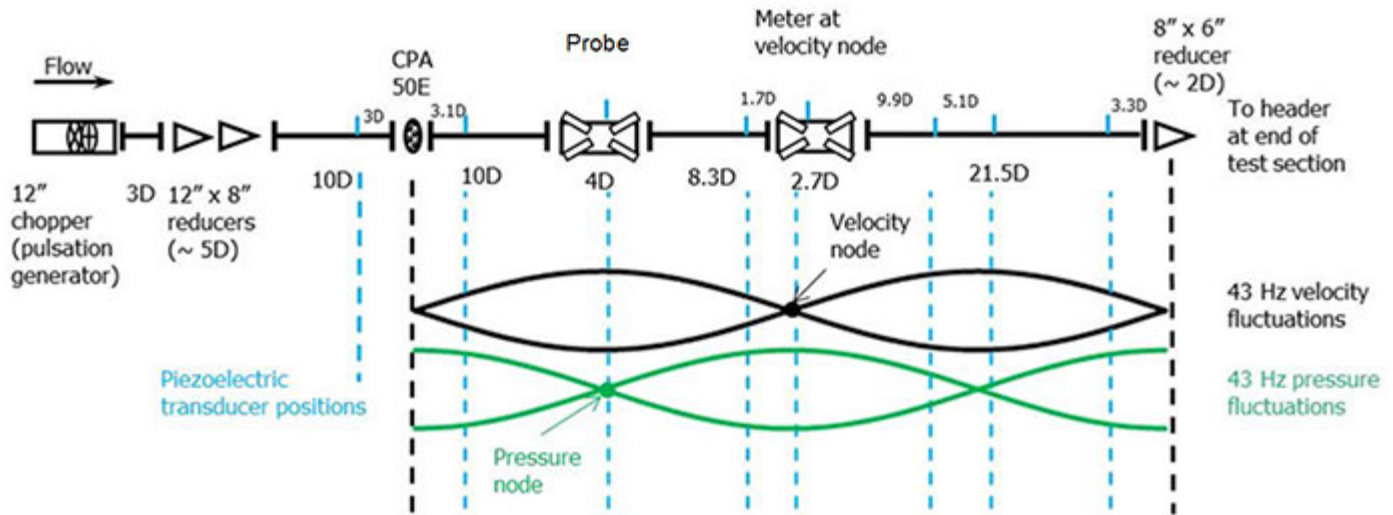


Figure 2: Pressurized natural gas pipeline test section schematic and example acoustic standing wave caused by pulsations.

**Accomplishments** — The hot-wire anemometer tool survived the testing process and collected useful data. In addition, promising research in the field of natural gas pipeline flow pulsation was performed. The hot-wire tool was able to clearly detect velocity pulsation frequencies, including harmonics of the induced frequency. It was also able to measure directly the magnitude of the velocity pulsations, which is an entirely new capability for the MRF. From the data collected with the hot-wire anemometer tool, the effects of pulsations on flow profile in natural gas were directly measured. An example of these findings is shown in Figure 3 as an animation of the changing flow profile over the course of a pulsation cycle.

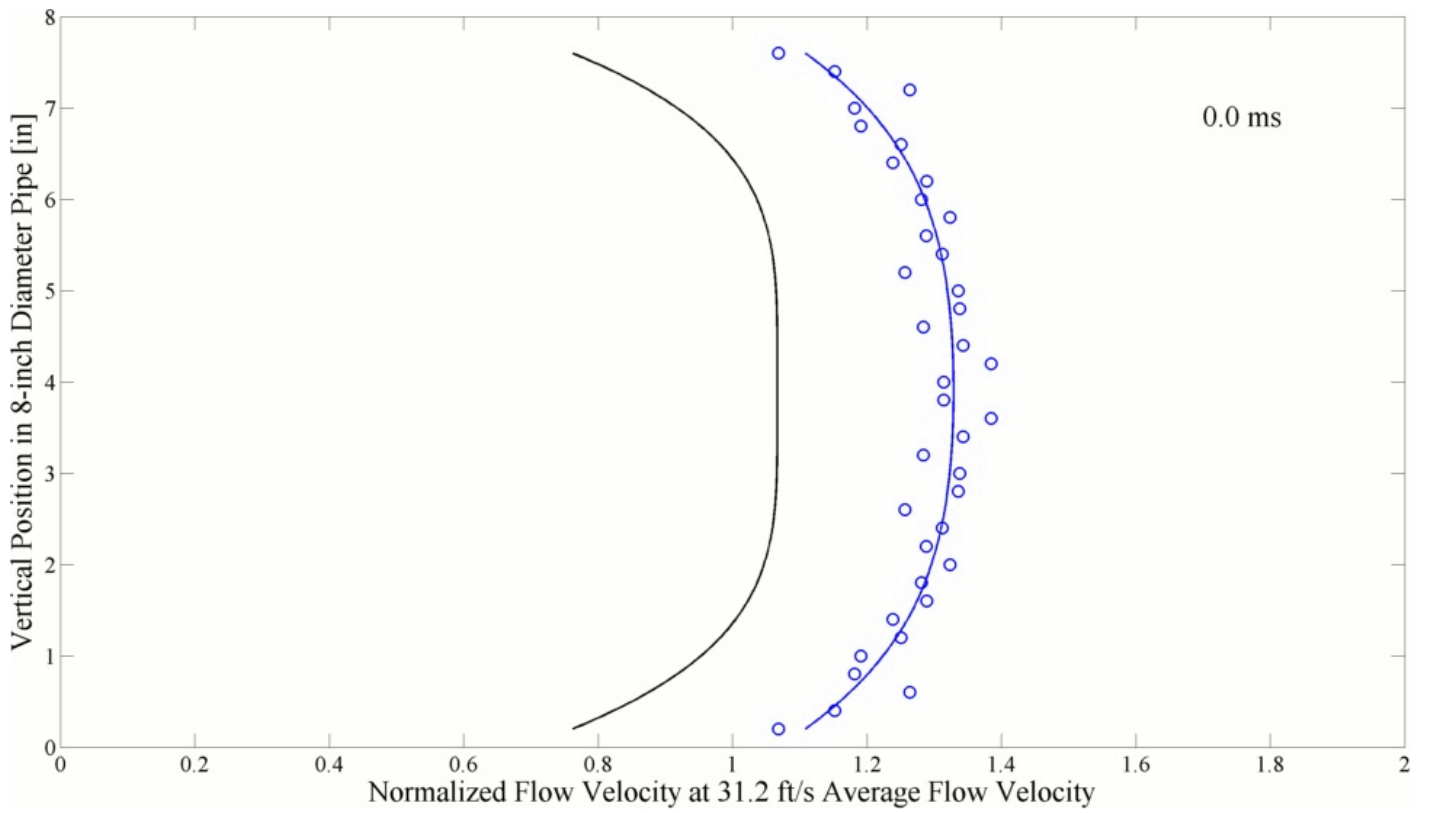


Figure 3: Animation of flow profile distortion caused by pulsation based on direct velocity measurements.

[Click to view animation.](#)

## 2016 IR&D Annual Report

---

### Field Testing of Rotating Equipment Vibration Modes Using Operational Modal Analysis, 18-R8608

#### Principal Investigators

[Jason Wilkes](#)

J. Jeffrey Moore

Tim Allison

Natalie Smith

Jonathan Wade

Dr. Klaus Brun

Inclusive Dates: 08/01/15 – Current

**Background** — The energy industry and particularly the natural gas and hydrocarbon segments depend on the centrifugal compressor to produce, process, liquefy, and transport many different gases. Centrifugal compressors use one or more impellers to impart angular momentum to the flowing gas to produce an increase in pressure, which is referred to as head. As the head developed in the compressor increases, the pressures surrounding the impellers and the rotor assembly become higher, and the dynamic behavior at shaft and impeller seals, axial thrust balance pistons, and impellers becomes more complex. Although state-of-the-art methods are often employed to predict the stability of such rotating equipment prior to commissioning in the field, these units are often shop-tested using externally mounted shakers to assess rotordynamic stability at various operating conditions. This process is costly and requires modifications to the compressor to allow for the installation of an exciter at one end of the shaft.

In recent years, a new technique has been successfully employed to measure the dynamic stability of compressors using only the excitation of the gas as it interacts with the shaft and impellers. This process is termed operational modal analysis (OMA). This technique has been applied successfully in other industries for some time; however, its application in rotating equipment is relatively new and is not well understood. The intention of the proposed investigation is to advance the state of the art for applying OMA to rotating equipment, providing expertise in a market that is sure to grow in the next decade.

**Approach** — SwRI proposes to develop an OMA algorithm, apply it to a high-pressure compressor, and compare results to a conventional forced-excitation parameter technique applied to the same compressor. To measure forced-excitation operating modes, a proprietary exciter will be developed that will serve as a low-cost option for original equipment manufacturers to measure operating modes when the OMA algorithm is not sufficient. The expected outcome of the project is that the two methods will agree well, and publication of the research findings will help to market this new capability to our clients. Additionally, the research program will aid in the setup of a



*Figure 1: Compressor assembly*

new high-pressure compressor that is expected to generate new and exciting experimental work.

**Accomplishments** — During this fiscal year, the primary focus of the project has been to prepare for the compressor facility. The main research compressor was donated by a commercial company in exchange for test data at high compressor discharge temperatures that will be taken after the conclusion of this project. The remainder of the driveline (gearbox and motor) was procured and arrived in June. A compressor skid was installed in an existing facility and designed to allow for the installation of different pieces of rotating equipment, increasing the utility of the driver and gearbox for future research needs. The driveline will be capable of driving equipment having a power of 3MW at a max speed of 14,000 rpm. The skid was designed, fabricated, machined, and delivered. The driveline was installed on the skid using a 30-ton crane, and the equipment was aligned. Following rough alignment, the 80,000-pound skid was moved as an assembly following installation and grouting of the sole plates. The details of the lube oil, dry gas seal, and instrumentation requirements were finalized and these systems were completed. The individual components of the facility are being commissioned, and the compressor will undergo low- and high-pressure commissioning.

## 2016 IR&D Annual Report

---

### Hydrogen and Methane Gas-Phase Detonations, 18-R8614

#### Principal Investigators

Nicholas Mueschke

Alexandra Joyce

Inclusive Dates: 01/01/16 – Current

**Background** — The explosive combustion of hydrogen ( $H_2$ ), methane ( $CH_4$ ), or other hydrocarbon gases results in a rapidly expanding volume of hot gaseous reaction products. Depending on the conditions, the combusting gases may result in the formation of a detonation wave. The high-pressure shock waves created by detonations are hazardous and may cause significant damage. The blast loads from a detonation event typically represent the worst-case scenario for flammable gas releases and is of significant concern in chemical processing, nuclear, automotive, and other industries. Current tools used to predict detonation overpressures may not provide accurate blast loads in situations involving enclosed gaseous releases, complex geometries, inhomogeneous mixtures, and large gas volumes. The goal of this work is to develop a new state-of-the-art predictive capability for simulating the dynamics of gas phase detonations. One challenge to accomplishing this objective includes addressing the multiscale nature of the problem where the detonation wave and combustion region is sub-millimeter in scale, moves at supersonic speeds, and the structural domain of interest is typically large. Also, some mixtures of gases require complex chemical kinetics models to properly simulate the progress of the chemical reaction, heat release rate within the reaction zone, and detonation wave properties.

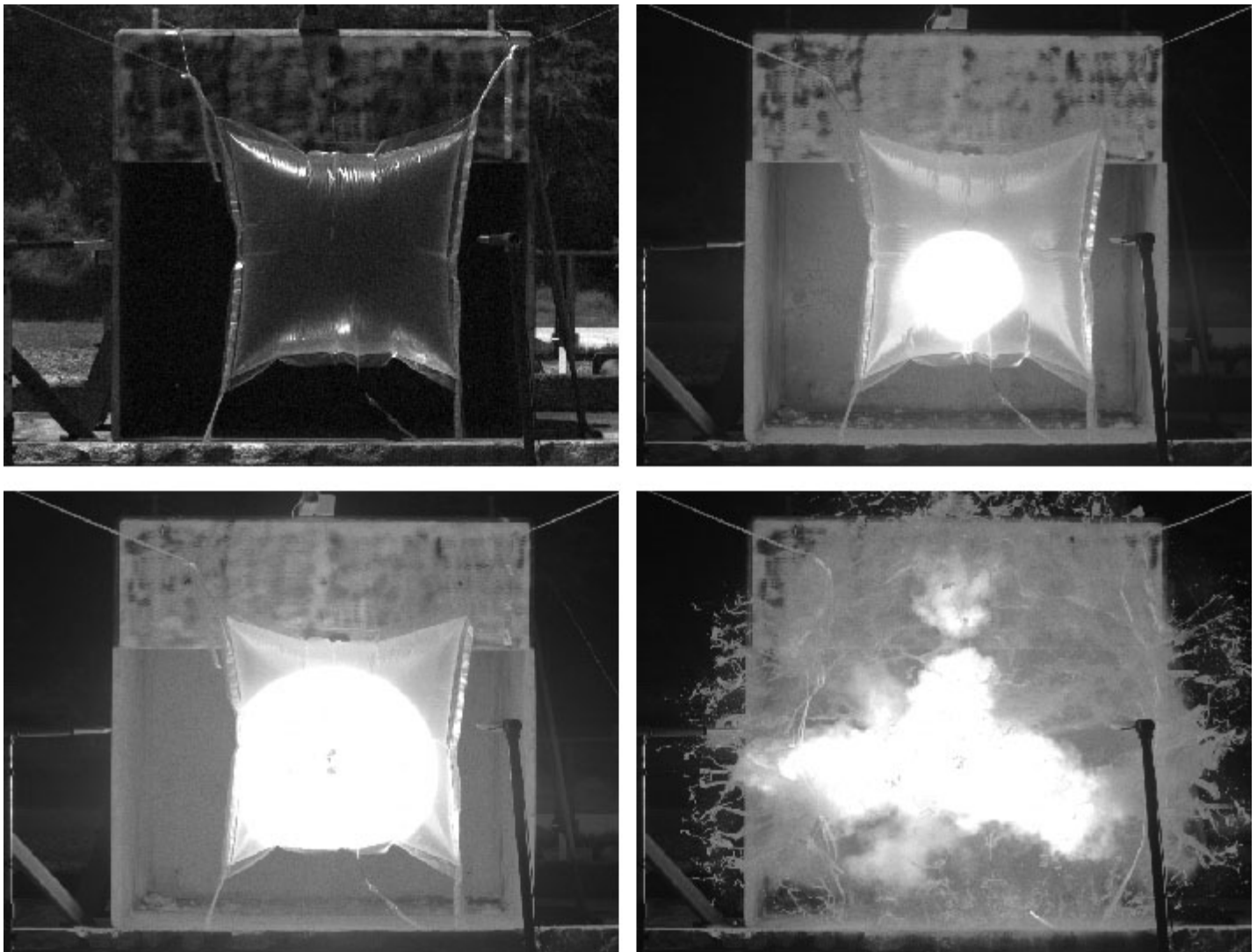


Figure 1: Detonation of stoichiometric  $\text{CH}_4\text{-O}_2$  gas mixture

[View a video of the detonation.](#)

**Approach** — The primary objective of this work is to develop a new computational capability to simulate gas-phase detonations for real-world scenarios that involve large-scale, complex domains and heterogeneous, multicomponent mixtures. This is being accomplished through a combined numerical and experimental approach. Different chemical reaction kinetics models and numerical integration strategies are being evaluated to determine their predictive accuracy, computational efficiency, and numerical resolution requirements. In particular, simplified global reaction kinetics, partial or reduced reaction kinetics, and complex complete reaction kinetics schemes are being evaluated. In addition, the ability to use coarse computational meshes that under-resolve the reaction zone and detonation wave are being tested. Experiments are being performed to measure the overpressures that occur in a partially confined structure in the event of a detonation. The experiments simulate small- and moderate-scale releases of hydrogen and methane. The blast wave overpressures exerted on the internal walls of the test fixture are measured using an array of high-resolution pressure transducers. These experiments will serve as a validation data set for the numerical simulation methods developed.

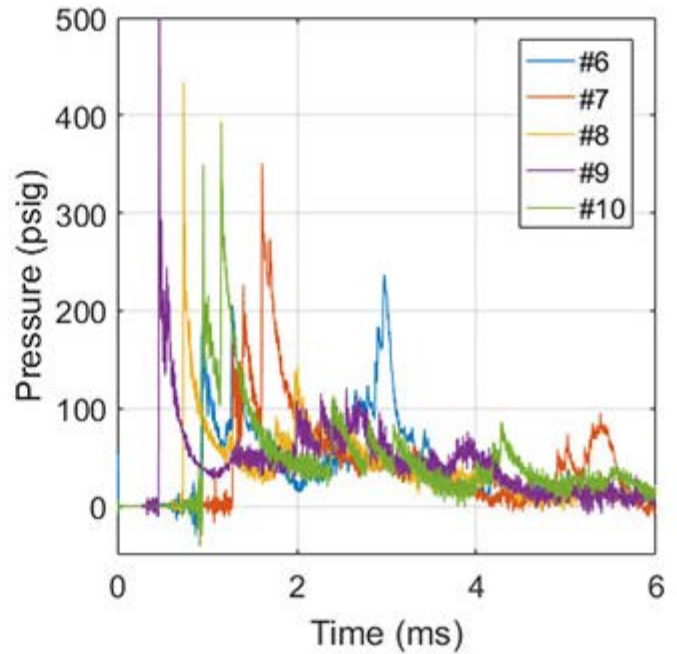


Figure 2: A bag containing a mixture of hydrogen-air within test fixture (left). Measured blast wave overpressure on back wall of structure at different sensor locations (right).

**Accomplishments** — Experimental measurements of detonation wave velocities and pressures have been recorded for a series of unconfined and partially confined hydrogen-air, hydrogen-oxygen, and methane-oxygen detonations. Figure 1 shows a detonation of a bag filled with a stoichiometric methane-oxygen mixture. The spherical expanding detonation wave was recorded using high speed videography at 22,000 frames per second. Figure 2 shows a configuration where a gas leak was simulated by a bag filled with hydrogen and air placed in one corner of the test fixture. Multiple configurations and mixtures have been tested. Figure 2 also shows a measurement of the high pressure blast wave loading of one wall of the confining structure. The development of the numerical algorithms to simulate such detonation events is still ongoing. Initial work has focused on testing different reaction kinetics models and numerical integration schemes in 1D. Figure 3 shows the results of a simulated hydrogen-air detonation using a global reaction kinetics model. As part of this project, the numerical simulation methods that provide the greatest accuracy and computational efficiency will be implemented within a 3D computational fluid dynamics code to allow for the simulation of more complex 3D detonation events.

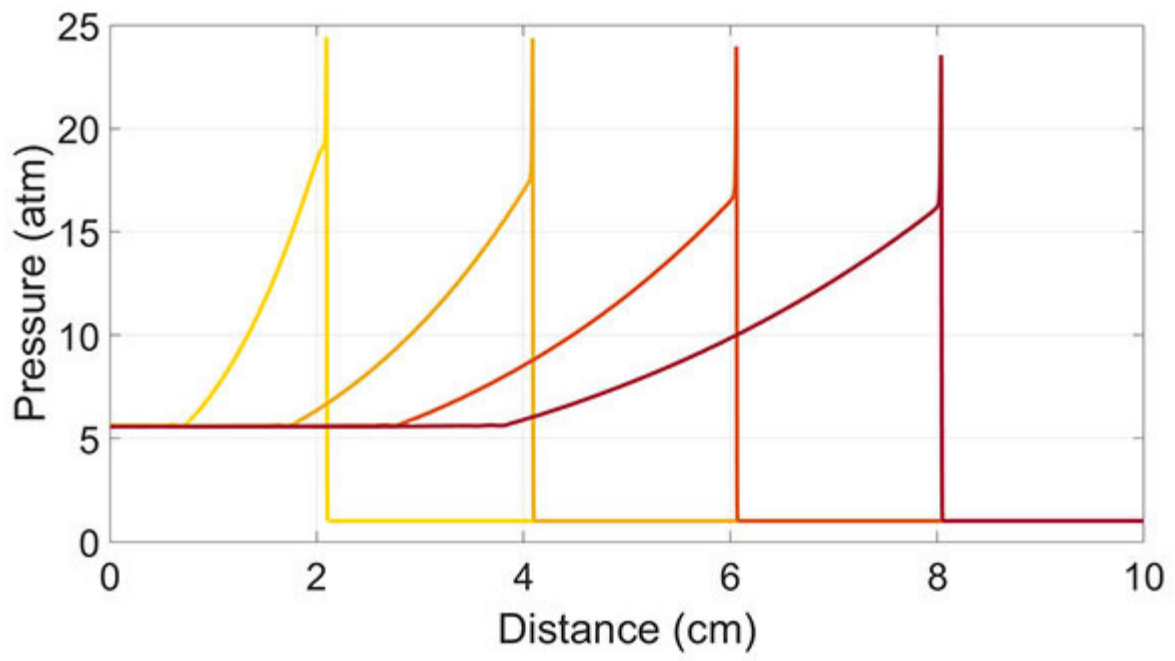


Figure 3. Simulation of hydrogen-air detonation wave

## 2016 IR&D Annual Report

### A Fundamental Assessment of $K_{ISSC}$ and $J_R$ Tearing Resistance Curves in Sour Brine Environment, 18-R8618

#### Principal Investigators

Baotong Lu

Carl Popelar

Inclusive Dates: 01/01/16 – Current

**Background** — The purpose of this project is to develop a theoretical foundation for developing practical methods to establish the threshold for sulfide stress cracking and fracture toughness in sour (wet H<sub>2</sub>S) environments. The thresholds for sulfide stress cracking ( $K_{ISSC}$ ) and fracture toughness ( $J_R$ ) are critical parameters in engineering critical analyses (ECAs) used by the oil and gas industry to ensure the long-term integrity of risers and flowlines in sour service. H<sub>2</sub>S is a common corrosive species that occurs during oil and gas production that significantly degrades the resistance to sulfide stress cracking and the fracture toughness. Unfortunately, the apparent  $K_{ISSC}$  determined from current standard practices depends on test conditions, which can result in significant non-conservative ECAs. Similarly, the degradation of the  $J_R$  tearing resistance in a sour environment is governed by the rate of hydrogen being transported to the crack tip and, hence, is dependent on loading rate, yet no guidance is currently available on what constitutes a sufficiently slow rate needed to obtain a conservative estimate of the toughness.

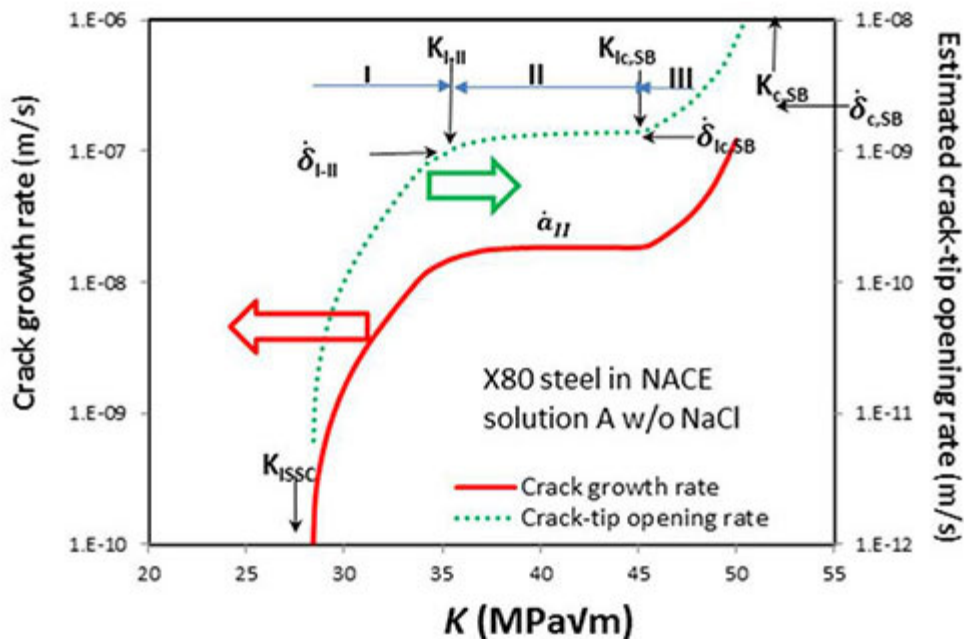


Figure 1: Cracking-tip opening rate ( $\delta$ ) during sulfide stress cracking under sustained loading

**Approach** — Fracture resistance degradation in sour environments is governed by the rate of hydrogen being transported to the crack tip. Thus, the issues with establishing  $K_{ISSC}$  and  $J_R$  can be rectified by a

quantitative model of the crack tip strain rate (CTSR) ahead of a growing crack. Such an analysis facilitates the quantitative assessment of the loading-rate effect on fracture toughness in sour environments as well as the dependence of  $K_{ISSC}$  on crack extension. Achieving this unifying CTSR model will result in improved ECAs for pipes in sour service. Key experiments are being conducted in a sour environment to measure  $K_{ISSC}$  and  $J_R$  tearing resistance to validate the applicability of this model. This project will eventually lead to establishing new methods for determining  $K_{ISSC}$  and  $J_R$  resistance in sour environments.

**Accomplishments** — Analytical expressions for the local strain at the tip of a growing crack have been developed. According to this model, the crack-tip strain is proportional to the crack-tip opening displacement (CTOD), which can be readily measured using standard methods. Further, the CTSR or rate of CTOD can then be expressed as a function of mechanical driving force for cracking (K or J) and crack growth rate ( $da/dt$ ) as a function of yield strength and Young's modulus, as demonstrated in Figure 1. This model provides a theoretical basis to quantitatively assess the loading-rate dependence of  $K_{ISSC}$  and  $J_R$  in sour environments.

## 2016 IR&D Annual Report

### Development and Validation of Liquid-Liquid Separation Modeling Techniques, 18-R8622

#### Principal Investigators

Amy B. McCleney

Rebecca A. Owston

Steven T. Green

Inclusive Dates: 01/01/16 – Current

**Background** — The overall objective of this work is to demonstrate the ability to perform accurate computational fluid dynamics (CFD) modeling of liquid-liquid separation, validating results against test data being collected under a separate Joint Industry Project (JIP). Separators are composed of large vessels with complex internals to promote coalescence of liquid droplets and/or eliminate mist from gas. The design of multiphase separators is a nontrivial task, requiring complex separation physics and knowledge of fluid properties, flow rates, and inlet mixing conditions. Proper sizing of separators has historically been strongly dependent on data collected at field-like conditions. However, most of the available data, design guidelines, and prediction models are based on air/water analyses at atmospheric conditions. Separator modeling using CFD represents an economical option for design, but caution must be used in the setup and interpretation of the data. Many examples are available in the literature of poor agreement between simulation results using particular models and experimental/field data. Therefore, there is a need for reliable methods to simulate separator efficiency and performance for oil and gas industry applications.

**Approach** — A three-dimensional solid model of the test separator and internals has been created as shown in Figure 1, and the fluid domain was discretized. Benchmark CFD simulations comparing the accuracy and complexity of different separator modeling techniques/simplifying assumptions were conducted using two different software packages. Numerical results were compared against experimental data. After determining the optimum submodels for obtaining high-accuracy liquid-liquid separation results, 11 parametric simulations were carried out that varied the viscosity, flow rate, and water cut in the separator. Numerical results from the parametric runs were compared against experimental data. Due to the

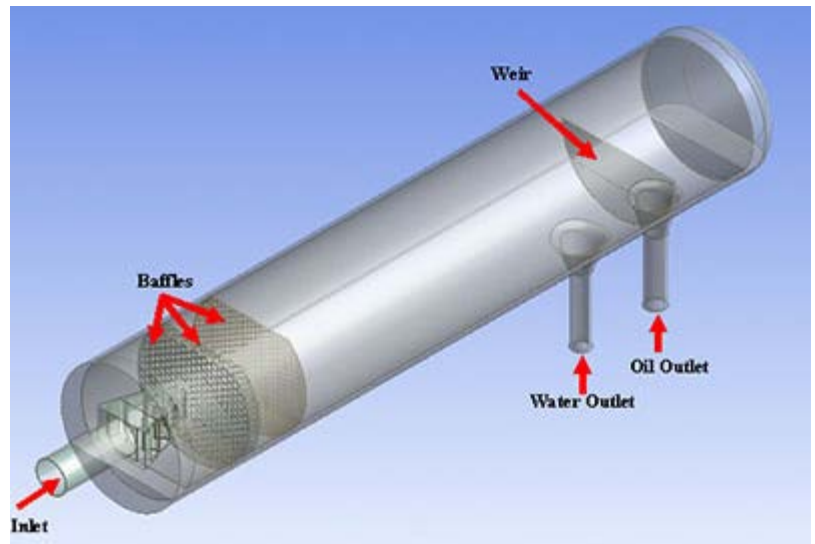


Figure 1: Solid model geometry of the liquid-liquid gravity test separator

unexpectedly high emulsion observed in certain experiments, this project also is investigating the effectiveness of emulsion submodels used in conjunction with the CFD. Two emulsion models from the literature and one developed under this project based on the JIP experimental data are being investigated.

**Accomplishments** — A wide range of multiphase modeling approaches, drag models, virtual mass models, meshing schemes, solution algorithms, and turbulence models were examined in the benchmark

phase. Using an optimum combination of submodels in the CFD setup, it was shown that overall separator efficiency could be matched within 2 percent of experimental data using either of the two software codes employed. For the parametric cases, separation efficiencies of simulations came within 5-7 percent of those observed in experiments. Spatial water cut comparisons within the separator also had a similar level of agreement. The largest error was found to be for cases known to have high emulsion between the oil and water phases experimentally. Thus, implementation of emulsion submodels into one of the commercial codes using user-defined functions has been carried out. Preliminary results indicate significant improvement in numerical results for those cases experiencing high emulsion. An example of these results is shown in Figure 2.

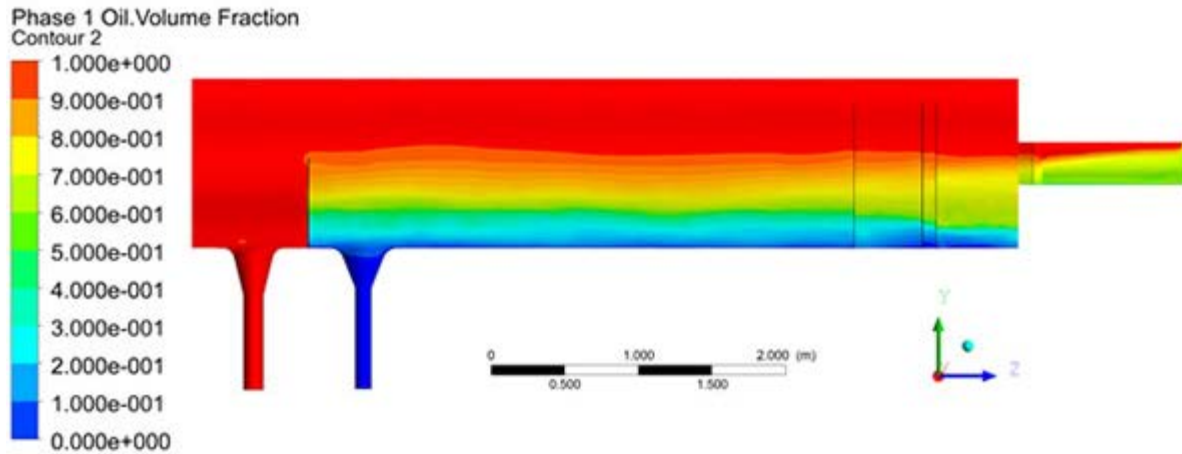


Figure 2: Volume fraction distribution of oil at the cross section of the separator for highest viscosity and water cut case

## 2016 IR&D Annual Report

---

### Improved Spatial Resolution for an Earth-Observing Infrared Spectrometer, 10-R8621

#### Principal Investigators

Robert A. Klar

Yvette D. Tyler

Inclusive Dates: 01/01/16 – 12/30/16

**Background** — Within the last decade, there has been rising awareness of climate change and its potentially detrimental consequences. Recognition that methane is a potent greenhouse gas has urged stricter governmental regulations and renewed focus on monitoring atmospheric methane. After researching several instruments, we found that those currently fielded do not have sufficient spatial resolution to meet the increasing demand for improved environmental monitoring. SwRI conceived of a concept for an atmospheric methane monitoring instrument.

**Approach** — The objective of this research is to devise, test, and validate a data-processing approach for reducing data volume while accurately measuring methane concentrations. To meet demands for improved environmental monitoring and improve upon the capabilities of predecessor instruments, we established the following performance goals for measuring methane and oxygen.

PERFORMANCE GOALS	PROPOSED RESEARCH
Minimum Signal to Noise Ratio (SNR)	100 <sup>1</sup>
Spatial Resolution	2 km x 2 km (land) 25 km x 25 km (ocean)
Spectral Resolution (Resolvance $R = \lambda / \Delta\lambda$ , $\lambda = 1640$ nm and 760 nm)	0.1 (16,400 and 7,600)
<i>1- measured at the poles (80° latitude)</i>	

The research seeks to take advantage of recent advancements in detector and readout technologies. In particular, we seek to exploit the processing capabilities included within the Teledyne SIDECAR® Application Specific Integrated Circuit (ASIC), which miniaturizes the drive electronics for infrared detectors. We also introduce a simplification to our original instrument concept by using a single larger detector (H2RG) instead of the two smaller ones.

**Accomplishments** — Windowing and accumulation data processing were implemented using the embedded processor on the SIDECAR. Images were acquired with the H2RG demonstrating the feasibility of doing data reduction at the front-end of the instrument. A lossless data compression algorithm is also currently being examined for possible implementation.

We have completed the design, fabrication, and assembly of a SIDECAR Interface Board (SCIB). The SCIB will be integrated with the data processing software to conduct a validation test of our prototype instrument front-end in the laboratory.



## 2016 IR&D Annual Report

### Compound-Eye Based Ultra-Thin Cameras, 14-R8545

#### Principal Investigators

Joseph Mitchell

Monica Rivera Garcia

Joey Groff

Jeffrey Boehme

Inclusive Dates: 03/24/15 – 09/23/16

**Background** — This 12-month project focused on developing a new imaging technique that can lead to an ultra-thin camera design. Although modern consumer electronics commonly obtains camera thicknesses of 5 to 6 mm, reducing camera thickness to approximately 2 to 3 mm opens up new device and form factor possibilities. In traditional camera designs, the thickness of the device is largely dictated by the camera optics, which typically consists of multiple stacked lens elements that must be carefully aligned. Nature has already solved the thickness problem with the compound insect eye, which uses an array of miniature lenses in front of one or more light-sensitive areas. The individual “sub-images” are then reconstructed in the insect nervous system and brain. However an insect compound eye is quite challenging to fabricate due to the curved surfaces involved, so a planarized design would make it compatible with existing integrated circuit (IC) fabrication techniques and avoid the need to align multiple lens elements.

**Approach** — The concept investigated in this project uses several layers of very thin micro-optical components directly above the image sensor to form an array of sub-images that are reconstructed into a single image. A masked microlens array provides the focusing mechanism and field stop, with each microlens producing a single sub-image. Beneath the microlenses is a double-layered array of apertures where the aperture positions are progressively offset from the microlenses toward the edge of the array to give each sub-image a slightly different field of view. With this design, the total camera thickness can approach 2 mm.

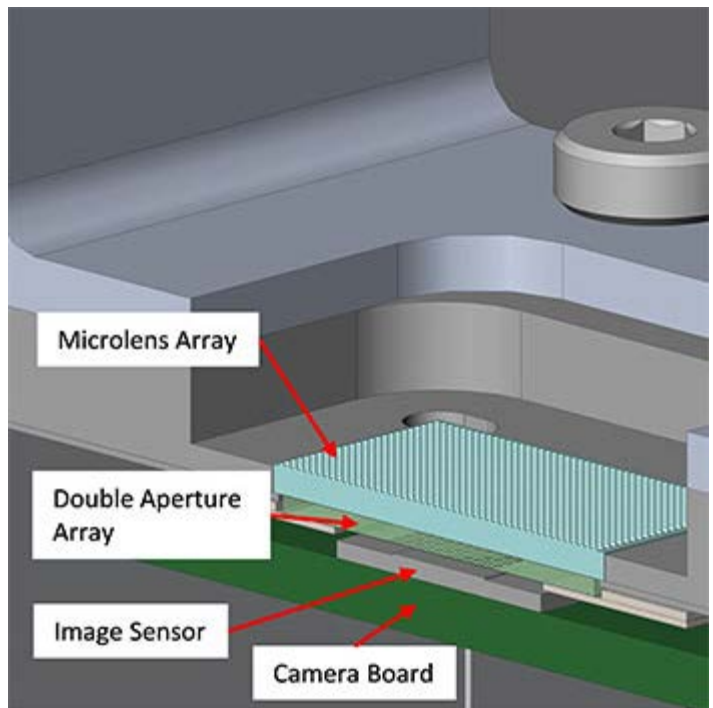


Figure 1: Illustration of compound-eye camera test configuration

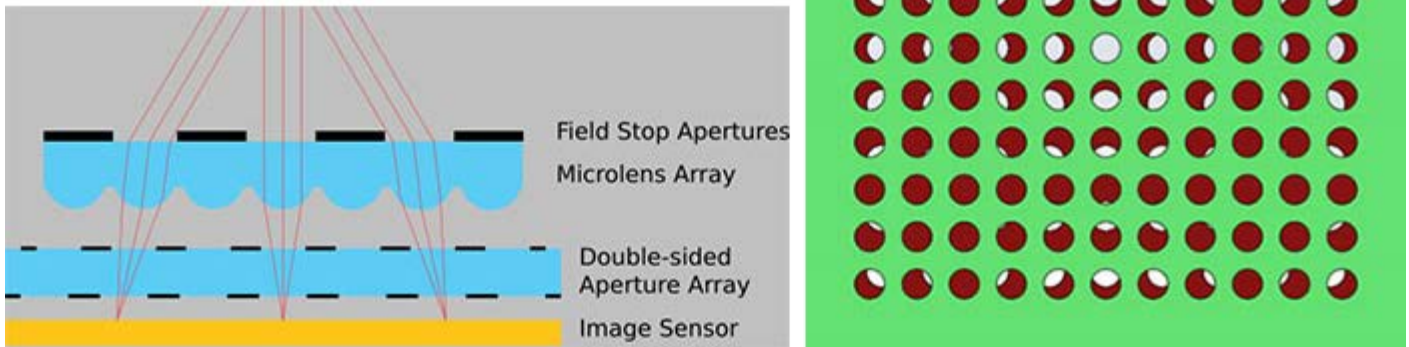


Figure 2: Illustration of compound-eye camera concept (left) and one double-aperture configuration (right)

The tasks in this project included:

- Develop a design for the ultra-thin camera concept in Zemax
- Develop post-processing code to turn the individual small field of view (FOV) sub-images into a single wide FOV image
- Acquire and fabricate the components to build a bench top demonstrator of the design
- Test the design against both camera test targets and real world scenes.

**Accomplishments** — During this project we developed four microlens/aperture configurations in Zemax from which five aperture array designs were fabricated. We developed a laboratory bench-top test fixture to quickly evaluate the designs using a modified five-megapixel image sensor connected to a microprocessor board for image display and capture. Images were acquired both with a standard target in the lab and of outdoor scenes. A post-processing routine was developed in MATLAB, which was tested on Zemax simulated sub-images.

There proved to be many challenges in fabricating the chromium-on-glass, double-sided aperture arrays with the primary challenge being the front-to-back alignment. During testing, we encountered image quality issues that were partially resolved by masking every other aperture with laser micromachined foil sheets to prevent sub-image crosstalk and by adding an additional field stop mask layer above the microlenses. Initial tests showed elimination of ghosting and major contrast improvements, but other issues remained due to the thickness and manual positioning of the foils, which would be resolved by a new aperture production run. Since the project had reached its conclusion, we were unable to follow up on our improvements, but we feel we have demonstrated that with a properly masked microlens array, we would have been able to reach our goal.

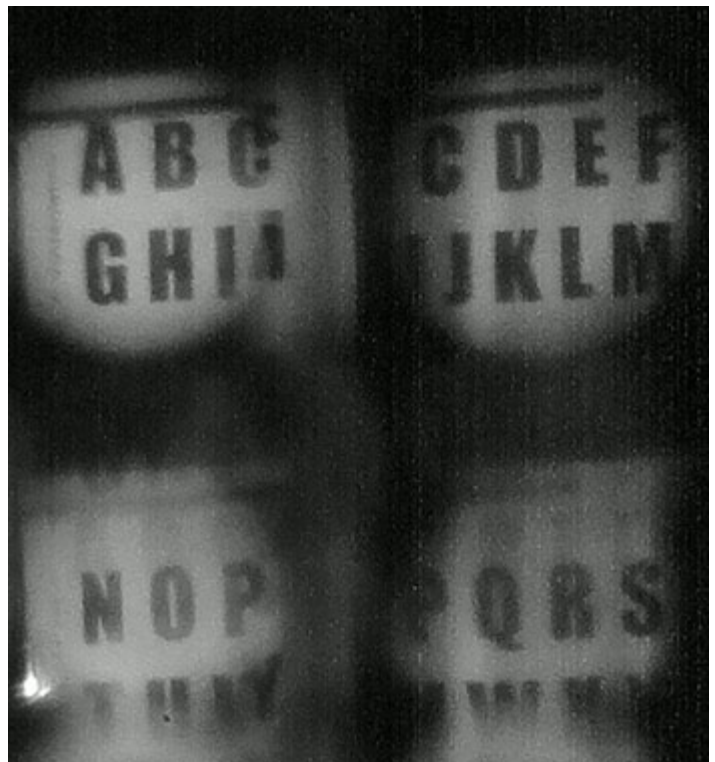


Figure 3: Sample sub-images of a test target

Since the project had reached its conclusion, we were unable to follow up on our improvements, but we feel we have demonstrated that with a properly masked microlens array, we would have been able to reach our goal.



## 2016 IR&D Annual Report

---

### **Multivariate Statistical Process Control for Cooling Towers, 14-R8656**

#### **Principal Investigators**

Tom Arnold

David Ogden

John White

Inclusive Dates: 04/11/16 – Current

**Background** — SwRI operates 12 comfort cooling towers that support HVAC systems in office buildings on campus. Comfort cooling towers use approximately 20 percent of the cooling tower water consumed campus wide. SwRI operates 29 process cooling towers supporting labs in technical divisions. Process cooling towers use approximately 80 percent of the cooling tower water.

Cooling towers are managed, in part, by maintaining a target pH and conductivity level of the water in the tower. Fresh water, referred to as make-up water, can be added, or bleed water removed from the tower to maintain the optimal levels of pH and conductivity. Prior to this project, pH, conductivity, make-up water usage, and bleed water readings were gathered by an outside contractor and reported on a weekly basis. An instance of a bleed valve being left open on a cooling tower went unaddressed using this existing measurement and reporting process. As a result, significant water usage and financial costs were incurred by SwRI.

**Approach** — The objective of this project was to determine if multivariate statistical process techniques can be used to detect anomalies in cooling tower operations. The following tasks will be completed to reach this objective:

- Task 1: Gather Data. Data on pH level, conductivity level, make-up water usage and bleed water usage all need to be collected in an automated fashion to enable the analysis and to perform more robust general monitoring of the cooling towers beyond this project. The purchase and installation of new cards, repair of meters, and running of conduits had to be performed to enable data collection.
- Task 2: Apply Statistical Methodologies to Cooling Tower Data. This task will examine other statistical means of monitoring the operation of the cooling tower. The use of multivariate approaches in particular will be considered.
- Task 3: Automate Anomaly Detection. Based on the identification of a suitable monitoring technique, the purpose of this task will be to implement the monitoring technique on the cooling towers.

**Accomplishments** — With the exception of a couple of towers, the work to integrate the data from the data collection system into the environment where nSPCT will run was completed. The server environments were configured and a demonstration customer site was configured.

As records for the process and comfort towers became available during Task 1, they were reviewed for reasonableness. On a couple of occasions, unusual looking results were referred for clarification and correction to SwRI personnel familiar with tower operation. Issues encountered included temperature and humidity meters reporting the same value for multiple days, temperature and humidity readings that did not match the values from other towers or from the local San Antonio weather station data, and overstated make-up water values. Individual readings are still being monitored. Data will soon be available so that the multivariate analysis techniques can begin to be reviewed.

---



## 2016 IR&D Annual Report

### Exploration of Encapsulation Methods of Subunit Vaccines, 01-R8576

#### Principal Investigators

Kenneth Carson

XingGuo Cheng

Inclusive Dates: 08/03/15 – 12/03/15

**Background** — Vaccination is one of the most effective tools for mitigating the impact of influenza epidemics and pandemics. However, commercially available flu vaccines are in general directed toward the specific strain(s) contained in the vaccine. Current flu vaccine strategies have two major drawbacks: lack of cross-protective immunity (i.e., the vaccine is not effective against multiple strains or types of flu) and lack of long-term effectiveness (i.e., the vaccine protection is short-lived and not potent enough.)

**Approach** — To overcome the above issues, this project combines the expertise and strength of two research teams in the infectious disease field of Ohio State University (OSU) and SwRI. The team at OSU, led by Professor Renukaradhya J. Gourapura (DVM, PhD) and Dr. Chang Lee, focused on developing highly effective antigens that target the highly conserved region of swine influenza virus proteins found in multiple viral strains. The team at SwRI focused on developing an optimal delivery platform for the antigens. Specifically, SwRI used its knowledge in encapsulation to develop extended release nanoparticle vaccine formulations (using chitosan, polylactide-co-glycolide-polyethylene glycol (PLGA-PEG) or lipids) with the goal of controlling release of the antigens while maintaining high loading efficiency and resulting in long-lasting immunity. To further increase the efficacy, SwRI included a novel adjuvant, monosodium urate crystals, developed through a SwRI project funded by the San Antonio Vaccine Development Center (SAVE). The nanoparticle formulations developed at SwRI were sent to OSU for testing for cross-protective immune response against influenza virus in the pig model.

**Accomplishments** — Based on the hydrophobicity and isoelectric points of peptides and the matrix materials used they can either be encapsulated inside the core of the particles, or the core or lipid bilayer of liposomes. The use of chitosan resulted in no usable nanoparticles. Particles of both the PLGA-PEG and liposomal formulations containing the mixture of peptides and adjuvant were submitted for testing in the pig influenza model at OSU. The vaccine was intra-nasally administered to swine challenged with SIV (swine influenza virus). Liposomal formulations showed positive results in the animal studies. We observed

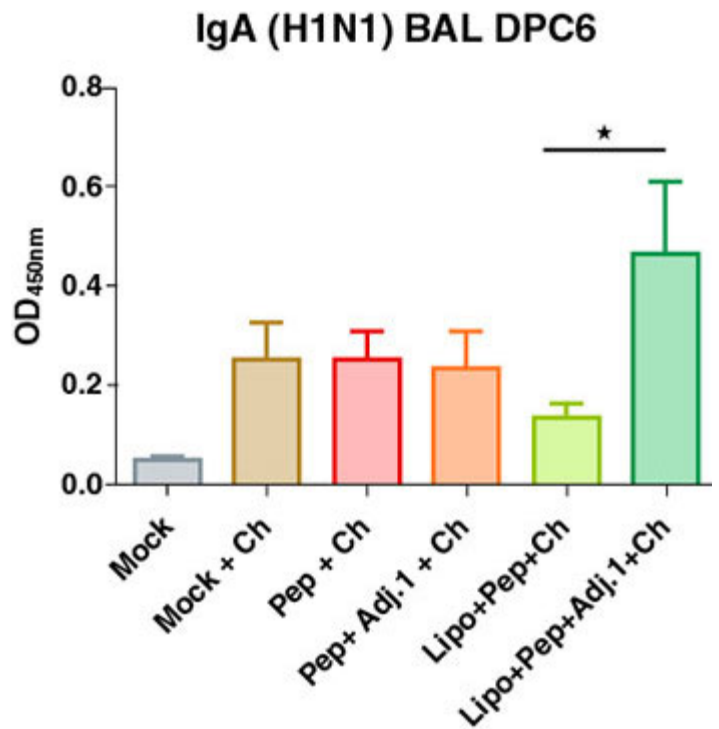


Figure 1: IgA (H1N1) levels found in the bronco-alveolar-gavage fluids six days post-challenge in a pig model. Green-peptide subunit vaccine mixture with adjuvant in a liposome was administered after a challenge of virus to pig animal model.

reduced gross lung lesion scores, interstitial pneumonia, H&E score, IL-10, IL-6, IFN-gamma levels in serum, lung lysate, and broncho alveolar lavage (BAL) fluid in liposomal formulation compared to non-treated control. In addition, the liposome vaccine formulation also illicit stronger IgA immune response instead of IgG immune response. This study demonstrates the promising efficacy of a liposomal flu subunit vaccine formulation.

## 2016 IR&D Annual Report

---

### Enhancing the Efficacy of a Chlamydia Subunit Vaccine through Encapsulation, 01-R8584

#### Principal Investigator

[XingGuo Cheng](#)

Inclusive Dates: 09/01/15 – 08/31/16

**Background** — Chlamydia trachomatis (CT) is the world's leading cause of bacterial sexual transmitted disease (STD) and the most commonly reported STD in the U.S. and Texas, with an increasing incidence rates over the last 10 to 15 years. There also is a huge health disparity in the frequency of the disease among the more than 100 million new global cases/year, and a huge economic and human health impact. Chlamydial infections in women induce upper genital tract pathology causing pelvic inflammatory disease, complications such as ectopic pregnancy and infertility, in addition to epididymitis in men, infant pneumonia in children that may lead to serious respiratory sequelae later in life, and certain serovars of CT cause trachoma, the major worldwide cause of preventable blindness. The vaccine candidate to be studied in this effort has been demonstrated to have a high degree of efficacy in two animal models of genital chlamydial infection. However, there is a need to further develop this promising vaccine as proposed in terms of longer-lasting protective immunity, easy and effective delivery, and improved efficacy to transition into humans.

**Approach** — This project connected the chlamydia research at The University of Texas at San Antonio (UTSA) with liposomal encapsulation research at SwRI. In Aim 1, UTSA provided SwRI selected subunit chlamydia vaccine (short peptides and CPG adjuvant), and SwRI used nano liposome encapsulation technology to encapsulate the test vaccine. The liposome size was measured by dynamic light scattering, and the charges were measured using a Z-potential analyzer. The liposome fabrication process was also validated in large scale (multi-liters). In Aim 2, the liposome vaccine formulation was intranasally injected into mice with genital infection, and duration of chlamydial shedding and pathological upper genital tract (UGT) sequelae were monitored. Additionally, the extent of humoral (antibody mediated) and cellular responses will be measured.

**Accomplishments** — We have designed and synthesized five, short, truncated peptides that can be used as alternative chlamydia antigens to replace recombinant chlamydial protease/proteasome-like activity factor (rCPAF) protein, which previously demonstrated good immune protection in an animal model challenged with the bacteria. Based on each subunit chlamydia antigen peptide's hydrophobicity and characteristics, we are able to use liposome to encapsulate each peptide, as well as the adjuvant, CpG oligonucleotide, at high loading efficiency and small nano size (below 200 nm). The custom-made liposome-based vaccine formulations are currently being evaluated *in vivo* and will become a promising vaccine to prevent chlamydia STD.

# SOUTHWEST RESEARCH INSTITUTE®

## 2016 IR&D Annual Report

---

### **Development of a Low-Cost Robust Circulating Fluidized Technology for the Sustainable Production of Biofuels and Biobased Products, 01-R8585**

#### **Principal Investigators**

[Monica Medrano](#)

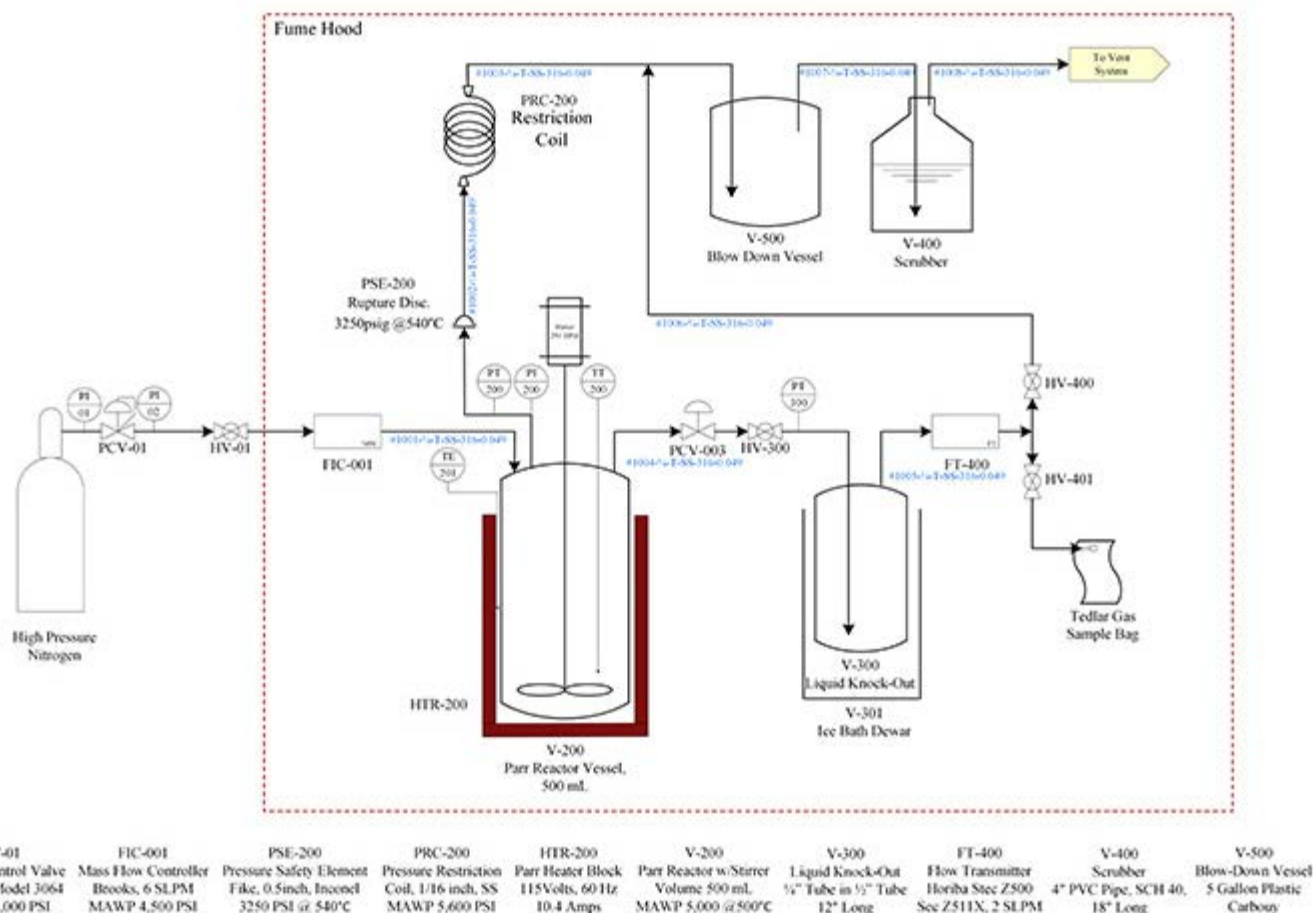
Jimell Erwin

Inclusive Dates: 09/01/15 – 12/30/16

**Background** — Southwest Research Institute (SwRI) completed the first year of working with The University of Texas at San Antonio (UTSA) in the UTSA-SwRI Connect Program to develop and demonstrate a novel biomass conversion technology to create cost-competitive, advanced biofuels and biobased products using SwRI's high-pressure, high-temperature hydrolysis process concept, patent applied for. The data from the present project will serve as input to the larger-scale supply chain model of the biomass industry under study at UTSA. The combined projects aim to model the performance and test the commercial viability of this new technology while considering uncertainties and risks by taking a holistic, source-to-use approach to test the economic viability of producing biofuels and new biobased products (possibly including byproducts) through a widely encompassing stochastic model of the whole supply chain counting factors such as soil type, crop(s) grown, weather pattern(s), transportation, conversion technology chosen, and other variables to make predictions about optimum crop technology choices, plant locations, and economics.

## R8585 UTSA Connect Project P&ID

Operating Conditions: 3250psig, 500°C



[Click for larger image.](#)

Figure 1: SwRI's experimental setup for small batch testing of biomass thermochemical conversion.

**Approach** — SwRI began with a literature review of thermochemical conversion processes currently used commercially or under development in research laboratories to convert biomass to fuels or chemicals. The three main thermochemical conversion processes are pyrolysis, gasification, and hydrothermal liquefaction. Based on current industry trends, SwRI chose to focus on pyrolysis as the most promising means of thermochemical conversion.

Using parameter values from the literature, SwRI completed a lumped kinetic model for switch grass pyrolysis reactions, which predict yields based on moisture and ash content of the biomass. This is consistent with the data being amassed in the model development. Additionally, a design-of-experiments statistical matrix was generated and completed to test the effects of moisture content, ash content, operating pressure (subcritical vs. supercritical), and reactor atmosphere composition (hydrogen vs. nitrogen). For the experiments, both switch grass and poplar were used due to the similarity of moisture and ash composition within each species.

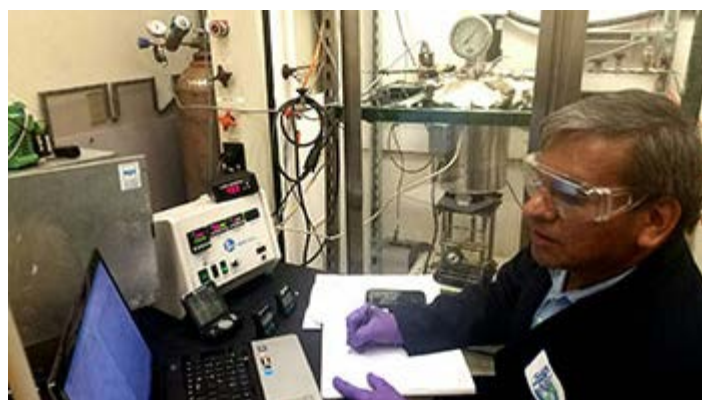


Figure 2: SwRI operator tests the effects of supercritical hydrogen atmospheres on biomass pyrolysis.

**Accomplishments** — SwRI has completed eight experiments that show that biomass type, ash content, and atmosphere (hydrogen/nitrogen) appear to have measurable effects on product yields, with moisture and pressure showing little impact. Additionally, there appear to be interactions with the ash content of the biomass and the reactor atmosphere (hydrogen/nitrogen).